PLACE IN RETURN BOX
to remove this checkout from your record.
TO AVOID FINES return on or before date due.

DATE DUE MAGIC 2	DATE DUE	DATE DUE
JAN 1 1 1998		
C6 0 3 0[illegible] NOV 2 2 200[illegible]		
MAY 0 3 2010		

d

o

lo

we

wa

ga

lo

re

or

not

str

gat

von

Goo

serv

test

dyna

ABSTRACT

LONGITUDINAL PLASTIC WAVE PROPAGATION

IN ANNEALED ALUMINUM BARS

by

Leonard Efron

In this investigation aluminum rods were subjected to dynamic compressive impact loading of duration of the order of 500 microseconds in order to study the propagation of longitudinal plastic waves. Two independent series of tests were conducted. In the first, an electro-magnetic transducer was used, while in the second, etched foil resistance strain gages yielded records of surface strain at the same gage locations. Strain rates on the order of 100 in/in/sec were reached.

Test results indicated that any given level of velocity or strain propagates along the bar with a constant velocity, not affected by the strain rate within the small range of strain rates encountered. However, the velocities of propagation observed differed noticeably from those predicted by von Karman rate-independent theory based on the static curve. Good agreement was found between the propagation speeds observed for different levels of velocity (averaged over all tests) and predictions of von Karman theory based on a single dynamic stress-strain curve differing from the static curve.

That the apparent applicability of a single dynamic curve

a
p
t
b

fr
pr
It
be
ev
ab
it

is
mo

th
bo
dif
end
whe
fir
the
bou
gage

and rate-independent theory to this kind of plastic wave propagation is consistent with rate-dependent theory for a material with a very slight rate dependence, was demonstrated by the results of computer solutions for rate-dependent theory.

The wave propagation speed versus strain level plots from the transient strain records showed consistently lower propagation speeds than those based on the velocity records. It is believed that the strain gage response actually lags behind the strain in the material, but considerably more evidence is needed before final conclusions can be drawn about the lag in the strain measurements and the reasons for it.

The velocity recording technique for non-magnetic materials is believed to give good results, but it may be possible to modify it to make it more nearly a routine type of test.

In order to apply the strain-rate-dependence theory to the experimental measurements made, it is necessary to have boundary values at $x = 0$. To avoid the three-dimensional difficulties associated with the stress at the actual impacted end of the bar and test one-dimensional theory in a region where it should be applicable, it was decided to take the first gage station (six diameters from the impacted end of the bar) as $x = 0$, and use the recorded velocity there as a boundary condition to predict the velocity versus time at gage stations further along the bar.

A numerical computer solution was obtained using the

r
T
t
v
v
a
t
ra
al
co
wi
me
a
be

co
co
a
ra
lo
eq

rate-dependent theory with a power law for rate dependence. The computer solution did predict a constant wave propagation speed for any given level of velocity, but the constant values predicted did not agree well with the experimental values from the velocity records. This lack of agreement appears to be mainly the result of using a rather poor fit to the static curve in the computations, since von Karman rate-independent theory using the same fitted static curve also gave poor agreement with the experiments. Since the computer solutions with rate-dependent theory were consistent with a single dynamic curve, and since the velocity measurements correlate with a single dynamic curve, it appears that a little ingenuity in curve-fitting could produce agreement between the rate theory and the experiments.

For the case of linear strain rate dependence, previously considered by Malvern (1950), a new computer solution for a constant stress boundary condition indicated the formation of a plateau of constant strain in agreement with von Karman rate-independent theory, if the load is applied for a duration long enough for the material at the impacted end to reach equilibrium.

LONGITUDINAL PLASTIC WAVE PROPAGATION

IN

ANNEALED ALUMINUM BARS

by

Leonard Efron

A THESIS

Submitted to
Michigan State University
in partial fulfillment of the requirements
for the degree of

DOCTOR OF PHILOSOPHY

in
Mechanics

Department of
Metallurgy, Mechanics and Materials Science

1964

L

a

t

P

t

a

g

Le

va

T,

ta

to

Ap

ti

al

as

ACKNOWLEDGMENTS

I wish to express my sincere appreciation to Professor Lawrence E. Malvern who suggested this problem. I shall always be grateful for his invaluable guidance and counsel throughout this research.

Thanks are also given to Professor William A. Bradley, Professor George E. Mase and Professor David Moursand for their services on my guidance committee. Appreciation is also expressed to Professor Charles S. Duris for his suggestions concerning numerical methods, to Dr. William W. Lester for his suggestions and assistance in developing the velocity transducer used in this study, and to Mr. William T. Bean for his advice regarding resistance strain gage technique. Note is also made of the assistance rendered to me by my fellow graduate students in Metallurgy and Applied Mechanics.

The project was supported by the National Science Foundation under Grant No. G-24898.

To my wife Joy, who is as perfect as her typing, I will always be thankful for her understanding, encouragement and assistance in the completion of this dissertation.

TABLE OF CONTENTS

C

CH

BI

AP

LIST OF FIGURES

P

c

t

c

a

o

p

s

p

f

CHAPTER I

INTRODUCTION

1.1 Purpose

The mechanical behavior of engineering materials has long been known to exhibit marked differences under conditions of impact and high rates of loading as compared to the results obtained during static testing. Theories taking into account the effects of strain rate in stress-strain relations were offered as early as 1909. The concept of a rate-of-strain dependence in dynamic deformations of metals was naturally extended to studies of stress wave propagation.

It is the purpose of this investigation to study the propagation of longitudinal plastic waves in aluminum rods, caused by dynamic compressive impact loading of duration of the order of 500 microseconds. Cross section particle velocity and surface strains from two independent series of tests are examined with special attention to the possible existence of strain rate effects.

The data from the velocity transducers is compared with predictions of a strain-rate-independent theory and also a strain-rate-dependent theory. Consideration is given to the possibility of using a single dynamic stress-strain curve for the material to account for the wave propagation observed.

In order to apply the strain-rate-dependence theory t

r

c

t

t

p

w

o

f

wl

fi

ba

bo

th

tr

fl

the

sol

pro

gov

com

*Sup
Bit

to the experimental measurements made, it is necessary to have boundary values at x = 0. However, at the actual end of the bar, the stress state is three-dimensional and a load-time history obtained from the transmitter bar would not be the proper boundary condition for the one-dimensional wave propagation. Bell[27*] has found that the one-dimensional wave is formed in a distance along the bar equal to about one diameter. In order to avoid the three-dimensional difficulties and test the one-dimensional theory in a region where it should be applicable, it was decided to take the first gage station (6 diameters from the impacted end of the bar) as x = 0, and use the recorded velocity there as a boundary condition to predict the velocity versus time at the other three gage stations further along the bar.

All calculations are for a semi-infinite rod and the transient experimental data are all obtained before any reflections arrive from the far end.

Associated with this study is a re-examination, using the high speed CDC-3600 digital computer, of some previous solutions of strain-rate-dependent longitudinal plastic wave propagation. Iterative procedures were used to solve the governing system of nonlinear equations. Difficulties in computation were encountered. The criteria for convergence

---

*Superscript numerals indicate references as listed in the Bibliography.

L

e

a

d

ar

sp

co

of

in

to

on

the

ini

ela

(17

Ven

190

teen

of the iteration process was found to be a function of strain-rate and the degree of material strain rate dependence.

1.2 Background

Thomas Young (1773-1829) included in his Course of Lectures on Natural Philosophy and the Mechanical Arts, London, 1807, a discussion of one-dimensional waves in an elastic bar due to longitudinal impact with another bar and concluded that $\sigma = \frac{Ev}{c}$ where σ is the stress at impact due to an imposed boundary velocity v. The quantities E and c are Young's Modulus and the elastic wave propagation speed respectively, which are material constants. This correct result perhaps marks the beginning of the history of stress wave propagation in solids.

In 1821 Navier (1785-1836), then Professor of Mechanics in Paris, presented a memoir giving the equations for vibratory motion of an elastic medium composed of particles acting on one another with forces directed along the lines joining them, and proportional to the product of displacement and initial distance between them. This paper for a particular elastic solid was followed by a series of works by Cauchy (1789-1857), Poisson (1781-1840), Green (1792-1841), St.-Venant (1797-1886), Stokes (1819-1903), Lord Kelvin (1824-1907), Lord Rayleigh (1842-1919) and others during the nineteenth century.

Their researches were carried on not only in an attempt to discover the laws governing vibrating bodies, but to understand the nature of light, the transmission of which was believed due to the vibrations of a perfectly elastic aether. Thus, many of the early studies of stress wave propagation in an elastic medium were prompted by an interest in electromagnetic phenomena. The twentieth century opened with our understanding of the governing equations for longitudinal waves (irrotational dilatation), transverse waves (equivoluminal distortion) in extended elastic bodies and Rayleigh surface waves in the form known to us today.*

In an extended elastic medium obeying Hooke's Law, longitudinal waves are propagated with a velocity

$$c = \left(\frac{\lambda + 2\mu}{\rho}\right)^{\frac{1}{2}} \tag{1.1}$$

where λ and μ are Lamé's constants and ρ is the mass density, whereas one dimensional wave analysis applied to longitudinal vibrations of rods yields

$$c = \left(\frac{E}{\rho}\right)^{\frac{1}{2}} \tag{1.2}$$

where E is Young's Modulus.

---

*For a review of the early history of elastic wave propagation, see:

Whittaker, E. T., A History of the Theories of Aether and Electricity, Vol. 1, Nelson, London, 1951 and Harper, N. Y., 1960, Chapter V.

Love, A. E. H., The Mathematical Theory of Elasticity, Dover, N. Y., 1944, Introduction and Chapter XIII.

(

f

t

s

w

n

of

to

te

in

whi

pla

deve

This latter result is only approximate since we assume that plane sections of the rod remain plane and the stress is uniform across the section.

As physicists gave up their quest for the elusive aether, interest in stress wave propagation slackened. However, technological advances began making use of metals and other materials past their proportional and elastic limits and into the plastic region. It also became apparent that many materials of interest exhibited mechanical properties under conditions of dynamic loading which differed significantly from the properties determined during static loading tests.

L. H. Donnell[1] (1930) introduced the first scheme for treating longitudinal wave propagation in a medium with a stress-strain relation deviating from Hooke's Law. Stress waves in a long bar were analyzed by a superposition technique in which the stress wave was treated as a succession of incremental steps in stress. Each increment was assumed to travel at a velocity determined by the slope of the material static stress-strain curve at the stress level of the increment. The wave velocities thus obtained are

$$c = \left(\frac{1}{\rho} \frac{d\sigma}{d\epsilon} \right)^{\frac{1}{2}} \tag{1.3}$$

which reduces to Equation (1.2) for a Hookean material.

World War II brought a surge of interest in elastic-plastic wave propagation. Studies were made in the light of developments in armor-piercing shells and armor plates. The

I
i
I
a
c
c
a

t
b
sc

me
sc
ge
ma

al
sho
as

ith
(19
the
plas

problem was treated independently by von Karman[2,3] (1942) in the United States, Taylor[4] (1940) in England, and Rakhmatulin[5] (1945) in Russia. The von Karman-Taylor theory assumes a single-valued strain-rate-independent stress-strain curve which is concave towards the strain axis (thus precluding the possibility of shock waves being built up) and assumes that radial inertia effects are negligible.

Whereas von Karman used Lagrangian co-ordinates, Taylor treated the problem using an Eulerian co-ordinate system, but later showed that by a suitable transformation, the two solutions are identical.

Experiments were carried out shortly after the development of this theory by Duwez and Clark[6]. The results showed some discrepancies from the predictions, which it was suggested might be attributable to strain-rate effects in the material.

The hypothesis of material strain-rate dependence had already been offered. It had been suggested that stress should be considered as a function of strain rate as well as the level of strain as early as 1909.

Among the proposed functional relationships was a logarithmic relationship suggested empirically by both P. Ludwik[7] (1909) and H. Deutler[8] (1932). L. Prandtl[9] (1928) reached the same conclusion as the result of a physical theory of plastic flow. The relation may be written

$$\sigma(\epsilon, \dot{\epsilon}) = \sigma_1(\epsilon) + k \ln \dot{\epsilon} \qquad (1.4)$$

w

ra

s

o

wh

wh

st

the

by

whe

The

rate

Thus

plas

where $\sigma_1(\epsilon)$ is the stress at a strain of ϵ when the strain rate, $\dot{\epsilon}$, is unity. The factor k could be a function of strain.

Another relation which has been proposed is a power law of the form

$$\sigma(\epsilon, \dot{\epsilon}) = \sigma_1(\epsilon)\, \dot{\epsilon}^n \tag{1.5}$$

where n may be a function of strain.

In a more general form the relation can be written

$$\sigma = \phi(\epsilon_p, \dot{\epsilon}_p) \tag{1.6}$$

where the subscript refers to nominal plastic strain and strain rate. L. Malvern[10,11] developed a one-dimensional theory for longitudinal stress-wave propagation as in a rod, by rewriting Equation (1.6) as

$$E_o \dot{\epsilon}_p = g(\sigma, \epsilon) \tag{1.7}$$

where E_o (Young's Modulus) is introduced for convenience. The elastic components of the deformation are considered rate independent, and hence we obtain

$$E_o \dot{\epsilon}_e = \dot{\sigma} \tag{1.8}$$

Thus, the constitutive equation which is the flow law when plastic deformation occurs is given by

$$\dot{\epsilon} = \dot{\epsilon}_e + \dot{\epsilon}_p$$

$$E_o \dot{\epsilon} = \dot{\sigma} + g(\sigma, \epsilon) \tag{1.9}$$

M
s
w
T
ar
a
is
th
wh
tr
pla
to
rat
for
on
such
of t

Malvern gave a numerical solution for the case of a linear strain-rate-dependence

$$\sigma = \sigma_o + \frac{1}{k} \dot{\epsilon}_p \tag{1.10}$$

where σ_o represented the static stress-strain relation

$$\sigma_o = f(\epsilon)$$

Thus

$$\dot{\epsilon}_p = k \left[\sigma - f(\epsilon) \right]$$

and

$$E_o \dot{\epsilon} = \dot{\sigma} + k \left[\sigma - f(\epsilon) \right] \tag{1.11}$$

The relation $f(\epsilon)$ was chosen to represent approximately a hardened aluminum alloy, and one result of the solution is that small plastic strains propagate at a velocity greater than that predicted by the strain-rate-independent theory, whereas larger strains are progressively retarded.

The special case σ_o = constant had previously been treated numerically by Sokolovsky.[12,11]

Most experimental work has shown the formation of a plateau of uniform strain at the impact end of rods subjected to constant velocity loadings, as predicted by the strain-rate-independent theory. The numerical solution of Malvern for a strain-rate-dependent theory, which was carried out on desk calculators, did not indicate the formation of any such region of uniform strain in the first 100 microseconds of the impact.

a
i
e
p
s

us
di
a
Th
ga
Be
pre
inc
ind
pul
the
exp
appe
Howe
and
elas

Prop
the

Experiments by Bell[13] on steel bars and Sternglass and Stuart[14] with copper strips involved the propagation of incremental impact loads superimposed upon static loads in excess of the elastic limit. The wave fronts were found to propagate at the elastic wave velocity and not at the lower speed predicted by von Karman theory.

Alter and Curtis[15] subjected lead bars to impact loading using a Hopkinson Pressure Bar[16] with a stepped increase in diameter. Due to reflections within the bar, the result was a plastic preloading to the lead followed by a second impact. The wave front of the second disturbance was found to propagate at the elastic wave velocity. More recent studies by Bell and Stein[17] of incremental loading waves in dynamically pre-stressed aluminum, using a similar set-up in which the increment exceeded the original elastic limit of the material, indicated that only the initial portion of the subsequent pulse travelled at the elastic wave speed. The remainder of the pulse appeared to propagate at the plastic wave speeds expected from rate-independent theory. All these results appeared to contradict the rate-of-strain independent theory. However, other studies of wave propagation in lead by Bodner and Kolsky[18] suggest that lead should be treated as a visco-elastic material for small amplitude plastic waves.

Attempts to establish a physical basis of plastic wave propagation in crystalline solids based on the laws governing the generation and motion of dislocations have been made by

Ca
th
co
gr
g(
nc
th
ra
nu

ma
ba
the
str
sho
The
min
men
pen
str
rat
stra
the

to d
alum

Campbell, Dorn, Hauser, Simmons, et al.[19-24] They have shown that Equation (1.9) is a good approximation for the material constitutive equation. The experiments conducted by this group using a Hopkinson split pressure bar device showed that $g(\sigma, \epsilon)$ was independent of stress and strain histories, but not a simple function of $\sigma - f(\epsilon)$. In discussion of these theories, Dorn has said that they suggest a greater strain rate effect in pre-strained aluminum than in annealed aluminum, and this agrees with their experimental observations.[23,24]

Using a diffraction grating technique, Bell[25-27] has made studies of constant velocity impact on annealed aluminum bars and found agreement with the strain-rate-independent theory on the basis of a "dynamic" rather than the static stress-strain curve. Kolsky and Douch[28] made studies of short bars of pure copper, pure aluminum and aluminum alloy. They found no appreciable strain rate dependence for the aluminum alloy. For the copper and pure aluminum their measurements indicated a rate-of-strain dependence, but a rate-independent theory gave reasonable agreement if a single dynamic stress-strain relation appropriate to the actual range of rates of straining in the test was used. The copper at low strain rates did, however, exhibit a strain rate effect of the nature predicted by Malvern.

Lindholm,[29] in a series of tests in which short (length to diameter ratios from 0.2 to 2.0) specimens of high purity aluminum were subjected to strain cycling at widely variant strain rates, has shown that the prior strain rate history of the specimen has a significant effect on plastic flow behavior when reloading is at a high strain rate. Dynamically reloaded specimens indicated an annealing recovery effect with a characteristic time on the order of seconds. These findings do not agree with the concept of a single dynamic stress-strain relation.

A strain-rate-dependent theory would result in the higher increments of strain in a pulse being propagated at slower speeds than predicted by the rate-independent theory based on the static curve. Such apparent slowing has been observed,[30] but it is the contention of some researchers that the apparent decrease in wave propagation speed for large strains is due to the failure of the measuring devices to faithfully follow the deformation.

Strain gages of both the wire and foil type have been used to successfully monitor "static" strains into the plastic range, but controversy still exists as to their ability to respond accurately to large strains at high strain rates. It has been suggested by Bell[31] that the strain rate dependence indicated from earlier wave propagation experiments was due to a lag in the gage response. When compared to measurements made with his diffraction grating technique, he found that wire resistance strain gages gave errors which were related to the maximum slope of strain-time curve. Tests at a strain rate of 1000 in/in/sec and a maximum amplitude of 2.5% indicated errors of 26% at a point one-half inch away from the impact end of a one-inch diameter specimen. At a distance equal to $3\frac{1}{2}$ diameters from the impact end (with a much lower strain rate) the error was on the order of 10%.

The problem at hand is to determine the three dependent variables (stress, strain, velocity) in terms of the two independent variables x and t. With the exception of the techniques of dynamic photoelasticity with birefringent materials or use of the Hopkinson Pressure Bar, we are restricted experimentally to techniques for measuring strain or particle velocity. The higher the strain rate and strain magnitude, the higher the required frequency response of the transducer.

For further background information concerning dynamic stress-strain relations and anelastic stress waves, the reader is referred to references 32 through 35 as listed in the Bibliography.

2.

fo

te

im

at

di

ar

an

eff

one

at

has

For

sio

sta

the

a di

CHAPTER II

FUNDAMENTALS

2.1 Strain-Rate-Independent Theory

The rate-independent theory of von Karman was derived for a long, thin unstretched wire subjected to an impulsive tension load at one end. The analogous treatment for an impulsive compressive load, also using Lagrangian co-ordinates, is described below. The governing equations for one-dimensional longitudinal stress wave propagation in a bar are obtained by assuming that plane sections remain plane and that the stress is uniform across them. Lateral inertia effects are assumed negligible. These assumptions make the one-dimensional theory incorrect in the immediate vicinity at a suddenly impacted end of the bar, since, as Bell[27] has shown, a three-dimensional wave pattern exists there. For this reason, in comparing experiments with one-dimensional theory, we will take input data from the first gage station three inches from the end.

Lagrangian Co-ordinates will be used. Let u(x,t) be the displacement at time t of the cross section initially at a distance x. Loading occurs at the section x = 0. Then

$$\epsilon = \frac{\partial u}{\partial x} \tag{2.1}$$

$$v = \frac{\partial u}{\partial t} \tag{2.2}$$

where ϵ is the strain and v is the particle velocity at the section under consideration. Compressive stress and strain are reckoned positive, while displacement and particle velocity are considered positive when they are to the left (negative x-direction). In the cases treated in Chapter IV, the compressive wave moving to the right produces negative displacement and velocity.

Differentiating the first equation with respect to time and the second with respect to x, we obtain the equation of continuity

$$\frac{\partial \epsilon}{\partial t} = \frac{\partial v}{\partial x} \tag{2.3}$$

The equation of motion for an element of the bar gives

$$\frac{\partial \sigma}{\partial x} = \rho \frac{\partial v}{\partial t} \tag{2.4}$$

If strain is assumed to be a single valued function of stress, we can rewrite (2.4) as

$$\frac{\partial^2 u}{\partial t^2} = \frac{d\sigma}{d\epsilon} \frac{\partial^2 u}{\partial x^2} \tag{2.5}$$

which we recognize as the one dimensional wave equation for waves propagating with the velocity $c = \sqrt{\frac{d\sigma}{d\epsilon} / \rho}$. One obvious solution is[36]

$$u = v_1 t + \epsilon_1 x \tag{2.6}$$

which corresponds to a constant velocity impact at x = 0 on a semi-infinite bar and from Equation (2.1) represents a c

n

w

o

a

ϵ

ar

in

poi

fir

at

c_o^2

in

constant strain ϵ_1.

Letting $S = \frac{d\sigma}{d\epsilon}$ we see that a compression wave of magnitude ϵ_1 will propagate at a speed c_1 given by

$$c_1{}^2 = \frac{x^2}{t^2} = \frac{S}{\rho} \tag{2.7}$$

where S is evaluated at $\epsilon = \epsilon_1$.

Thus, the complete solution requires the consideration of three regions for the case of constant velocity impact at $x = 0$.

(a) $0 < x < c_1 t$ where $\epsilon = \epsilon_1$

(b) $c_1 t < x < c_o t$ where the relation $\frac{x}{t} = \sqrt{\frac{S}{\rho}}$ holds and c_o is the elastic wave propagation velocity

(c) $x > c_o t$ where $\epsilon = 0$

In the field of the solution [region (b) above] , σ and ϵ are positive, decreasing toward the right, while u and v are negative, increasing toward the right (i.e. decreasing in magnitude), and v is decreasing with time at any one point (increasing in magnitude).

Unless the constant velocity imposed at $x = 0$ has a finite rise time from $v = 0$, we have a discontinuity in strain at $x = c_o t$. Here, $S = E_o$ (Young's Modulus) and we have $c_o{}^2 = \frac{E_o}{\rho}$ which is the result in the elastic case.

Fig. (2.1) shows the relation between ϵ and $\beta = \frac{x}{t}$ in the three regions.

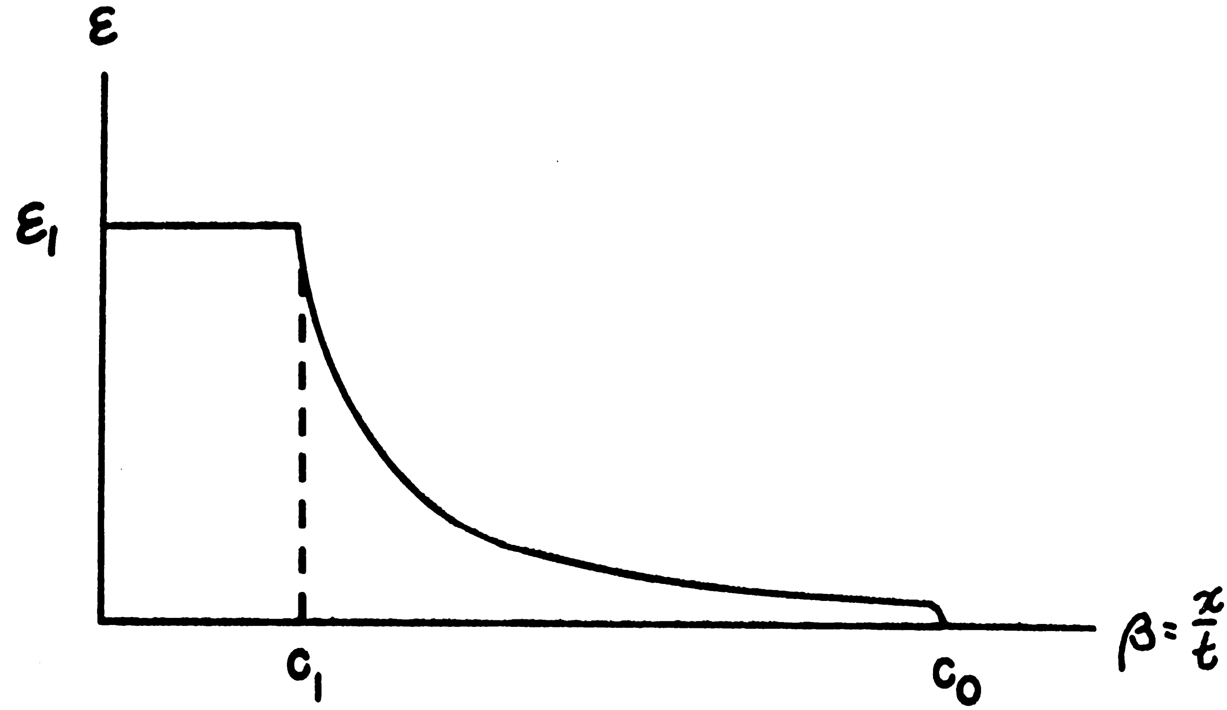

FIG (2.1) SCHEMATIC REPRESENTATION OF THE STRAIN DISTRIBUTION DUE TO CONSTANT VELOCITY IMPACT IN A RATE INDEPENDENT MATERIAL

2.2 Strain-Rate-Dependent Theory

In addition to Equations (2.3) and (2.4) a third equation is provided by the constitutive equation of the material. We will assume the flow law in the general form given by Equation (1.9)

$$E_o \frac{\partial \epsilon}{\partial t} = \frac{\partial \sigma}{\partial t} + g(\sigma, \epsilon) \qquad (2.8)$$

Thus, we now have a system of three quasi-linear first order differential equations. Although the equations are linear in the derivatives, the term $g(\sigma, \epsilon)$ may be non-linear in σ and ϵ.

The system is rewritten

$$\begin{aligned} E_o \frac{\partial \epsilon}{\partial t} - \frac{\partial \sigma}{\partial t} &= g(\sigma, \epsilon) \\ \frac{\partial \epsilon}{\partial t} - \frac{\partial v}{\partial x} &= 0 \qquad (2.9) \\ \frac{\partial \sigma}{\partial x} - \rho \frac{\partial v}{\partial t} &= 0 \end{aligned}$$

which we see is of the form

$$L_k \left[u\right] = a_{ki} u_x^{\,i} + b_{ki} u_t^{\,i} = G_k \qquad \begin{array}{l} \text{Summed } i = 1,2,\ldots,N \\ \text{N Eqs. } k = 1,2,\ldots,N \end{array} \qquad (2.10)$$

where the subscripts x and t denote partial derivatives.

The system will be shown to be hyperbolic and hence suitable for numerical solution by the method of characteristics.[37,38] We seek a combination

$$L \equiv \lambda_k L_k = \lambda_k G_k \quad \text{Summed } k = 1,2,\ldots,N \qquad (2.11)$$

such that it represents interior differentiation in only one direction, the direction given by the ratio $\frac{dx}{dt} = \frac{x_p}{t_p}$,

where the subscripts denote differentiation with respect to the parameter p along the curve being sought. If such a direction exists, we have

$$\frac{\lambda_k a_{ki}}{\lambda_k b_{ki}} = \frac{\frac{dx}{dp}}{\frac{dt}{dp}}$$

Thus,

$$\lambda_k(a_{ki}dt - b_{ki}dx) = 0 \qquad (2.12)$$

which represents N equations for i = 1,2,...,N.

Returning to Equation (2.11) we multiply by dx to obtain

$$Ldx = \lambda_k a_{ki}\, dx\, u_x{}^i + \lambda_k b_{ki}\, dx\, u_t{}^i$$

and then substitute from Equation (2.12) to obtain

$$Ldx = \lambda_k a_{ki} u_x{}^i dx + \lambda_k a_{ki} u_t{}^i dt$$

$$= \lambda_k a_{ki} du_i = \lambda_k G_k dx$$

with the final result

$$\lambda_k(a_{ki}du^i - G_k dx) = 0 \qquad (2.13)$$

Equation (2.11) is now multiplied by dt and the procedure repeated to obtain an additional relation

$$\lambda_k(b_{ki}du^i - G_k dt) = 0 \qquad (2.14)$$

Equations (2.12), (2.13), (2.14) are N + 2 homogeneous linear algebraic equations for the N multipliers λ_k. For these equations to be satisfied by a non-trivial solution, it is required that all the NxN determinants of the coefficients of λ_k vanish.

The determinant obtained from Equation (2.12) will define the characteristic base curves in the base x,t-plane, while the others furnish the interior differential equations, holding along the characteristic base curves.

For the system of Equations (2.10) we have

$$u^i = \begin{bmatrix} \sigma \\ \epsilon \\ v \end{bmatrix} \qquad a_{ki} = \begin{bmatrix} 0 & 0 & 0 \\ 0 & 0 & -1 \\ 1 & 0 & 0 \end{bmatrix} \qquad b_{ki} = \begin{bmatrix} -1 & E_o & 0 \\ 0 & 1 & 0 \\ 0 & 0 & -\rho \end{bmatrix}$$

$$G_k = \begin{bmatrix} g(\sigma, \epsilon) \\ 0 \\ 0 \end{bmatrix}$$

From Equation (2.12)

$$\lambda_1(a_{11}dt-b_{11}dx) + \lambda_2(a_{21}dt-b_{21}dx) + \lambda_3(a_{31}dt-b_{31}dx) = 0$$

$$\lambda_1(a_{12}dt-b_{12}dx) + \lambda_2(a_{22}dt-b_{22}dx) + \lambda_3(a_{32}dt-b_{32}dx) = 0$$

$$\lambda_1(a_{13}dt-b_{13}dx) + \lambda_2(a_{23}dt-b_{23}dx) + \lambda_3(a_{33}dt-b_{33}dx) = 0$$

Sul

and

wher

wave

isti

the

teri

Substituting from above

$$(dx)\lambda_1 + (0)\lambda_2 + (dt)\lambda_3 = 0 \tag{2.15}$$

$$(-E_o dx)\lambda_1 + (-dx)\lambda_2 + (0)\lambda_3 = 0 \tag{2.16}$$

$$(0)\lambda_1 + (-dt)\lambda_2 + (\rho\, dx)\lambda_3 = 0 \tag{2.17}$$

and we require

$$\begin{vmatrix} dx & 0 & dt \\ -E_o dx & -dx & 0 \\ 0 & -dt & \rho dx \end{vmatrix} = dx(-\rho\, dx^2 + E_o dt^2) = 0$$

Hence, the characteristic curves are

$$\begin{aligned} dx &= 0 \\ dx &= +c dt \\ dx &= -c dt \end{aligned} \tag{2.18}$$

where $c = \sqrt{\frac{E_o}{\rho}}$ represents the speed of propagation of the wave front.

Since there are as many distinct families of characteristics (all of which are real) as the order of the system, the system is completely hyperbolic. The method of characteristics is therefore applicable for the solution.

Equations (2.13) and (2.14) are

$$(-g dx)\lambda_1 + (-dv)\lambda_2 + (d\sigma)\lambda_3 = 0 \tag{2.19}$$

$$(-d\sigma + E_o d\epsilon - g dt)\lambda_1 + (d\epsilon)\lambda_2 + (-\rho dv)\lambda_3 = 0 \tag{2.20}$$

an

te

dx

or

sin

tion

-d

Thus,

The determinant formed by Equations (2.19), (2.16) and (2.17) is

$$\begin{vmatrix} -gdx & -dv & d\sigma \\ -E_o dx & -dx & 0 \\ 0 & -dt & \rho dx \end{vmatrix} = dx(E_o d\sigma dt + pgdx^2 - E_o \rho dxdv) = 0$$

We now examine the conditions required for the bracketed term to vanish along the characteristic curves. Along $dx = cdt$ we have

$$E_o d\sigma dt + \rho gc^2 dt^2 - E_o \rho cdtdv = 0$$

or

$$d\sigma - \rho \, cdv = -gdt$$

since

$$E_o = \rho \, c^2$$

Along $dx = -cdt$ we similarly obtain

$$d\sigma + \rho cdv = -gdt$$

Finally, we consider the determinant formed by Equations (2.15), (2.20) and (2.17)

$$\begin{vmatrix} dx & 0 & dt \\ -d\sigma + E_o d\epsilon - gdt & d\epsilon & -\rho dv \\ 0 & -dt & \rho dx \end{vmatrix} = \begin{array}{l} dx(\rho d\epsilon dx - \rho dvdt) \\ \quad + dt^2(d\sigma - E_o d\epsilon + gdt) = 0 \end{array}$$

Thus, along $dx = 0$, we have

$$d\sigma - E_o d\epsilon = -gdt$$

and

are

C
D

pli

How

pro

to

whe

k h

The differential equations defining the characteristics and the interior differential equations holding along them are summarized below.

Characteristic Diff. Equation	Interior Diff. Equation Along the Characteristic	
$dx = cdt$	$d\sigma - \rho c dv = -g(\sigma, \epsilon)dt$	(2.21)
$dx = -cdt$	$d\sigma + \rho c dv = -g(\sigma, \epsilon)dt$	(2.22)
$dx = 0$	$d\sigma - E_o d\epsilon = -g(\sigma, \epsilon)dt$	(2.23)

The form of $g(\sigma, \epsilon)$ will not in general permit an explicit integration of the interior differential equations. However, the system can be treated by numerical integration procedures. For this purpose, the following transformations to non-dimensional variables is introduced.

$$
\begin{aligned}
S &= \frac{\sigma}{E_o} \\
E &= \epsilon \\
V &= \frac{v}{c_o} \\
T &= kt \\
X &= \frac{k}{c_o}\, x \\
G &= \frac{1}{kE_o}\, g(\sigma, \epsilon)
\end{aligned}
\tag{2.24}
$$

where $c_o = \sqrt{\frac{E_o}{\rho}}$ is the elastic wave propagation speed and k has units of $\sec^{-1}$ and a magnitude chosen for convenience depe

tion

tics

solu

of th

three

tics.

shock

by th

where

and ve

from e

of an

sults

and th

depending on the form of $g(\sigma, \epsilon)$.

The characteristic curves and interior differential equations are now given by

$$dS - dV = -GdT \text{ along the curve } dX = dT \qquad (2.25)$$

$$dS + dV = -GdT \quad \text{" \quad " \quad "} \quad dX = -dT \qquad (2.26)$$

$$dS - dE = -GdT \quad \text{" \quad " \quad "} \quad dX = 0 \qquad (2.27)$$

From Fig. (2.2) we see that there are three characteristics passing through each point in the X,T-plane. Thus, the solution at any point P can be obtained if we have knowledge of the dependent variables at points A, B and C by solving three difference equations along the appropriate characteristics.

The conditions across the leading edge of an elastic shock wave traveling in the positive direction, represented by the line $x = c_o t$ in the x,t-plane are

$$\Delta \sigma = -\rho c_o \Delta v \qquad (2.28)$$

$$\Delta v = -c_o \Delta \epsilon \qquad (2.29)$$

$$\Delta \sigma = \rho c_o^2 \Delta \epsilon = E_o \Delta \epsilon \qquad (2.30)$$

where $\Delta\sigma$, $\Delta\epsilon$ and Δv are the jumps in stress, strain and velocity as the wave passes. The first condition results from equating impulse to change of momentum for the traversing of an element of the bar by the shock wave. The second results from continuity of the displacement across the shock, and the third follows from the first two and $c_o = \sqrt{\frac{E_o}{\rho}}$.

FIG (2

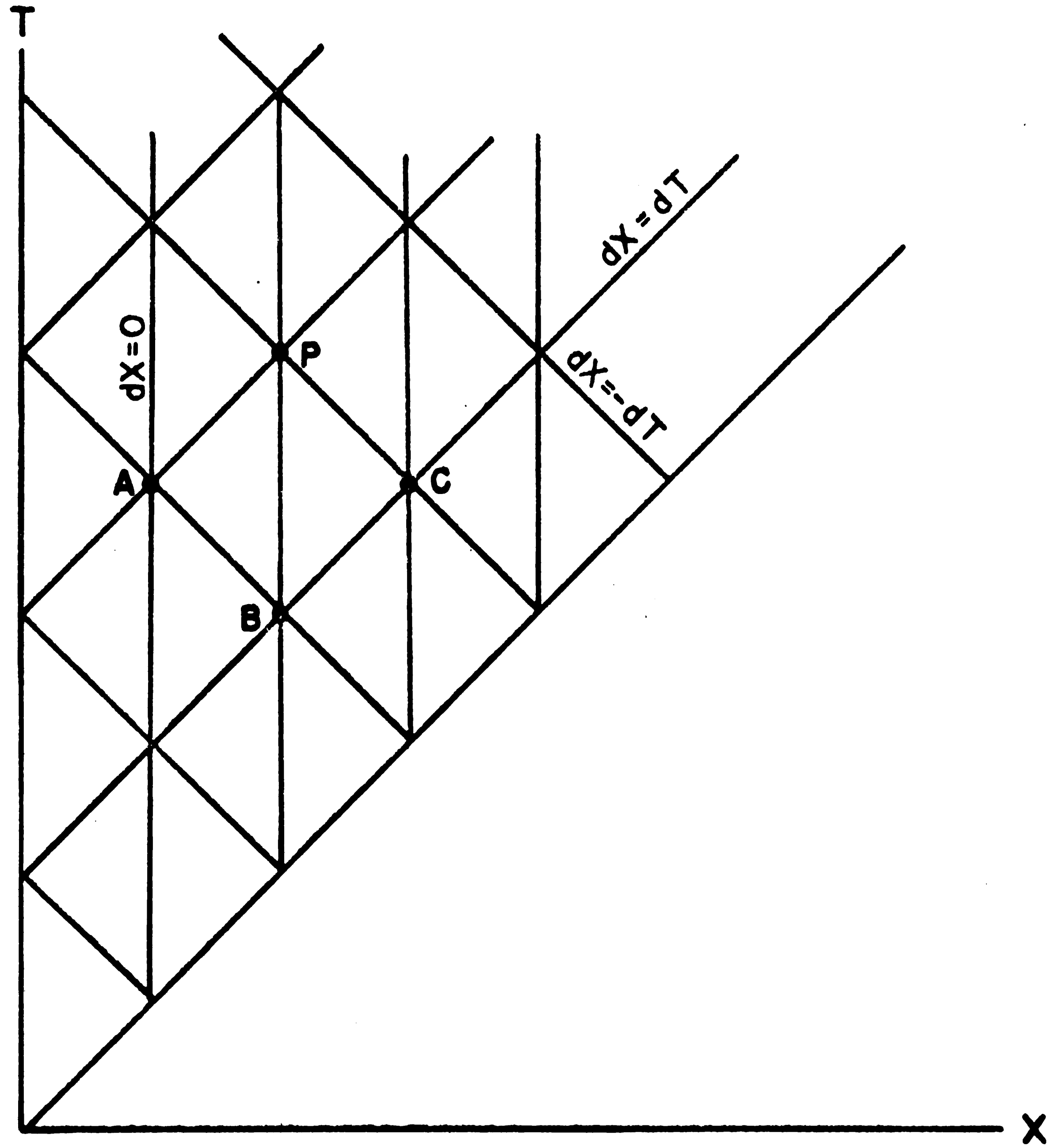

FIG (2.2) THE CHARACTERISTICS IN THE X,T-PLANE

Thu

cec

jus

equ

(se

alo

t =

tio

all

tha

stre

one

the

for

use

pria

Thus, in a semi-infinite bar with an undisturbed region preceding the shock, we obtain $\sigma = \rho c_o^2 \epsilon = -\rho c_o v$ on $x = c_o t$ just after the shock passes, and the interior differential equation along the characteristic can be integrated to obtain (see Malvern[11])

$$-\tfrac{1}{2}t = \int_{\sigma_o}^{\sigma} \frac{d\bar{\sigma}}{g\left(\bar{\sigma}, \frac{\bar{\sigma}}{c_o^2}\right)} \qquad (2.31)$$

along $x = c_o t$ where $\sigma_o = -\rho c_o v_o$ is the stress at $x = 0$, $t = 0$.

If there is no shock wave, but rather a gradual transition from an elastic to a plastic stress wave, we have

$$\sigma = \sigma_y = \rho c_o^2 \epsilon = -\rho c_o v$$

all along the curve $x = c_o(t-t_y)$ where $t = t_y$ is the time that the loading at the boundary $x = 0$ reaches the yield stress σ_y.

For the case of point P along $x = 0$, we assume at least one of the dependent variables to be prescribed and hence the equations along $X = 0$ and $dX = -dT$ will be sufficient for solution.

In writing the finite difference equations, we must use the average value of G along the element of the appropriate characteristic curve.

2.3 Numerical Procedure

Rewriting Equations (2.25), (2.26) and (2.27) as difference equations along the appropriate characteristics as shown in Fig. (2.3) we obtain

$$
\begin{aligned}
(S_p - S_a) - (V_p - V_a) &= -\Delta T\,\frac{G_p + G_a}{2} \\
(S_p - S_c) + (V_p - V_c) &= -\Delta T\,\frac{G_p + G_c}{2} \qquad (2.32) \\
-(S_p - S_b) + (E_p - E_b) &= \Delta T(G_p + G_b)
\end{aligned}
$$

These equations are solvable by iteration techniques in the form

$$(S_p^{\,i} - S_a) - (V_p^{\,i} - V_a) = -\tfrac{1}{2}\Delta T(G_p^{\,i-1} + G_a) \qquad (2.33)$$

$$(S_p^{\,i} - S_c) + (V_p^{\,i} - V_c) = -\tfrac{1}{2}\Delta T(G_p^{\,i-1} + G_c) \qquad (2.34)$$

$$-(S_p^{\,i} - S_b) + (E_p^{\,i} - E_b) = \Delta T(G_p^{\,i-1} + G_b) \qquad (2.35)$$

We begin with an initial guess for the value of G_p and solve for $S_p^{\,i}$, $E_p^{\,i}$, $V_p^{\,i}$ after which $G_p^{\,i} = G_p^{\,i}(S_p^{\,i}, E_p^{\,i})$ may be evaluated.

The process is then repeated to obtain $S_p^{\,i+1}$, etc. and the iteration continued until the new values of S_p, E_p, and V_p differ by less than some pre-determined amount from the values in the preceding iteration. Three types of "typical points" must be considered for a wave propagating in a semi-infinite bar, or before reflections occur in a finite bar: (a) general interior point, (b) impacted end (x = 0) and

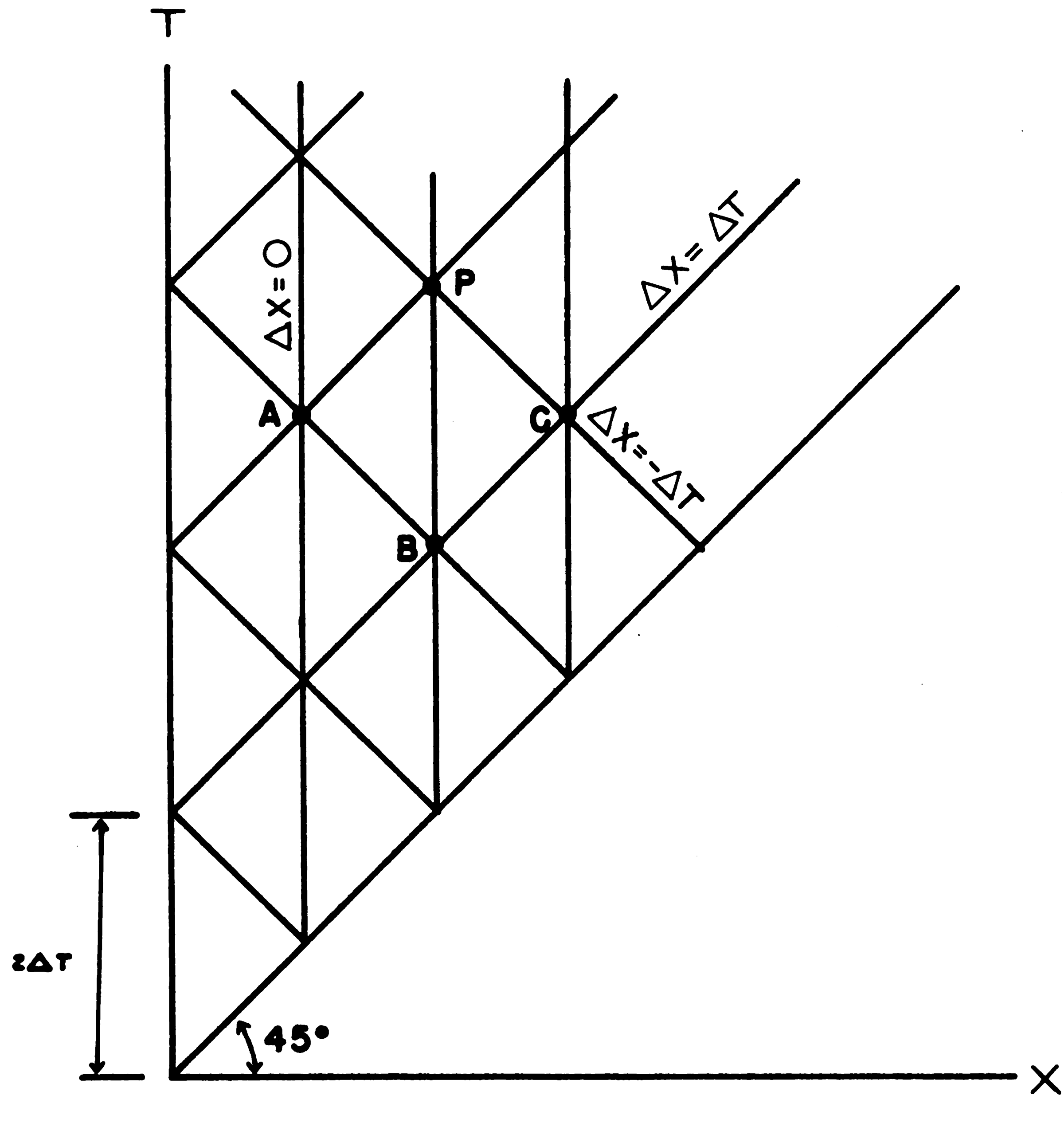

FIG (2.3) FINITE DIFFERENCE GRID USED IN NUMERICAL SOLUTION

(c) plastic wave front.

(a) General Interior Point

The equations for a general interior point are

$$
\begin{aligned}
S_p^{\,i} - V_p^{\,i} &= S_a - V_a - \tfrac{1}{2}\Delta T(G_a + G_p^{\,i-1}) \\
S_p^{\,i} + V_p^{\,i} &= S_c + V_c - \tfrac{1}{2}\Delta T(G_c + G_p^{\,i-1}) \qquad (2.36) \\
-S_p^{\,i} + E_p^{\,i} &= -S_b + E_b + \Delta T(G_b + G_p^{\,i-1})
\end{aligned}
$$

the solution of which is

$$
\begin{aligned}
S_p^{\,i} &= \tfrac{1}{2}(D_a + D_c) - \tfrac{1}{2}\Delta T G_p^{\,i-1} \\
E_p^{\,i} &= \tfrac{1}{2}(D_a + D_c) + D_b + \tfrac{1}{2}\Delta T G_p^{\,i-1} \qquad (2.37) \\
V_p^{\,i} &= S_c + V_c - \tfrac{1}{2}\Delta T G_c
\end{aligned}
$$

where

$$
\begin{aligned}
D_a &= S_a - V_a - \tfrac{1}{2}\Delta T G_a \\
D_b &= -S_b + E_b + \Delta T G_b \qquad (2.38) \\
D_c &= S_c + V_c - \tfrac{1}{2}\Delta T G_c
\end{aligned}
$$

(b) Impact End Point

Since we are not involved with any reflections from the striker bar, we need only consider propagations along $dX = 0$ and $dX = -dT$ at the boundary $X = 0$. Thus, we will have only two equations available. We consider individually the solution for three possible boundary conditions.

pa

In

ci

thr

The

The

The e

soluti

These boundary conditions are described here for the impact end of the bar, according to the one-dimensional theory. In the solution presented in Art. 4.5(b), we will use the velocity boundary condition applied at the first gage station three inches from the impact end.

(i) <u>Velocity Boundary Condition:</u> $V(0,T) = V_o(t)$

The equations for this point are

$$S_p^{\,i} + V_p^{\,i} = D_c - \tfrac{1}{2}\Delta TG_p^{\,i-1}$$

$$-S_p^{\,i} + E_p^{\,i} = D_b + \Delta TG_p^{\,i-1} \qquad (2.39)$$

$$V_p = V_o$$

The solution here is

$$S_p^{\,i} = (D_c - V_o) - \tfrac{1}{2}\Delta TG_p^{\,i-1}$$

$$E_p^{\,i} = (D_c + D_b - V_o) + \tfrac{1}{2}\Delta TG_p^{\,i-1} \qquad (2.40)$$

$$V_p = V_o$$

(ii) <u>Stress Boundary Condition:</u> $S(0,T) = S_o(t)$

The equations for this boundary condition are

$$S_p + V_p^{\,i} = D_c - \tfrac{1}{2}\Delta TG_p^{\,i-1}$$

$$-S_p + E_p^{\,i} = D_b + \Delta TG_p^{\,i-1} \qquad (2.41)$$

$$S_p = S_o$$

solution of which yields

$$S_p = S_o$$

$$E_p^{\ i} = D_b + S_o + \Delta TG_p^{\ i-1} \qquad (2.42)$$

$$V_p^{\ i} = D_c - S_o - \tfrac{1}{2}\Delta TG_p^{\ i-1}$$

(iii) Strain Boundary Condition: $E(0,T) = E_1(t)$

This final boundary condition enables us to obtain the solution $S(0,T)$ for all T by solving Equation (2.27) which is now an ordinary differential equation for S in the independent variable T. For the complete solution, we write the equations

$$S_p^{\ i} + V_p^{\ i} = D_c - \tfrac{1}{2}\Delta TG_p^{\ i-1}$$

$$-S_p^{\ i} + E_p = D_b + \Delta TG_p^{\ i-1} \qquad (2.43)$$

$$E_p = E_1$$

whose solution is

$$S_p^{\ i} = (-D_b + E_1) - \Delta TG_p^{\ i-1}$$

$$E_p = E_1 \qquad (2.44)$$

$$V_p^{\ i} = (D_b + D_c - E_1) + \tfrac{1}{2}\Delta TG_p^{\ i-1}$$

(c) Plastic Wave Front

For an impact loading with a finite rise time, the conditions at the leading edge have already been described and transformed to

$$S = E - V$$

along

$$X = T - T_o = T - \frac{t_y}{k} \qquad .$$

where t_y is the time at which $\sigma = \sigma_y$ at $x = 0$.

A shock wave propagating along $X = T$ is treated by transforming Equations (2.28), (2.29) and (2.30) to obtain

$$\Delta S = -\Delta V \tag{2.45}$$

$$\Delta V = -\Delta E \tag{2.46}$$

$$\Delta S = \Delta E \tag{2.47}$$

Rewriting Equation (2.25)

$$-dT = \frac{dS - dV}{G} = \frac{2dS}{G}$$

we obtain

$$-\tfrac{1}{2}T = \int_{S(0,0)}^{S} \frac{ds}{G(s,s)} \tag{2.48}$$

along $X = T$ which is the transformation of Equation (2.31).

2.4 The Iteration Scheme

A system of equations

$$\left\{ f_k(x_1, x_2, \ldots, x_n) = 0 \right\} \qquad k = 1,2,\ldots,m \tag{2.49}$$

is called normal if $m = n$. If the system is reduced to the form

$$\left\{ x_j = \phi_j(x_1, x_2, \ldots, x_n) \right\} \qquad j = 1,2,\ldots,n \tag{2.50}$$

we can use the method of iteration to construct a series of solutions

$$x_j^{\,1},\ x_j^{\,2}, \ldots,\ x_j^{\,r}, \ldots$$

by means of the formula

$$\left\{ x_j^{\,i+1} = \phi_j(x_1^{\,i},\ x_2^{\,i}, \ldots, x_n^{\,i}) \right\} \qquad i = 1, 2, \ldots, r-1 \tag{2.51}$$

where, under certain conditions, the solution may be made as accurate as one pleases for sufficiently large r.

The iterative scheme for non-linear equations will always converge if the following two conditions are satisfied.[39]

1. Denoting the system solution as

$$\left\{ x_j \right\} = \left\{ \alpha_j \right\}$$

it is required that $\left\{ x_j^{\,i} \right\}$ be "close" to the solution with the degree of proximity determined by the functions $\left\{ \phi_j \right\}$.

2. The second condition, which is the only one required of linear systems, is associated with the Jacobian matrix of the system

$$J\left\{ x_j \right\} = \begin{bmatrix} \dfrac{\partial \phi_1}{\partial x_1} & \dfrac{\partial \phi_1}{\partial x_2} & \cdots\cdots & \dfrac{\partial \phi_1}{\partial x_n} \\ \dfrac{\partial \phi_2}{\partial x_1} & & & \vdots \\ \vdots & & & \\ \dfrac{\partial \phi_n}{\partial x_1} & \cdots\cdots & \cdots\cdots & \dfrac{\partial \phi_n}{\partial x_n} \end{bmatrix} \tag{2.52}$$

For a linear system the elements $\frac{\partial \phi_i}{\partial x_j}$ of the matrix are constants, whereas for non-linear equations they will, in general, be functions of $x_1, x_2, \ldots, x_n$.

A necessary and sufficient condition (if the first condition is satisfied) for iterative convergence is that all the eigenvalues of the matrix J evaluated at $\{x_j\} = \{\alpha_j\}$ have moduli less than unity. This is a difficult condition to check. It can only be hoped that if the moduli of the eigenvalues of $J\{x_j^o\}$ are less than unity, the eigenvalues of $J\{\alpha_j\}$ will be likewise for $\{x_j^o\}$ sufficiently close to $\{\alpha_j\}$.

An alternative, less difficult, sufficient (but not necessary) condition for convergence of the iteration process is that the sum of the elements of every column or every row of the Jacobian matrix $J(\alpha_1, \alpha_2, \ldots, \alpha_n)$ be less than unity. Thus, at least one of the following two systems of inequalities must be satisfied.

$$\sum_{j=1}^{n} \left| \frac{\partial \phi_i}{\partial x_j} \right| < 1 \qquad (2.53)$$

or

$$\sum_{i=1}^{n} \left| \frac{\partial \phi_i}{\partial x_j} \right| < 1 \qquad (2.54)$$

for

$$\{x_j\} = \{\alpha_j\}$$

A second iterative scheme known as Seidel's method carries out the calculations according to

$$
\begin{aligned}
x_1^{i+1} &= \phi_1(x_1^{i}, x_2^{i}, \ldots, x_n^{i}) \\
x_2^{i+1} &= \phi_2(x_1^{i+1}, x_2^{i}, \ldots, x_n^{i}) \\
\cdot \quad & \quad \cdot \\
\cdot \quad & \quad \cdot \\
\cdot \quad & \quad \cdot \\
x_n^{i+1} &= \phi_n(x_1^{i+1}, x_2^{i+1}, \ldots, x_{n-1}^{i+1}, x_n^{i})
\end{aligned}
\tag{2.55}
$$

using in each line those values of x_j^{i+1} which are available.

The conditions of convergence for Seidel's method are different from the previous iteration method, and hence, one scheme may converge while the other diverges for the same set of initial estimates. It is however known that when any of the inequalities of Equation (2.53) are satisfied, the speed of convergence in Seidel's method is more rapid than for conventional iteration.[39]

In the numerical solution Seidel's method was utilized and the grid mesh size was determined by the choice of ΔT. As ΔT appears in the terms $\frac{\partial \phi_i}{\partial x_j}$ it was chosen so that at least one of the two sets of inequalities (2.53) and (2.54) were satisfied. For any given flow law the required increment ΔT will decrease with increasing strain rate.

An additional aid to improving convergence was to incorporate a technique known as "Aitken's δ^2 - process."

This permits an improvement in the solution after five iterations better than that which would be obtained by the usual next iteration. The method is particularly suited where convergence is oscillatory or like that of a geometrical progression, which appeared to be the case for the problem under consideration.

The equations were programmed in Fortran for the CDC-3600 computer at the Michigan State University Computer Center. The program is described in the Appendix.

CHAPTER III

THE EXPERIMENT

3.1 General Description

An adaption of a commercial Hyge shock tester was used to apply a compressive impact load having a duration of approximately 560 microseconds to aluminum bars of half-inch diameter. Two independent series of tests were conducted. In the first series, transient surface particle velocity records were obtained at four stations along the plastically deforming specimen by means of electromagnetic transducers. In the second series, etched-foil strain gages were used to monitor surface strains at the four stations.

Ideally, the strain and velocity measurements should have been conducted simultaneously on each specimen. This was impossible since the magnetic field would have induced an error signal in the foil gages as they translated during the passage of the wave.

The basic system is shown schematically in Fig. (3.1). Both the transmitter and striker are made of 9/16 inch diameter steel drill rod. The Hyge shock tester is capable of accelerating its piston and a five pound mass to a maximum velocity of 1200 in/sec in a distance of about 12 inches. At this point the piston is decelerated to zero in an additional four inches, while the striker is free to travel in

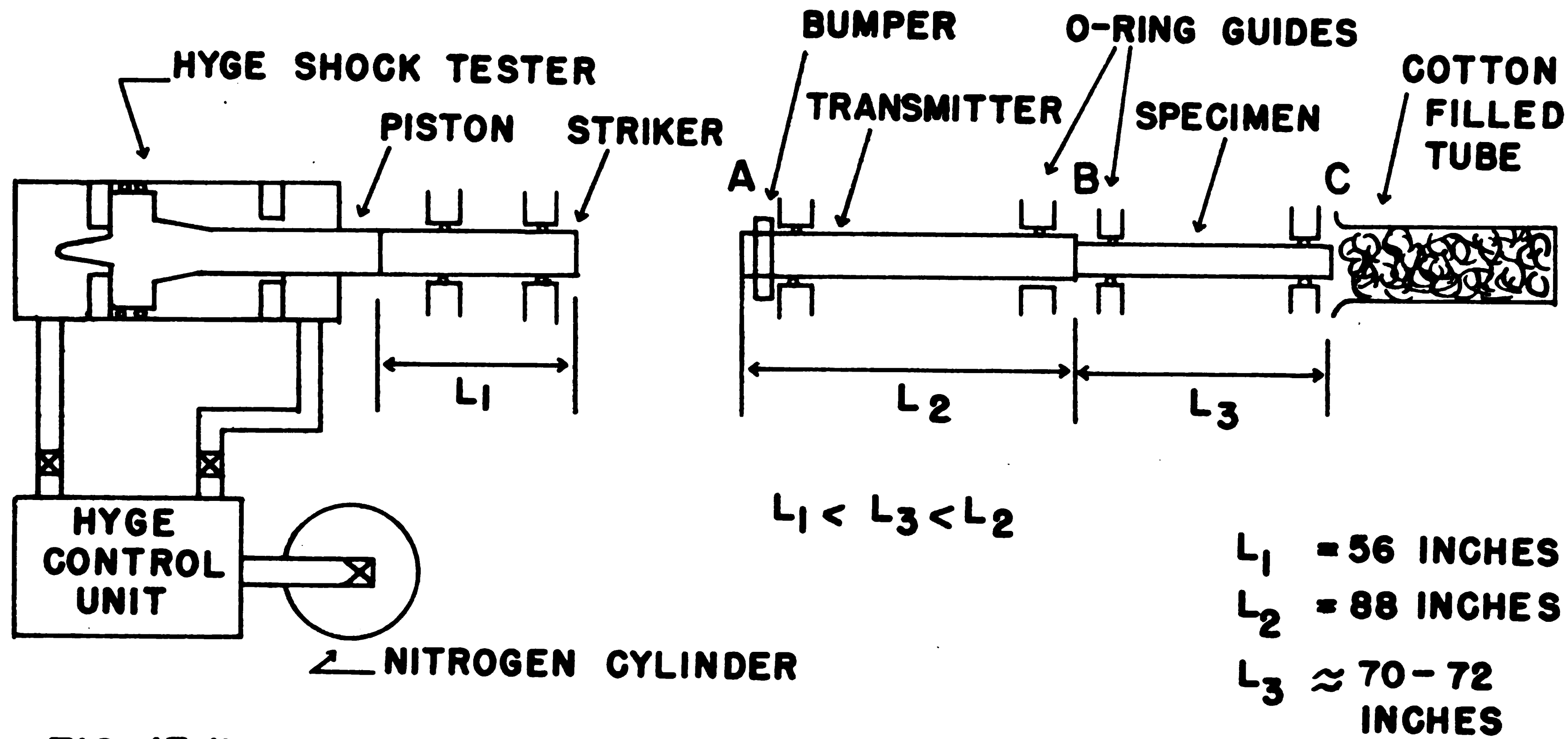

FIG (3.1) SCHEMATIC OF LOADING SET UP

it
tr
fr
sh
co
st
to
th
te
in
to
The
twi

the
mat
to
The
tens
retu
and
is s
late
wrap
from

its O-ring guides. When the striker makes contact with the transmitter bar AB, a compression wave is propagated outward from A to both the right and left. Since the striker is shorter in length than the transmitter, the bars remain in contact until the wave reflected from the left end of the striker returns to the interface. A wave normally incident to a free surface is reflected with a change in sign and hence the outgoing compression wave returns to the interface as a tension wave. Tension waves cannot be passed across the interface and hence the striker moves to the left with respect to the transmitter after the reflected tension wave arrives. The length of the compression wave transmitted is therefore twice the length of the striker bar.

We now turn our attention to the transmitter bar. When the wave front arrives at B, the acoustic and geometric mismatch will cause part of the pulse to be reflected and part to be transmitted as a compression wave into the specimen. The transmitter and specimen remain in contact until the tension wave reflected from the nearest free surface, C, returns to B. The specimen then begins moving to the right and is caught in the cotton filled tube. Sufficient energy is still trapped in the transmitter to cause it to also translate to the right, but the bumper, which is formed of a wrapping of plastic electrical insulating tape, prevents it from making a second contact with the specimen.

Friction in the O-ring guides and the spring action of the

int

3.2

110

of

lon

per

was

turn

face

650°

piec

dens

ing,

from

the u

well

3.3

I

the cotton decelerator bring the specimen to rest without introducing additional plastic strains.

3.2 Specimens

The specimens were all prepared from extruded Alcoa 1100 F aluminum (2S aluminum) bars with a nominal diameter of 0.5005 inches. Each bar was on the order of 58 inches long and had both faces turned to provide a flat surface perpendicular to the longitudinal axis. A one-inch piece was cut from each end of the bar before facing and this in turn was turned to a length of 1.000 $\pm$ .005 inches and also faced. Both bars and short specimens were then annealed at 650° F for one hour and furnace cooled.

Employing a chemical balance, several of the inch long pieces were weighed, first in air and then in water. The density of the aluminum was thereby found to be

$$\rho = 2.53\times10^{-4} \text{ lb sec/in}^4.$$

Static stress-strain curves were obtained, after annealing, from seven of the one-inch specimens. Four of them came from opposite ends of two specimens to serve as a check on the uniformity of material properties along each specimen as well as between specimens.

3.3 Velocity Transducer

It is well known that a current will flow in a conductor mo

Th

fi

wh

re

is

in

per

cov

as

are

wav

bee

vel

Earl

tran

the

bar.

tudi

Produ

where

moved through a magnetic field (for example, see reference 40). The relation between the voltage generated and the magnetic field is

$$e = -\int \overline{\beta} \cdot \overline{v} \times \overline{dL} \qquad (3.1)$$

where $\overline{\beta}$ is the magnetic field vector, $\overline{L}$ is the vector representation of length measured along the conductor and $\overline{v}$ is the velocity of the conductor with respect to the field.

Figs. (3.2) and (3.3) show a permanent horseshoe magnet in position about a bar so that the magnetic field is perpendicular to the longitudinal axis of the bar. Two Nyclad-covered strands of #30 copper wire are attached to the bar as indicated so that when the cross-section at which they are located has a velocity imparted to it by the passing stress wave, a current will flow in each. This method has previously been used by Ripperger and Yeakley[41] to detect particle velocities in aluminum bars subjected to short elastic pulses. Earlier efforts at developing a similar magnetic-inductive transducer were reported by Ramberg and Irwin.[42]

If the field is constant over the entire cross section, the effective length of the conductor is the diameter of the bar. Thus, $\overline{\beta}$, $\overline{L}$, and $\overline{v}$ are mutually perpendicular for longitudinal waves and Equation (3.1) reduces to the scalar product

$$e = \beta L v$$

where e is the potential difference between points B and E

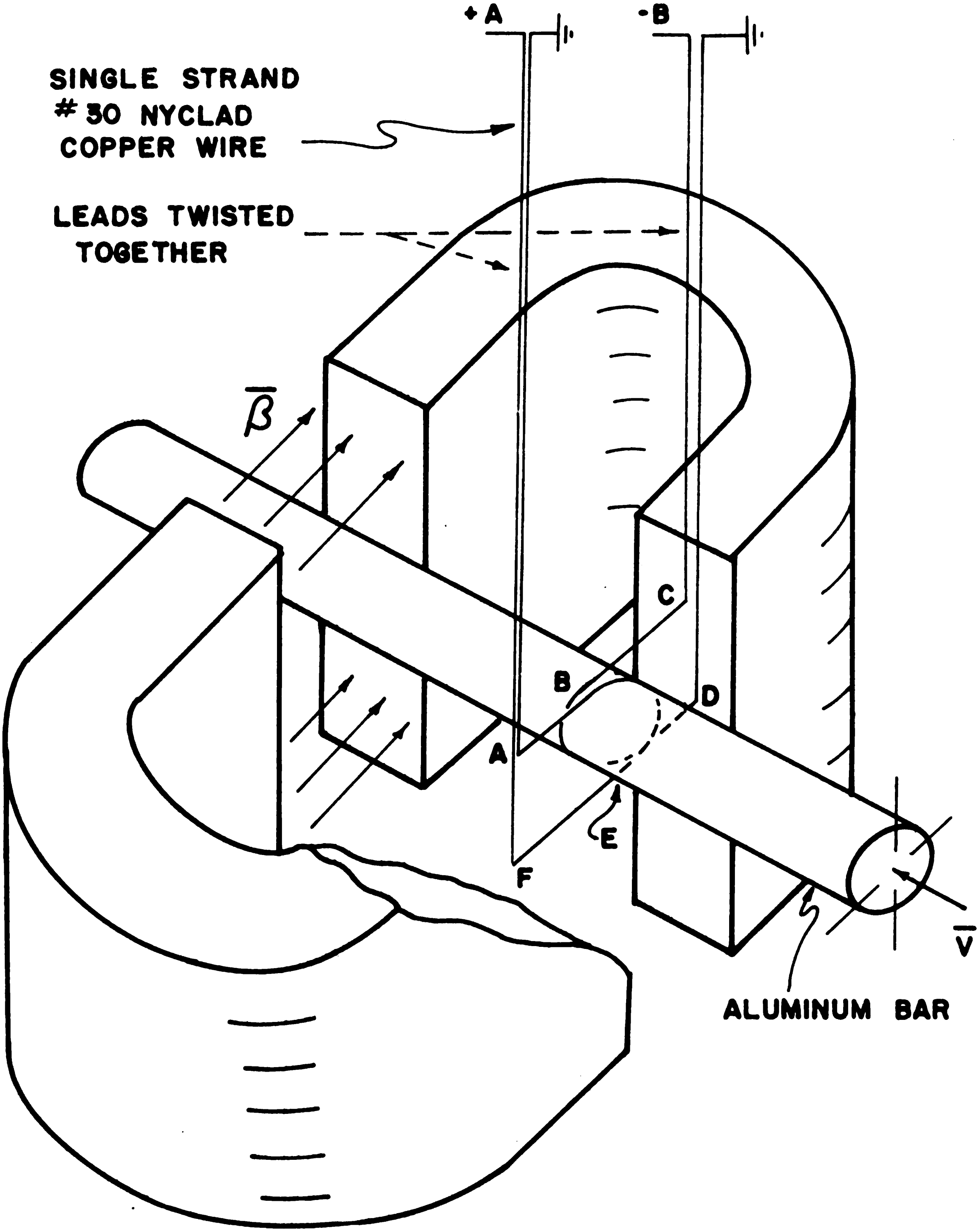

FIG (3.2) SCHEMATIC OF THE VELOCITY TRANSDUCER

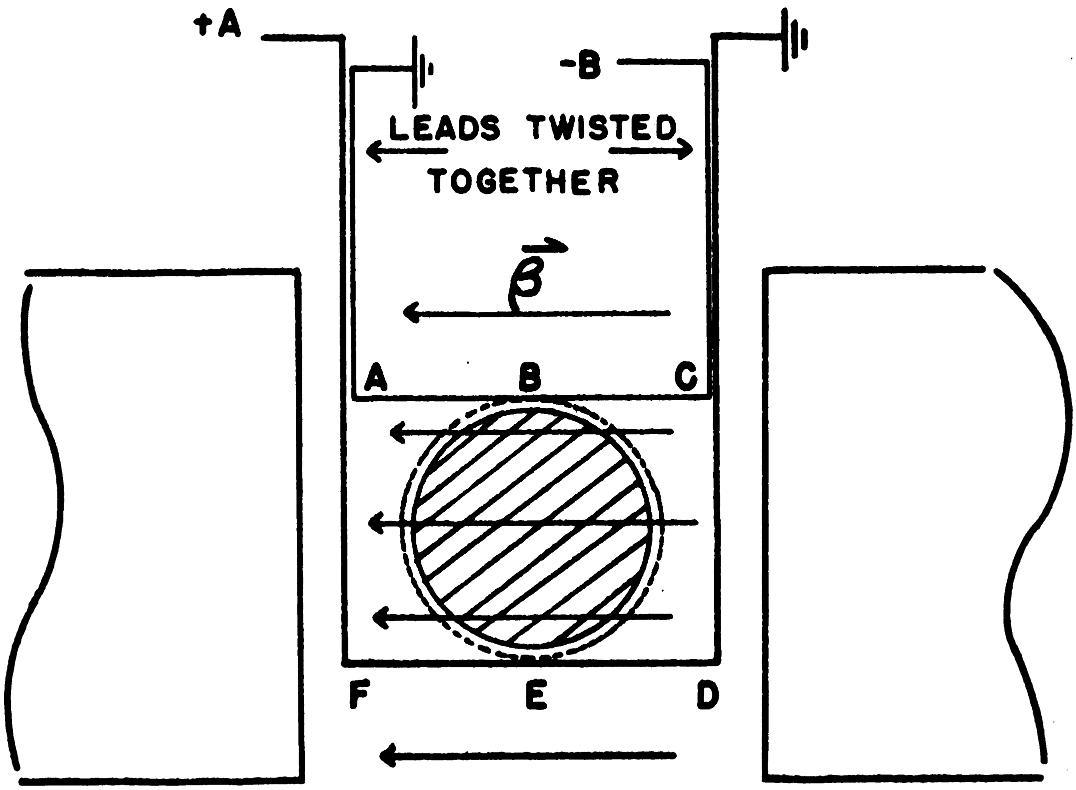

FIG (3.3) WIRE ARRANGEMENT AT GAGE SECTION in each wire for L = 2R. Thus, the induced voltage is directly proportional to the particle velocity.

Points A, C, D and F are rigidly fixed and hence, the four sections AB, BC, DE and EF can only rotate when the cross section translates. With these sections moving in horizontal planes, we find $\bar{\beta} \times \bar{L}$ perpendicular to $\bar{v}$ and hence their dot product vanishes and no contribution is made to the voltage generated in each loop. The sections AF and CD are rigidly cemented to a non-magnetic jig and hence do not move. Above points A and C the leads are twisted together so that any vibrations or motions will cause no additional signal to be generated. Two semi-circular loops of wire are used to eliminate any possible effects of bending in the bar.

The leads are connected as indicated in Figs. (3.2) and (3.3) to the input of a Tektronix D-Unit differential preamplifier, thus giving a two-fold increase in signal to

$$e = 2\beta dv \qquad (3.2)$$

where d is the diameter of the semi-circular loop of wire.

Four such measuring stations were set up using two sets of magnets from military-surplus magnetron tubes. Fig. (3.4) shows the gage arrangements and Figs. (3.5) and (3.6) are views of the physical set up.

3.4 Surface-Strain Transducer

Annealed constantan etched-foil resistance strain gages

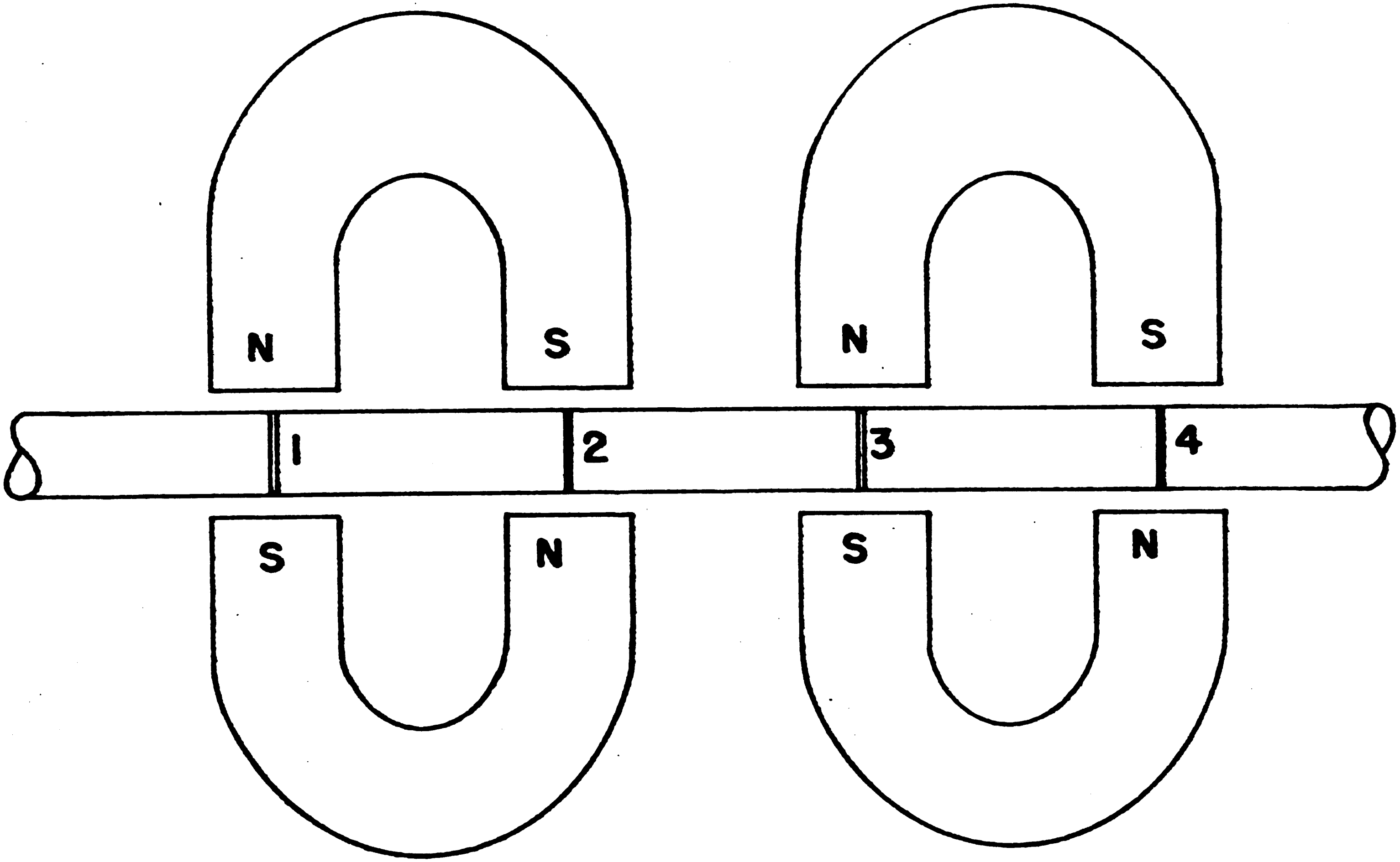

FIG (3.4) MAGNET ARRANGEMENT PROVIDING FOUR GAGE STATIONS

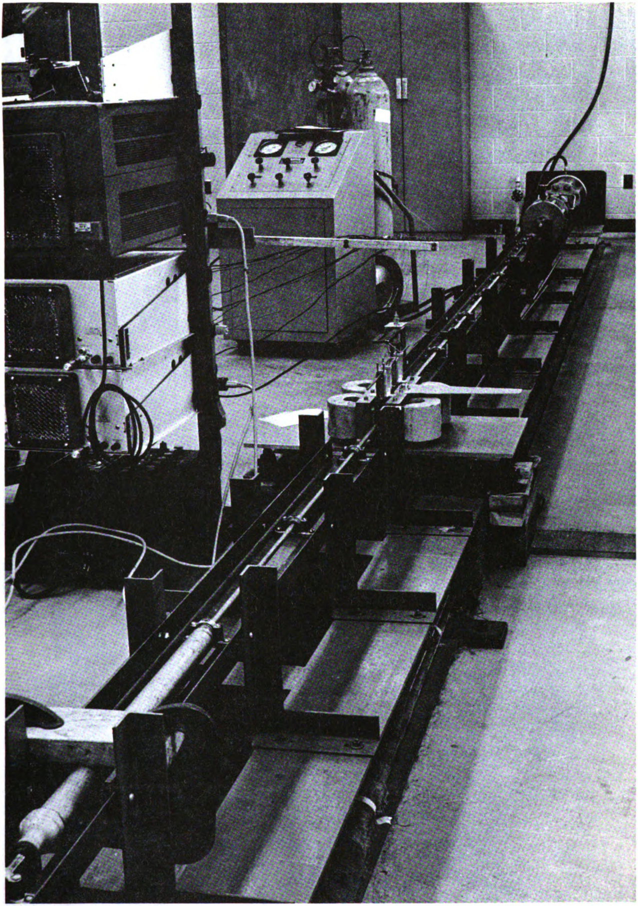

Fig. (3.5a) General View - Hyge and Test Set Up

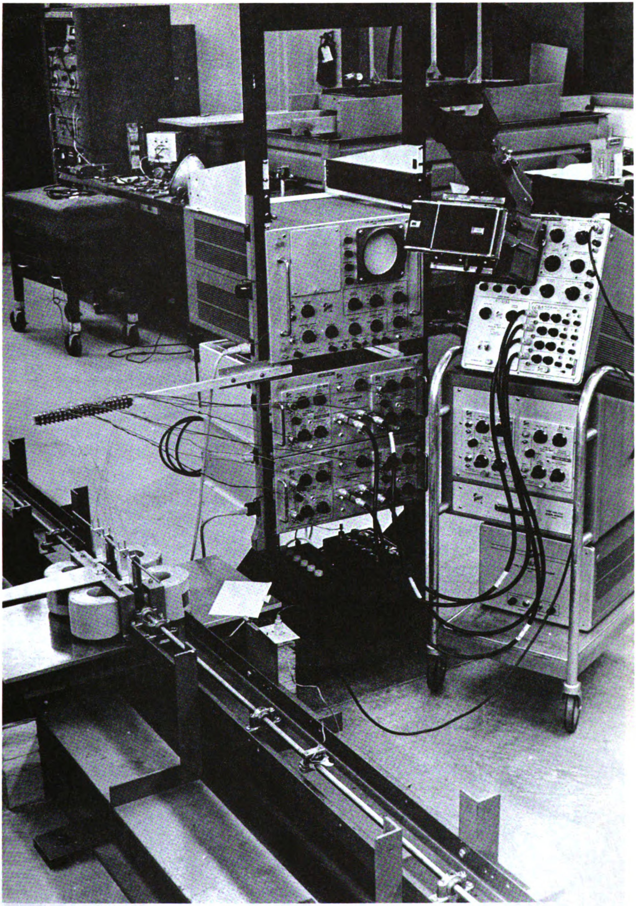

Fig. (3.5b) General View - Electronics and Recording Equipment

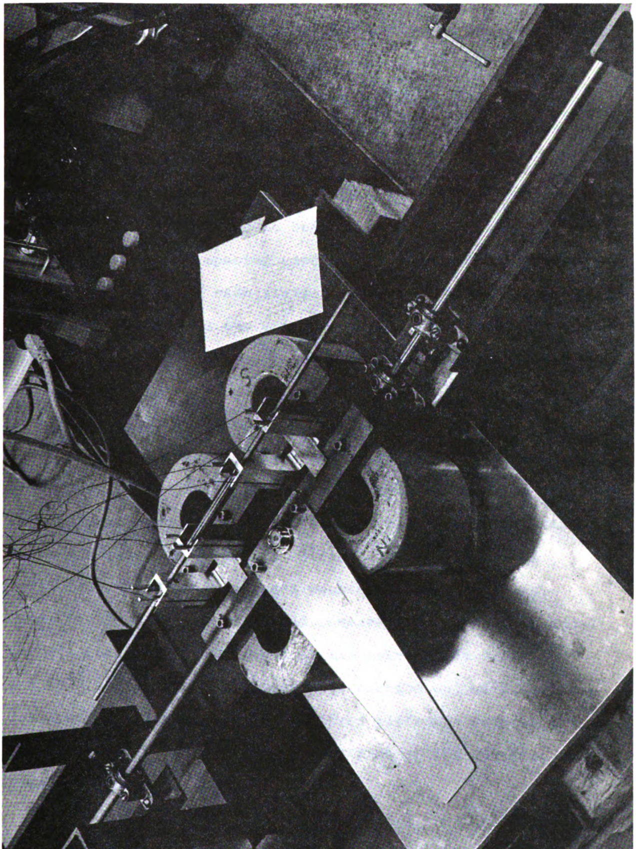

Fig. (3.6) Details - Velocity Transducer and Alignment Jig manufactured by Micro-Measurement, Inc. were selected for the dynamic tests. Type EP-03-125CA-120 gages having a length of 0.125 inch and width of 0.182 inch were chosen. Series EP gages are rated as accurate to 7% strain under static loading conditions. Dynamic strains on the order of 2-3% were anticipated.

The gages were mounted in pairs, diametrically opposed to cancel any effects due to bending, at four stations which corresponded to the spacing used in the velocity transducer tests. The gages at each station were connected in series and then installed as one arm of a Wheatstone bridge. Fig. (3.7) is a schematic of the strain gage bridge set up.

3.5 Static Test Procedure

The one-inch samples were subjected to compressive loading in an Instron testing machine. Recording accuracy of the Instron load measuring system was calibrated at better than 1% in the range of interest. Strain was measured to 5% using etched-foil strain gages mounted on the specimens. Three combinations of gages and cements were used as an added check. Load was applied at a strain rate on the order of 4×10^{-5} in/in/sec. Two tests were carried out with continuous loading while two others involved alternate loading and unloading as an aid in the determination of the apparent Young's modulus of the material.

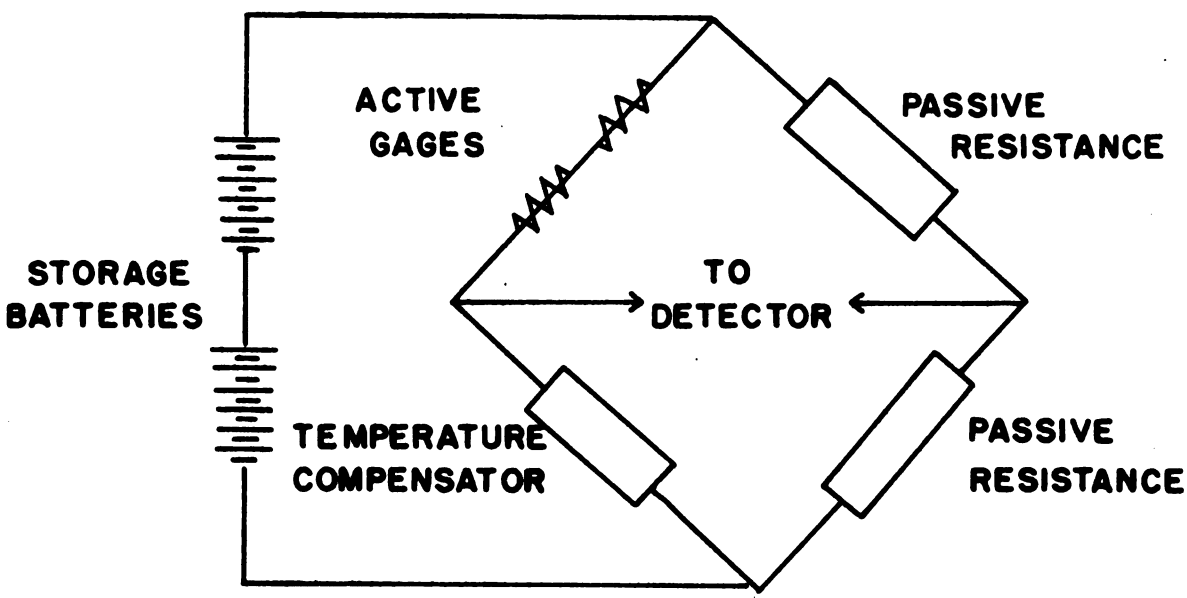

FIG (3.7) SCHEMATIC OF STRAIN GAGE BRIDGE

The test combinations are tabulated below.

Test	Parent Specimen	Micromeasurement Gage Type	Bonding Cement	Loading
1	11	EP-03-125AD-120	Eastman 910	continuous
2	11	EA-13-125AD-120	W.T. Bean RTC	alternate
3	13	EP-03-125AD-120	" " "	continuous
4	13	EA-13-125AD-120	" " "	alternate
5	5	EA-13-125AD-120	Eastman 910	continuous
6	7	EA-13-125AD-120	" "	"
7	8	EA-13-125AD-120	" "	"

Strain was read with a Baldwin Type-N static strain indicator. This instrument has a range of ± 3%. In order to use the N unit over a range from zero to minus five percent strain, the device illustrated in Figs. (3.8) and (3.9) was used.

The linearly tapered cantilever beam within the channel is made of beryllium copper which, after machining, was heat treated to a Rockwell hardness of C-43. This indicated a proportional limit on the order of 75,000 psi and a yield strength of well over 100,000 psi. Ultimate strength is about 175,000 psi. Young's modulus is 15 x 10^6 psi.

Due to the taper, the maximum bending stress in the beam, when loaded by the screw, occurs at a point two inches to the right of the support. With the beam loaded as shown

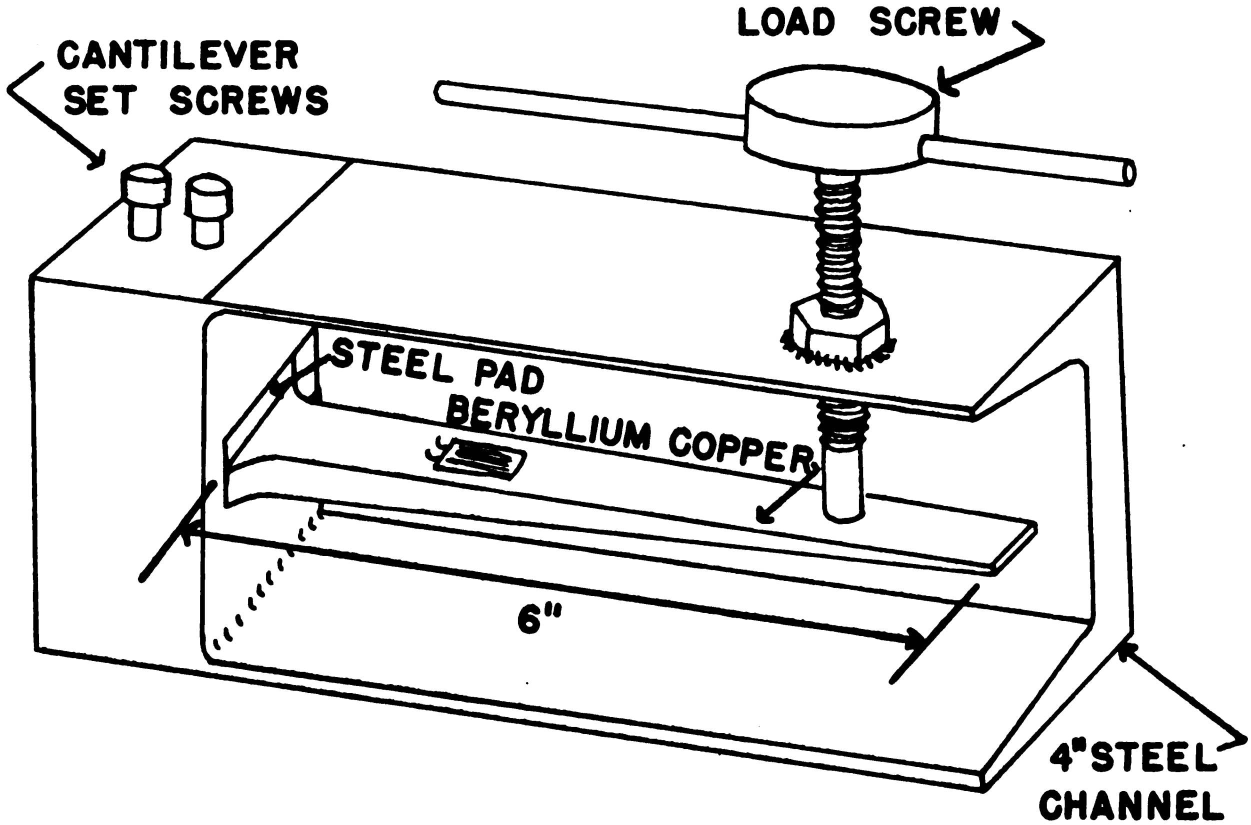

FIG (3.8) RANGE EXTENDER- UNLOADED

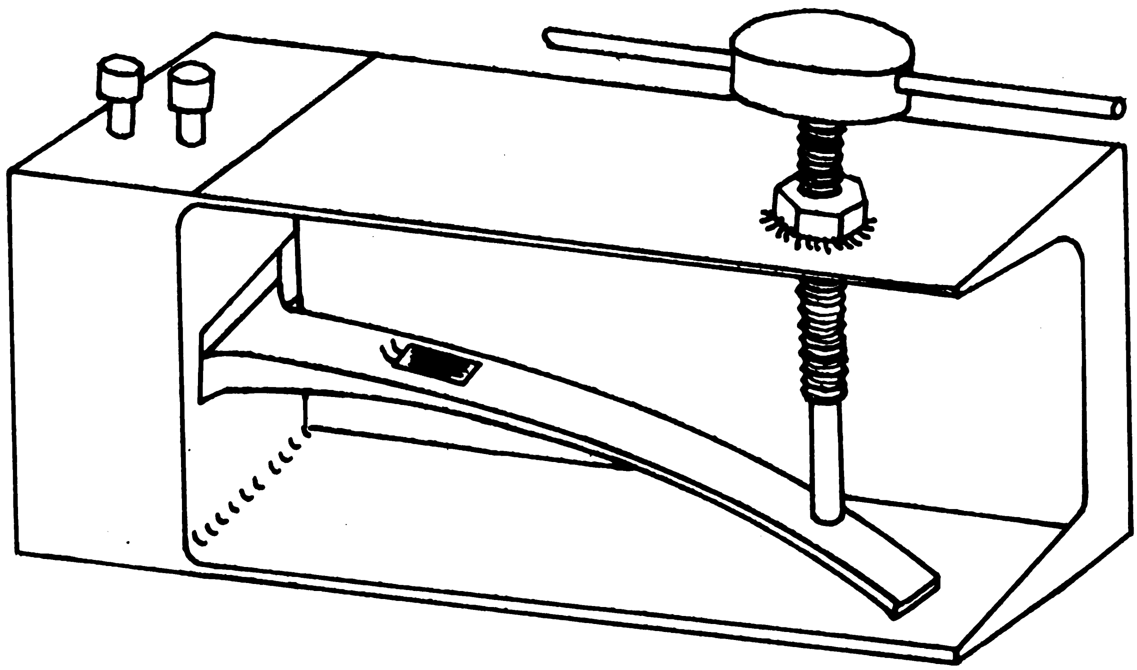

FIG (3.9) RANGE EXTENDER-LOADED

in Fig. (3.9), foil gages were mounted to both the upper and lower surfaces of the beam at the critical cross section. After appropriate curing of the bonding agent, the load was removed and the gages successively coated with Gagekote 1, 2 and 5* to provide electrical moisture and mechanical protection respectively. The beam was then rotated 180 degrees about its longitudinal axis, replaced in the fixture, and reloaded.

The type N unit indicated a total of about 21,000 microstrain for the sum of the magnitudes of strains on the two surfaces. Stability was excellent. Switching to four external arm operation, the fixture gages were used for one-half of the bridge. The one-inch sample specimen with its two 120 ohm diametrically opposed gages connected in series and an appropriate temperature compensator completed the circuit as illustrated in Fig. (3.10).

With no load on the Instron, the fixture was adjusted to permit the N unit to be balanced at a reading of +32,000 microstrain. As the Instron loaded the specimen, the continuous load curve traced by the machine was marked at predetermined increments of strain and a load-versus-strain record obtained until the N-unit indicated a reading of -18,000 microstrain. A stress-strain curve to 5% strain was thereby obtained.

---

*Supplied by W. T. Bean, Detroit, Michigan

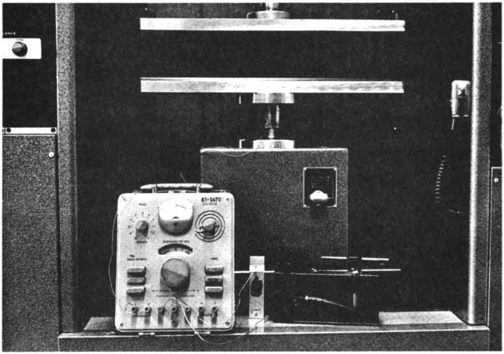

(a) Instron, specimen, temperature compensator, range extender and N-Unit

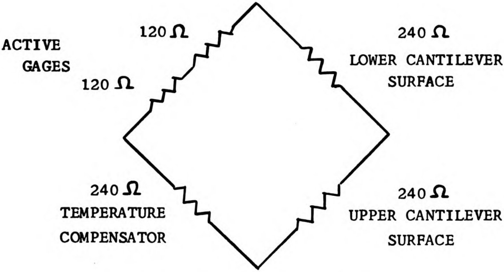

(b) Strain Gage Bridge Elements

Fig. (3.10) Details of the Static Stress-Strain Test Set Up

In order to check the linearity of the N-unit when using the cantilever fixture, the active gage was replaced by a second temperature compensator loaded elastically in bending. A balanced reading of +31,360 microstrain, i.e., a strain of 640 microstrain, was attained. The copper cantilever was then removed and the N-unit converted to two arm operation, balanced, and the reading recorded. The load was removed from the active gage and the N-unit balanced again. The change was found to be 640 microstrain which agreed with the previously obtained result. Changes in contact resistance were found to be negligible.

3.6 Velocity Transducer Calibration

Two pairs of magnetron magnets were rigidly mounted within magnesium spacers to an aluminum plate. Fig. (3.11) shows the general set up. The magnets were locked in place with the pole pieces aligned along parallel planes one inch apart.

The field mapping was done at the M.S.U. Cyclotron Laboratory. The system made use of a Rawson rotating-coil flux meter which was mounted on the cross-feed of a servo-controlled milling-machine carriage. A volume with a grid spacing of 0.1" was mapped within each pole gap.

The output of the flux meter is proportional to the magnetic field intensity. This signal was passed through a voltage-to-frequency converter and the frequency was then counted. As a count was finished, a coupler (built by the

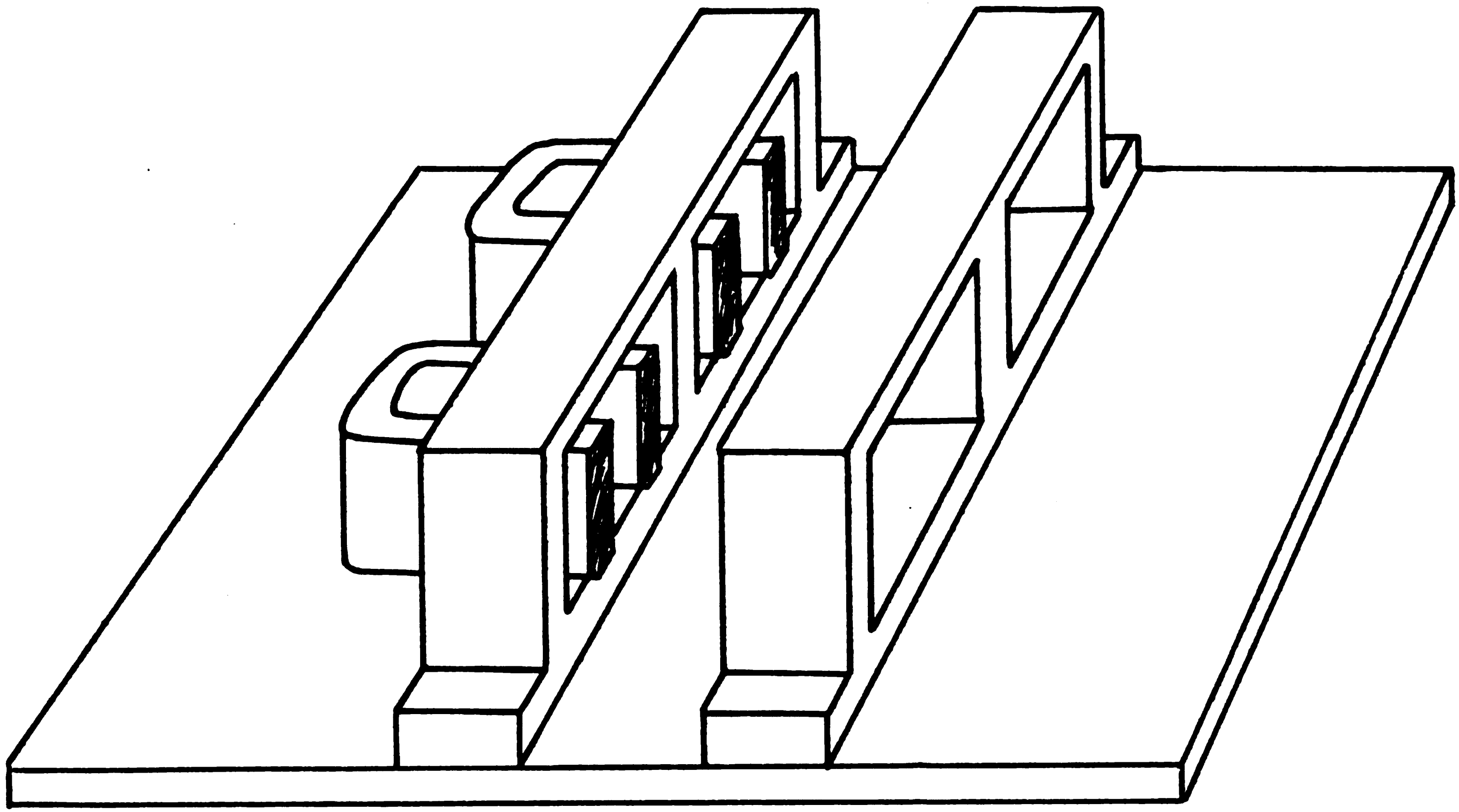

FIG (3.11) SCHEMATIC OF MAGNET SUPPORT FIXTURE

Cyclotron Lab) read the digital output of the frequency counter and the digits were then punched out by an IBM card punch.

Calibration of the system was performed by checking frequency counts against a bridge which can be used directly with the flux meter and a null galvonometer to obtain the flux density to the nearest gauss for the fields being mapped. The arrangement is described in Fig. (3.12).

The centers of the magnetic fields are shown in Fig. (3.13). If the wired cross sections on the specimen are located 0.1 inch forward of this point, a translation of 0.2 inch would result in a variation in the magnetic field through which the wire passes of less than 1%.

However, the field was not uniform across any section. Hence, the loop of wire was approximated by a circumscribed dodecagon and we have

$$e_o = \sum_{i=1}^{12} (\overline{\beta}_i \times \Delta\overline{L}_i) \cdot \overline{v} \tag{3.3}$$

where $\overline{\beta}_i$ is taken as the value of $\overline{\beta}$ at the midpoint of $\Delta\overline{L}_i$. Referring to Fig. (3.14) we have

$$\begin{aligned} e_o = \frac{\pi d}{12} [& (\beta_2 + \beta_6 + \beta_8 + \beta_{12})\cos 60^\circ \\ & + (\beta_3 + \beta_5 + \beta_9 + \beta_{11})\cos 30^\circ + \beta_4 + \beta_{10}]v \end{aligned} \tag{3.4}$$

The appropriate units are e_o in volts, β in webers/meter^2 (1 weber/m^2 = 10^4 gauss), ΔL (hence d) in meters.

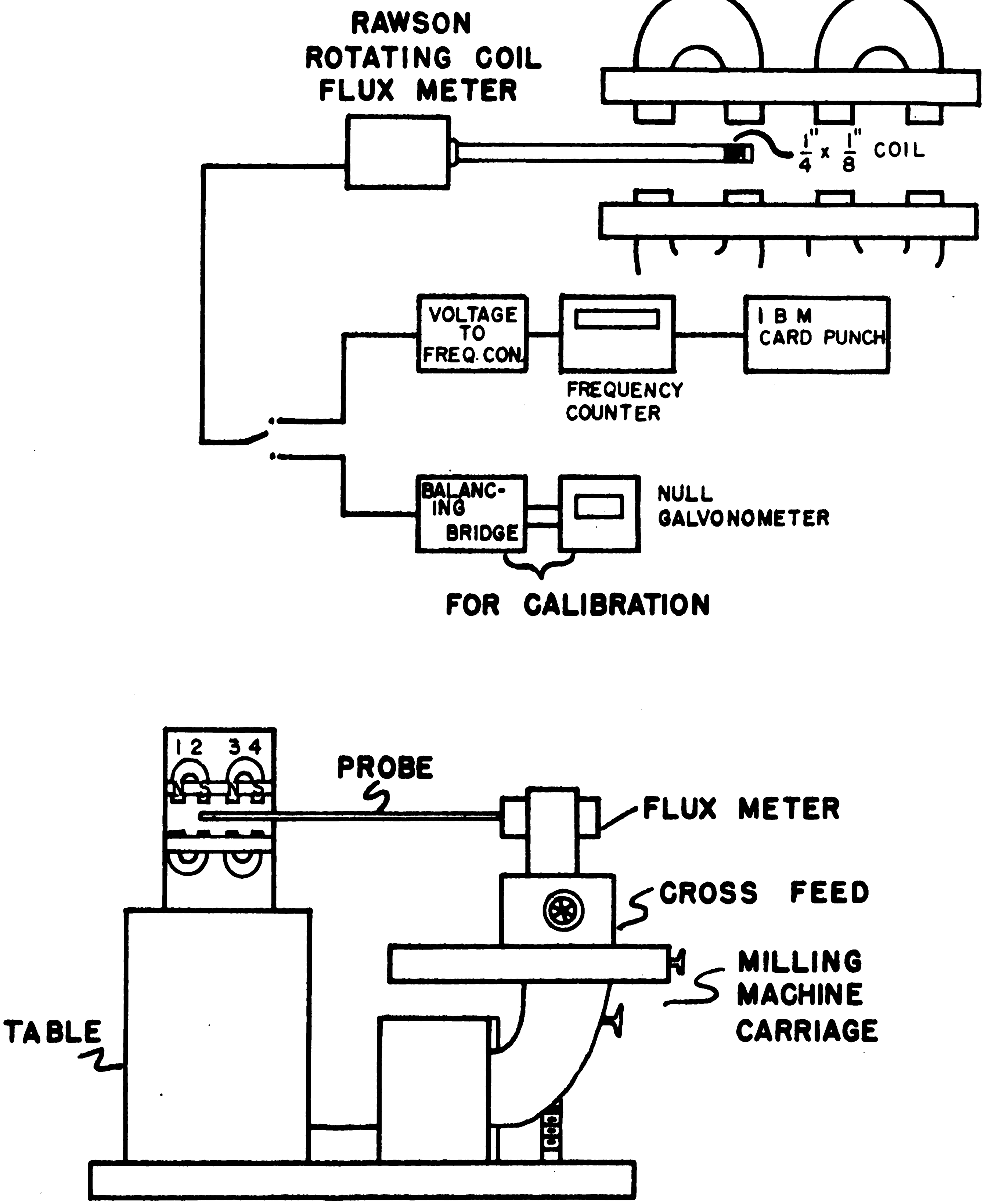

FIG (3.12) FIELD MAPPING SET UP

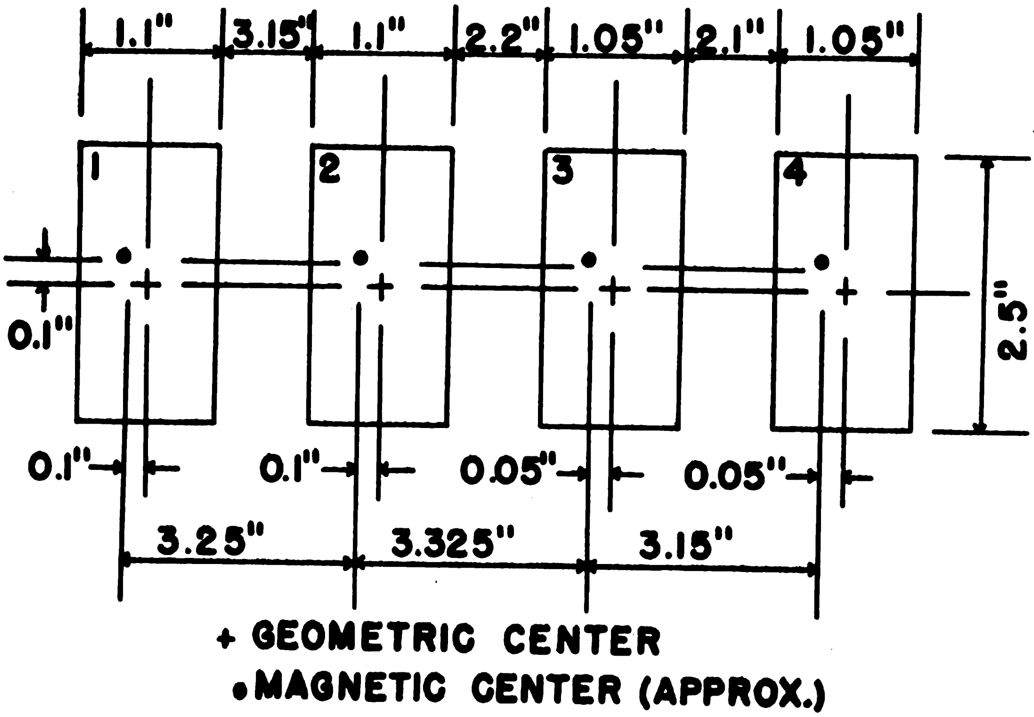

FIG (3.13) LOCATION OF MAGNETIC FIELD CENTERS

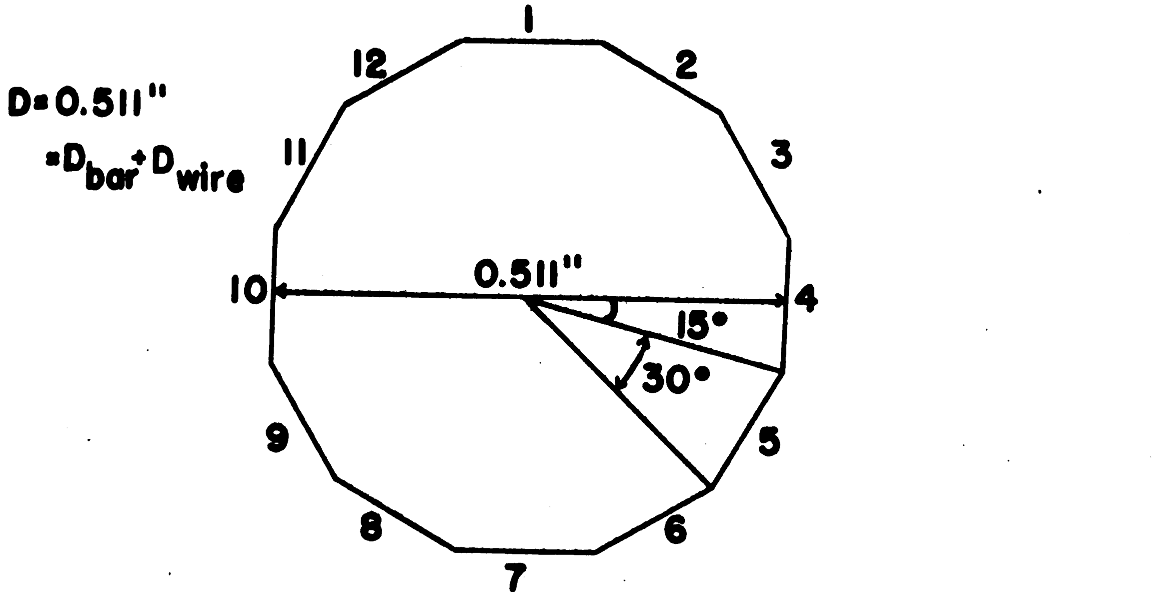

FIG (3.14) POLYGONAL APPROXIMATION OF WIRE LOOP

Equation (3.4) can be solved for v in the form

$$v = ke_o \qquad (3.5)$$

The following table gives the constants obtained for the four gage stations.

Station	x (in)	k (m/sec/ volt)	Max. Variation in 0.2 inch	β average (gauss)
1	3.000	118.6	-0.2 = -0.2%	3350
2	6.250	131.0	-0.6 = -0.5%	3250
3	9.575	138.8	-0.4 = -0.3%	2850
4	12.725	120.8	-0.4 = -0.4%	3275

Slight errors in either vertical or lateral placement of the wires would also result in variations in k on the order of less than 1%.

3.7 Velocity-Gage Tests

Circumferential scribe marks were made on the specimens at the appropriate intervals with the first mark three inches (six diameters) from the impact end. The wires were then bonded to the bar at the scribe marks using Armstrong C-4 epoxy cement with activator D. Curing was at room temperature for at least 36 hours. Heat from an incandescent lamp was used to aid curing during the first 12 hours. An aluminum jig served to maintain proper alignment during both cementing and testing. Special spacers which prevented lateral motion during cementing and moving were removed just prior to testing. In order to minimize the possibility of vibrations of the horizontal portions of the lead wires [see Figs. (3.2) and (3.3)] mass was added at these sections by applying a liberal coating of vaseline.

It was found that eddy currents were set up within the specimen in the region between the pole pieces during the passage of the stress wave. These currents modified the magnetic field so that when an uninstrumented aluminum bar was subjected to loading, a signal was detected in a free hanging loop of wire placed near it. No such signal was detected when a non-conducting polyethylene rod was substituted in place of the aluminum. The wave form generated was similar to that produced by a conventional magnetic pickup and is shown in Fig. (3.15). The maximum amplitude of the spikes was less than one-half millivolt and their presence was never detected on any of the records from instrumented specimens.

A series of tests were run in which particle velocities in the range 250 to 650 in/sec were obtained. The electronic circuitry and recording equipment used also monitored the strain gage tests and will be discussed later.

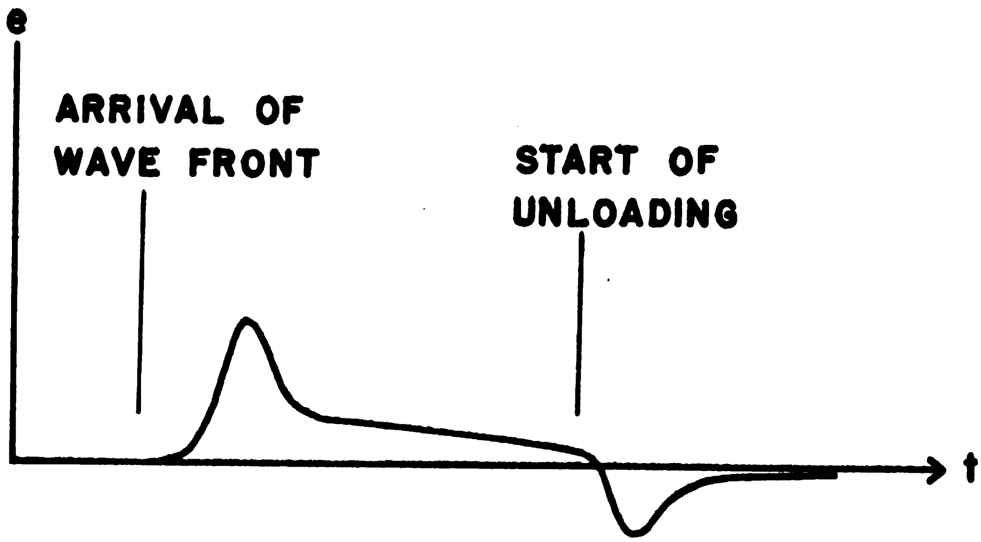

FIG (3.15) SCHEMATIC OF WAVE FORM PRODUCED BY EDDY CURRENTS

3.8 Strain Gage Tests

To increase the output of the strain gage bridge used in the dynamic tests, the passive half of the bridge consisted of 352-ohm resistors in the form of foil strain gages. The entire bridge was thus made relatively current insensitive. With two 120-ohm gages in series on the specimen and a 240-ohm temperature compensator, a 50% increase in output over a 240-ohm resistor bridge was attained. Two 12-volt storage batteries in series powered the bridge and kept power dissipation in the acceptable range for these gages.

The two 352-ohm gages for each station were mounted on opposite sides of 1/16-inch-thick strips of spring steel. These were mounted as cantilever beams in the fixture illustrated in Fig. (3.16). The beam was loaded until the bridge was nulled (possibly requiring a 180° rotation of the beam about its longitudinal axis). A sensitive center-zero galvonometer was used for this purpose.

The Baldwin Type-N static strain indicator was used to record the residual longitudinal strain by recording before and after balanced readings at each gage station.

A digital voltmeter was connected across the batteries to monitor voltage immediately prior to and after each test, but was not in the circuit during the test itself to prevent any possible noise in the system from this source.

A series of four tests were conducted in which the maximum dynamic strains varied over the range from about

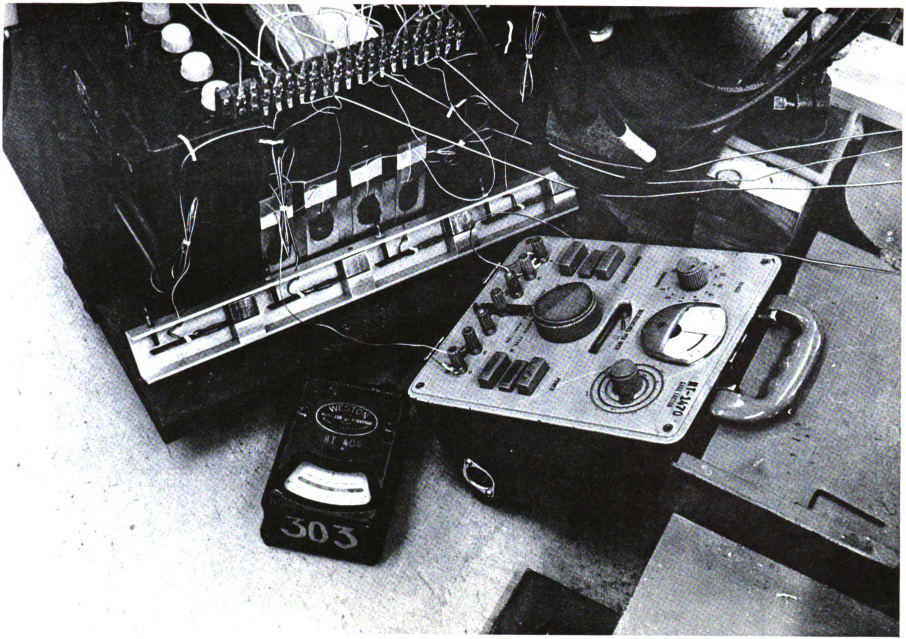

Fig. (3.16) Details - Dynamic Bridge Elements

0.5% to 1.0%. The first two were at the lower value, one using Eastman 910 and the second W. T. Bean RTC epoxy as bonding agents. No noticeable difference in response was noted. Eastman 910 was then used for the tests at higher strain levels because it simplified the specimen preparation. All gages were coated to provide electrical insulation and moisture and mechanical protection as in the static tests.

3.9 Electronics and Recording Equipment

Output from both the velocity and strain transducers was fed to Tektronix D-unit plug-in differential amplifiers in rack-mounted Tektronix 127 pre-amplifier power supplies. The frequency response ($\pm$3db) of the D-unit is 350kc at a gain of 100 and increases to 2mc at a gain of 2 when used with the 127 power supply with the push-pull output cables terminated in 170-ohms. Using single ended output reduced the signal gain by half. For all tests the D-unit was set at 20 mv/cm, and the single ended output resulted in a gain of $2\frac{1}{2}$.

The signal from each D-unit was then input to a Tektronix M-unit in a Tektronix Type 551 oscilloscope. The M-unit is an electronic switching unit which enables four signals to be displayed simultaneously on one beam of a scope. When all four channels are used in the chopped mode, the switching rate was found to be 960kc. This rate was found to be reliably constant and thereby provided a timing mark.

A Polaroid camera was used to make a permanent record of each test. After the graticule markings were photographed, the grid intensity was set to zero and the shutter locked open in the bulb position with the scope set on single sweep-external trigger. The trigger was provided by a barium titanate element clamped to the steel transmitter bar. The exact position was chosen so as to allow for any delay in the scope sweep mechanism.

The entire system was calibrated prior to each test using the internal square wave calibration signal in the scope. Several photos of square waves applied to each channel revealed that "eye error" was less than the rated ±3% calibration accuracy of the square wave.

CHAPTER IV

RESULTS

4.1 Static Stress-Strain Curves

Five of the one-inch sample specimens tested produced load-strain curves which varied by an amount on the order of the trace width of the Instron continuous pen recorder. These are shown as a single curve, the lower curve in Fig. (4.1). The two samples from parent specimen no.11 produced stress-strain curves which agreed with one another, but appeared to indicate a condition of work hardening when compared to the curve from the other specimens. This curve is shown as the upper curve in Fig. (4.1), but was ignored in the least squares curve fitting in obtaining $\sigma_o = f(\epsilon)$.

It should be noted that the slope of the upper curve is very nearly equal to that of the lower curve everywhere except for the region in the neighborhood of $\epsilon = 0.005$. Since the slope $\frac{d\sigma}{d\epsilon}$ will determine the speed of propagation of any level of strain in strain-rate independent theory, the speed predicted for most strain levels would still be about the same for both curves, according to the rate-independent theory. From the static tests involving alternate loading and unloading, Young's Modulus was found to be $E_o = 9.4 \times 10^6$ psi and hence, the specimens had a predicted elastic wave propagation speed of 1.93×10^5 in/sec.

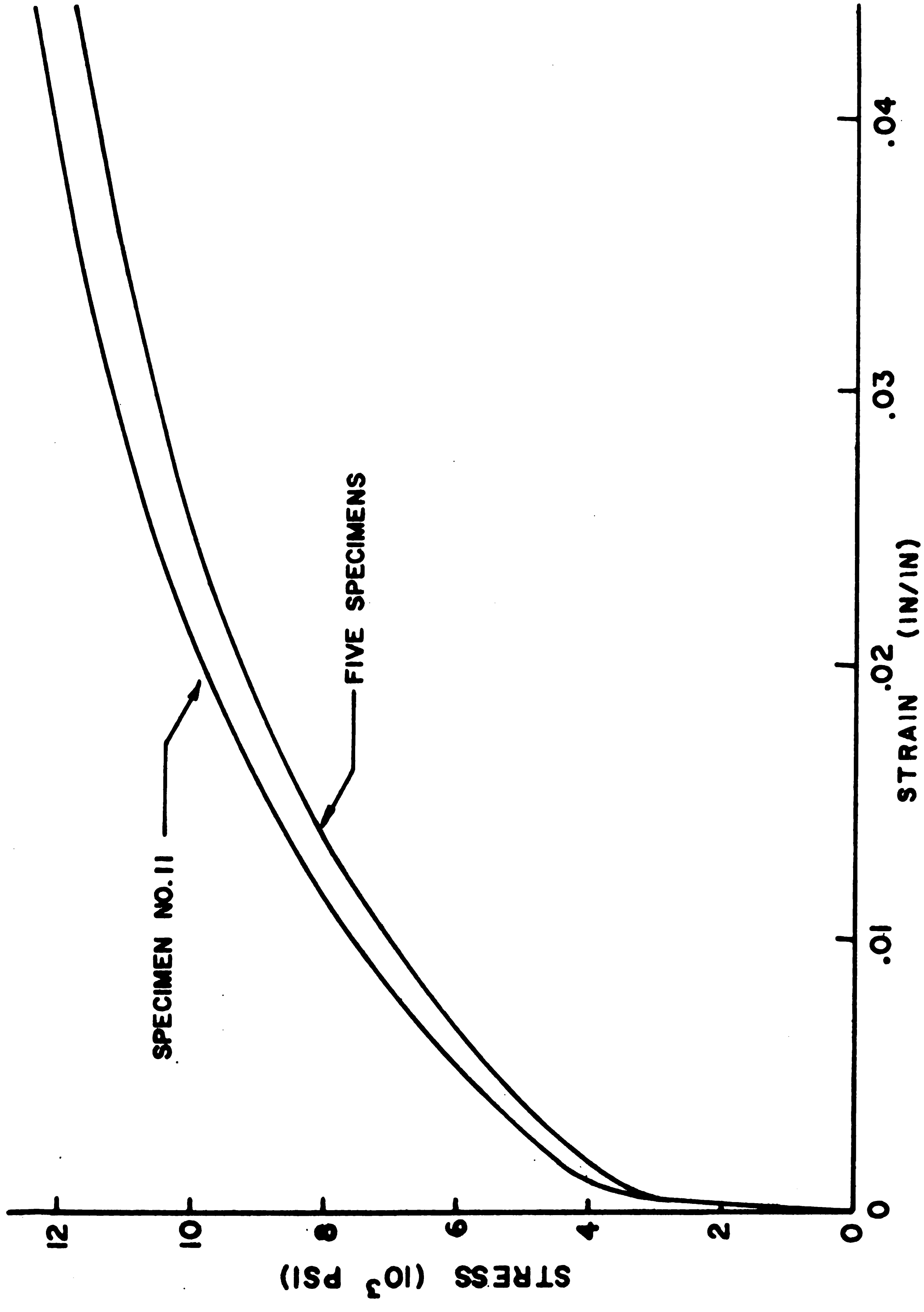

FIG (4.1) STATIC STRESS-STRAIN PROPERTIES (ALUMINUM 1100-O)

A best fit in the form

$$\sigma_o = f(\epsilon) = A\epsilon^B \qquad (4.1)$$

was obtained for the lower stress-strain curve data for strains up to two percent, as this is the range of the strains in all the dynamic tests. The resulting power law relation between stress and strain is

$$\sigma_o = 39{,}400\,\epsilon^{0.366} \qquad (4.2)$$

The fitted curve of Equation (4.2) is compared in Fig. (4.13) to the lower experimental static curve of Fig. (4.1). For strains in the range from yield to about $\epsilon = 0.001$ in/in, the fitted curve exhibits a steeper slope than the experimental curve, and therefore, the rate-independent theory based on this fitted curve will predict higher propagation speeds for these levels of strain than would be predicted with the actual experimental curve.

A second fit was made using only the data between $\epsilon = 0.005$ and $\epsilon = 0.02$. This gave the power law $\sigma_o = 29{,}400\,\epsilon^{0.311}$.

4.2 Velocity Test Results

The translation of the bar during the passage of the stress pulse resulted in strain in the horizontal elements AB, BC, DE and EF of Fig. (3.2) at each gage station. Translation of two tenths of an inch results in a 10% strain in these elements. The change in resistance of the copper wires for the time interval of interest was small with respect to the one Megohm input resistance of the D-unit.

Each specimen translated about one foot before being brought to a rest by the braking action of the cotton filled tube. The copper wires would invariably shear at the point where they enter the aluminum support jig. The epoxy bond appeared to hold up well except for occasional yielding at the points B or E indicated in Figs. (3.2) and (3.3).

Fig. (4.2) shows three typical oscilloscope trace records obtained with the velocity transducer. Fig. (4.2a) illustrates a test in which gage failure occurred after the sweep was completed. The gain for gage station one in the test was half of that for the other three channels, and each station has a different calibration factor due to differences in magnetic field strength. In Fig. (4.2b) we note slight disturbances occurring simultaneously at stations one and two and later at station three. The final trace record, Fig. (4.2c), illustrates transducer failure occurring first at the magnet forming stations one and two followed by failure at stations three and four. Failure occurs with catastrophic suddenness, and its onset is thus readily detectable.

The initial step, which propagates with no attenuation, is the leading elastic wave. This is then followed by the more slowly rising plastic stress wave. The reduced data in Fig. (4.3) for specimen No.7 shows that a nearly constant

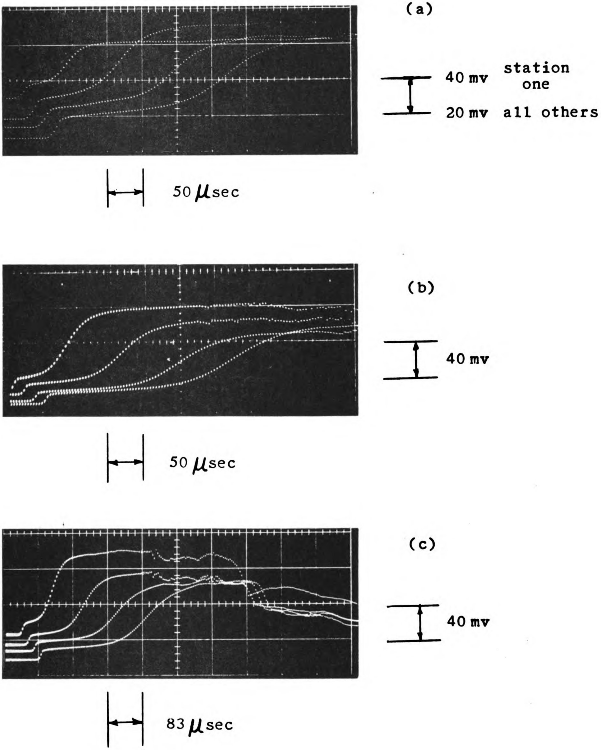

FIG. (4.2) TRACE RECORDS - PARTICLE VELOCITY TRANSDUCER (SWITCHING RATE 960 KC)

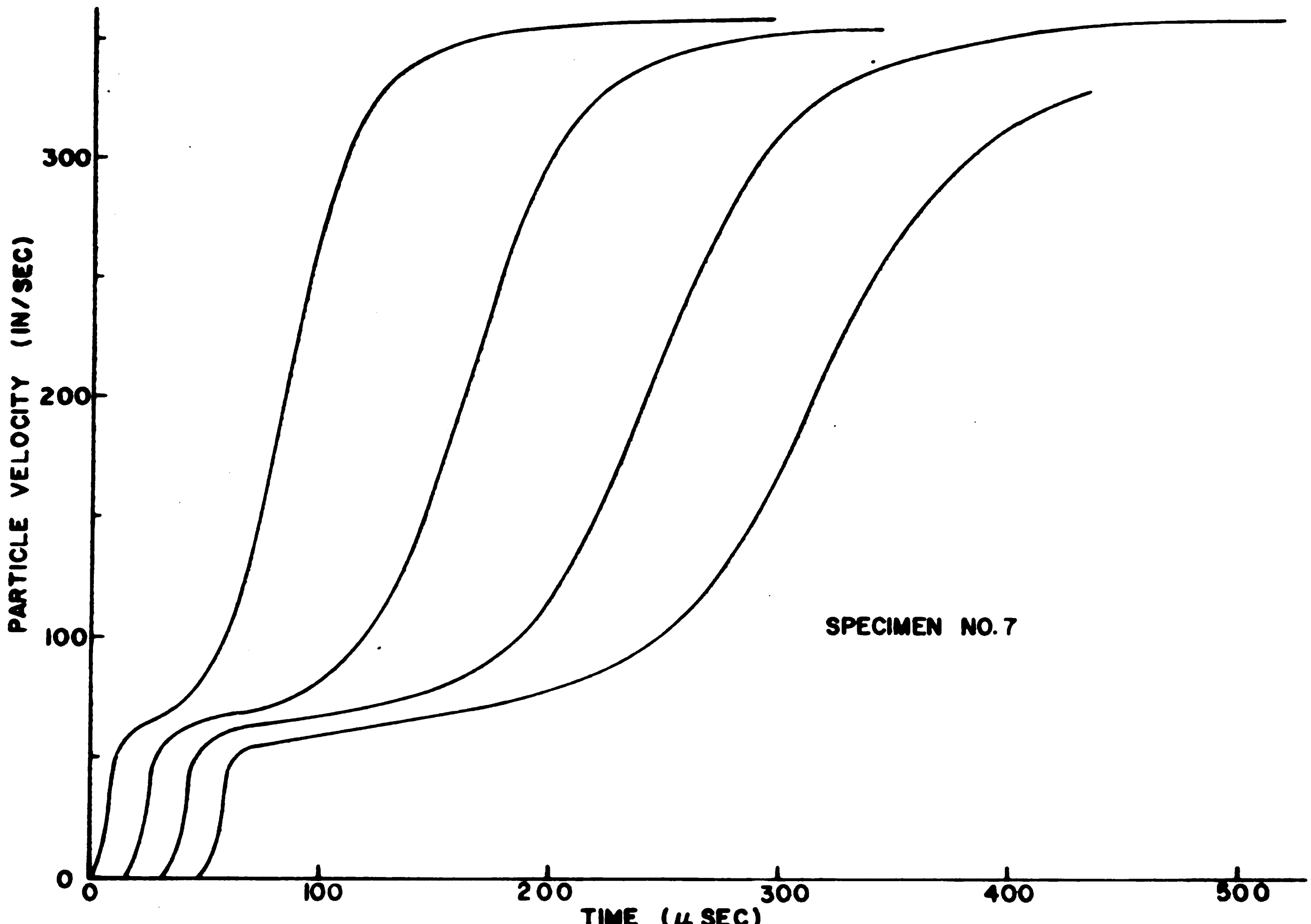

FIG (4.3) TYPICAL RECORD OF PARTICLE VELOCITY VS. TIME level of final velocity is reached, but in general, this value showed a slight decrease with increasing x. Station 4 did not appear to have reached equilibrium in any of the tests.

Negligible variation was noted in the speed of wave propagation for a given level of velocity on any single specimen. A larger variation was found between specimens. This scatter did not appear to be associated with the maximum velocity (and hence, strain rate) of the specimen as is shown in the table below.

Particle Velocity m/sec	Max. Variation in Wave Prop. Vel.		Number of Specimens
	Along Spec.	Between Spec.	
2	± 9.6%	± 8.5%	5*
3	± 2 %	± 7.5%	6
4	± 2.5%	± 5 %	6
5	± 1.5%	± 5.7%	6
6	± 2 %	± 2 %	4
7	± 2.5%	± 3 %	4
8	± 2.5%	± 4.7%	3

*The reading obtained from one specimen, in the region of the "knee," was discarded. The slope was small and hence, the errors in reading horizontal distances between traces was large.

No data is presented for particle velocities representative of the elastic range of the material, since a variation of ±1 microsecond (the approximate limit of trace readability) in horizontal distance between station records represents a variation of about ±8% in wave propagation speed.

The data for all these tests was averaged and the relation between c and v thus obtained is shown in Fig. (4.4). The elastic wave speed appears to be 196,500 in/sec giving $E_o = 9.77 \times 10^6$ psi for the apparent dynamic Young's Modulus. This is approximately four percent greater than the value, $E_o = 9.4 \times 10^6$ psi, determined from the static stress-strain records.

The vertical bars indicate the scatter in the experimental records. There was virtually no scatter for values of particle velocity up to about 50 in/sec. An examination of Fig. (4.3) shows that between particle velocities of 50 in/sec and 100 in/sec, the velocity versus time records exhibit a region in which we have an inflection point. This region of rapidly decreasing, then increasing, slopes increases in length at successive stations. Determination of wave propagation speeds here, for any level of particle velocity, is therefore subject to maximum error and this explains the greater scatter in this region.

This curve was examined in light of the von Karman theory by taking the derivative of Equation (2.1)

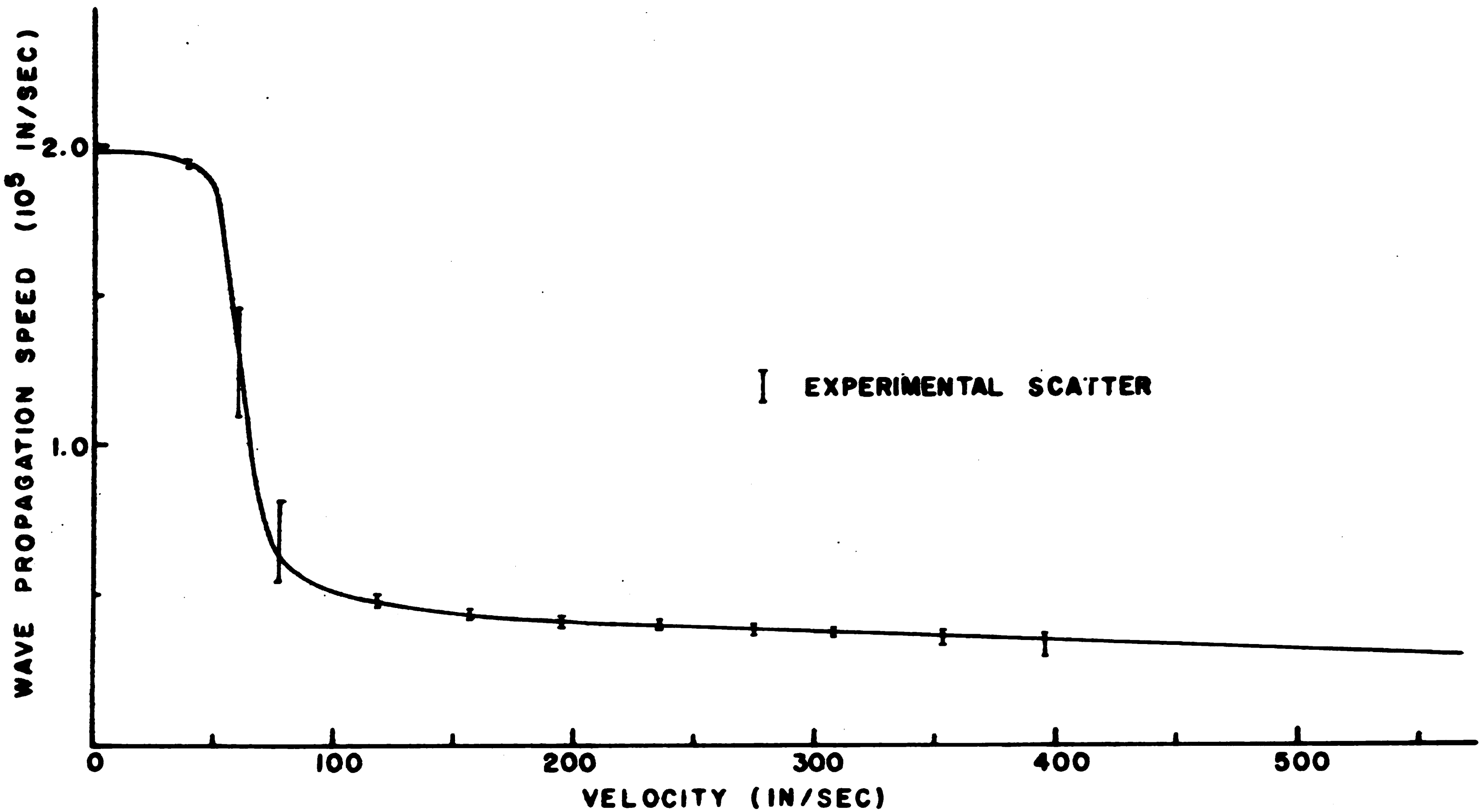

FIG (4.4) WAVE PROPAGATION SPEED VS PARTICLE VELOCITY (BASED ON AVERAGED DATA FROM SIX VELOCITY RECORDS)

$$v(\epsilon_0) = \int_0^{\epsilon_0} \sqrt{\frac{1}{\rho}\frac{d\sigma}{d\epsilon}}\, d\epsilon = \int_0^{\epsilon_0} c(\epsilon)\, d\epsilon \qquad (4.3)$$

in the form

$$\Delta\epsilon = \frac{\Delta v}{c(\epsilon)} = \sqrt{\frac{\rho}{\frac{d\sigma}{d\epsilon}}}\, \Delta v \qquad (4.4)$$

Thus, Fig. (4.5) of $\frac{d\sigma}{d\epsilon}$ versus ϵ was obtained. This curve was integrated with respect to ϵ and the resulting dynamic stress-strain curve is plotted in Fig. (4.6) with the previously obtained static stress strain curve.

In Fig. (4.7) the ϵ versus v curves are compared for

(1) von Karman theory based on the experimental static curve

and

(2) von Karman theory applied to work backward from the observed c versus v. This could be interpreted as based on von Karman theory using the single dynamic stress-strain curve of Fig. (4.6).

Comparison of the two shows that disagreement between them is slight. The single dynamic curve predicts propagation speeds in agreement with the averaged velocity test data, since it was in fact derived by working backward from the averaged velocity test data. The deviations of the measured propagation velocities in the individual tests from these averaged values did not appear to have any systematic

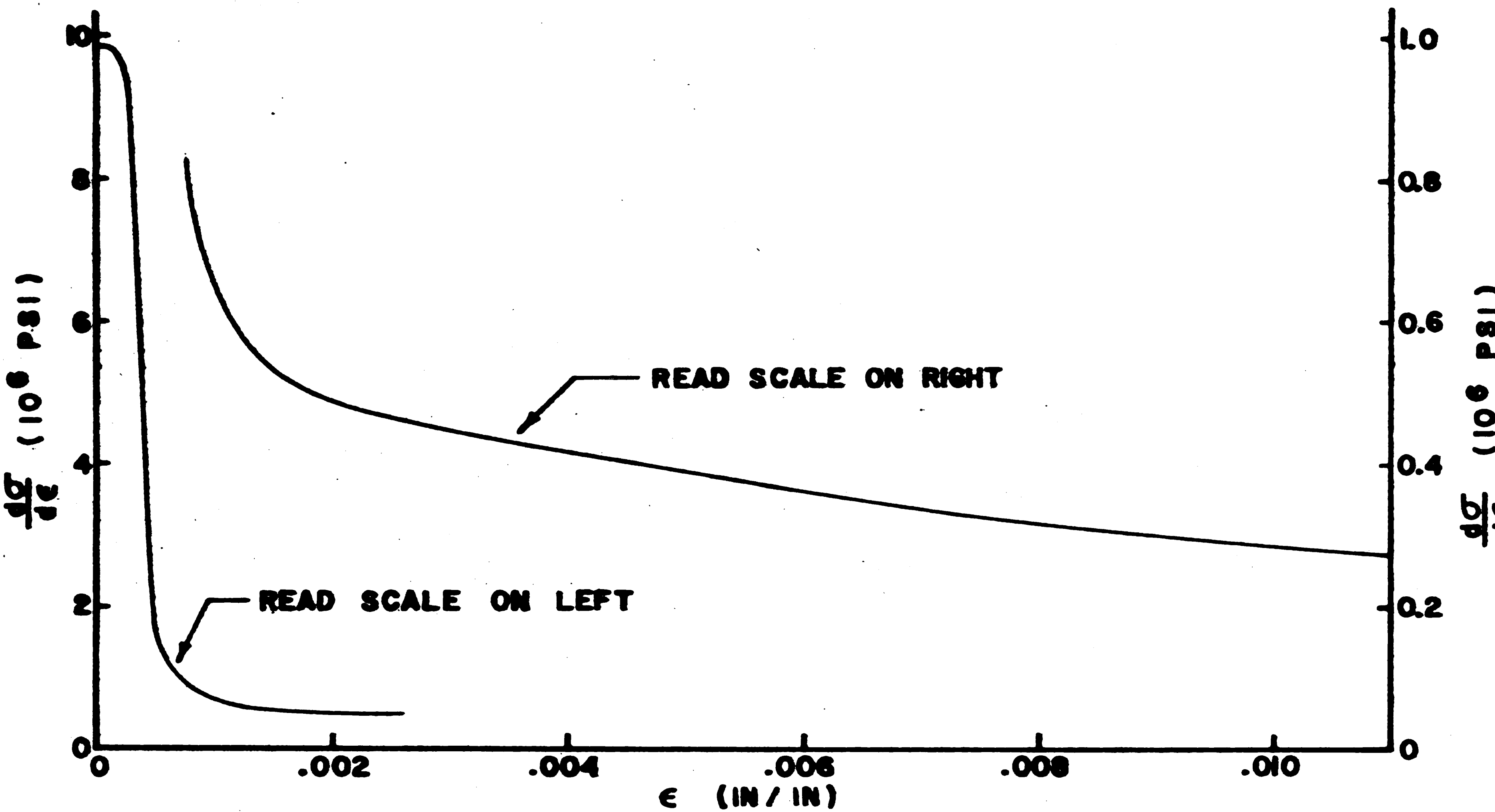

FIG (4.5) $\frac{d\sigma}{d\epsilon}$ VS ϵ [BASED ON VON KARMAN THEORY AND DATA OF FIG (4.4)]

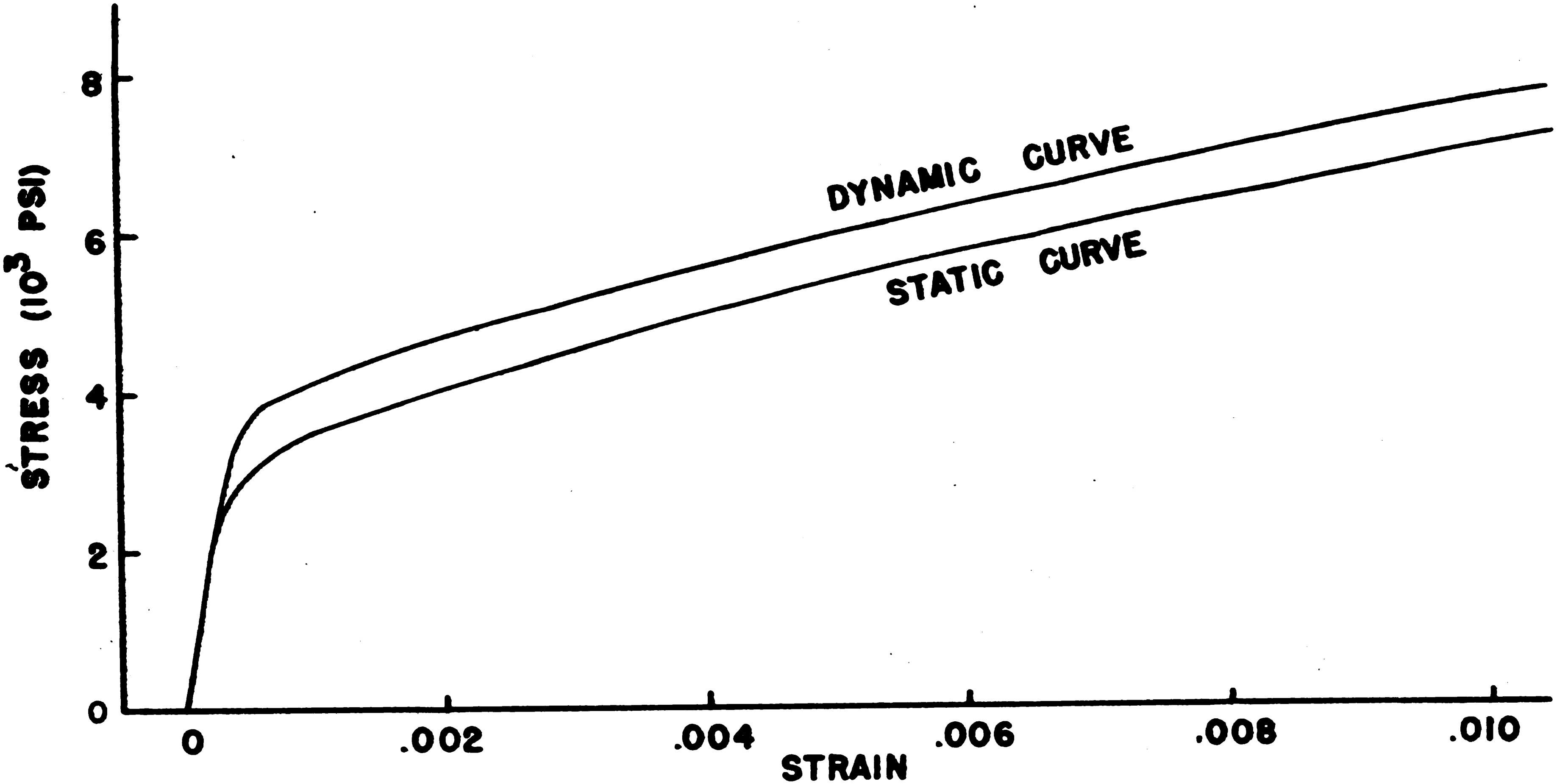

FIG (4.6) STATIC AND DYNAMIC STRESS - STRAIN CURVES (DYNAMIC CURVE BASED ON VON KARMAN THEORY AND VELOCITY TESTS)

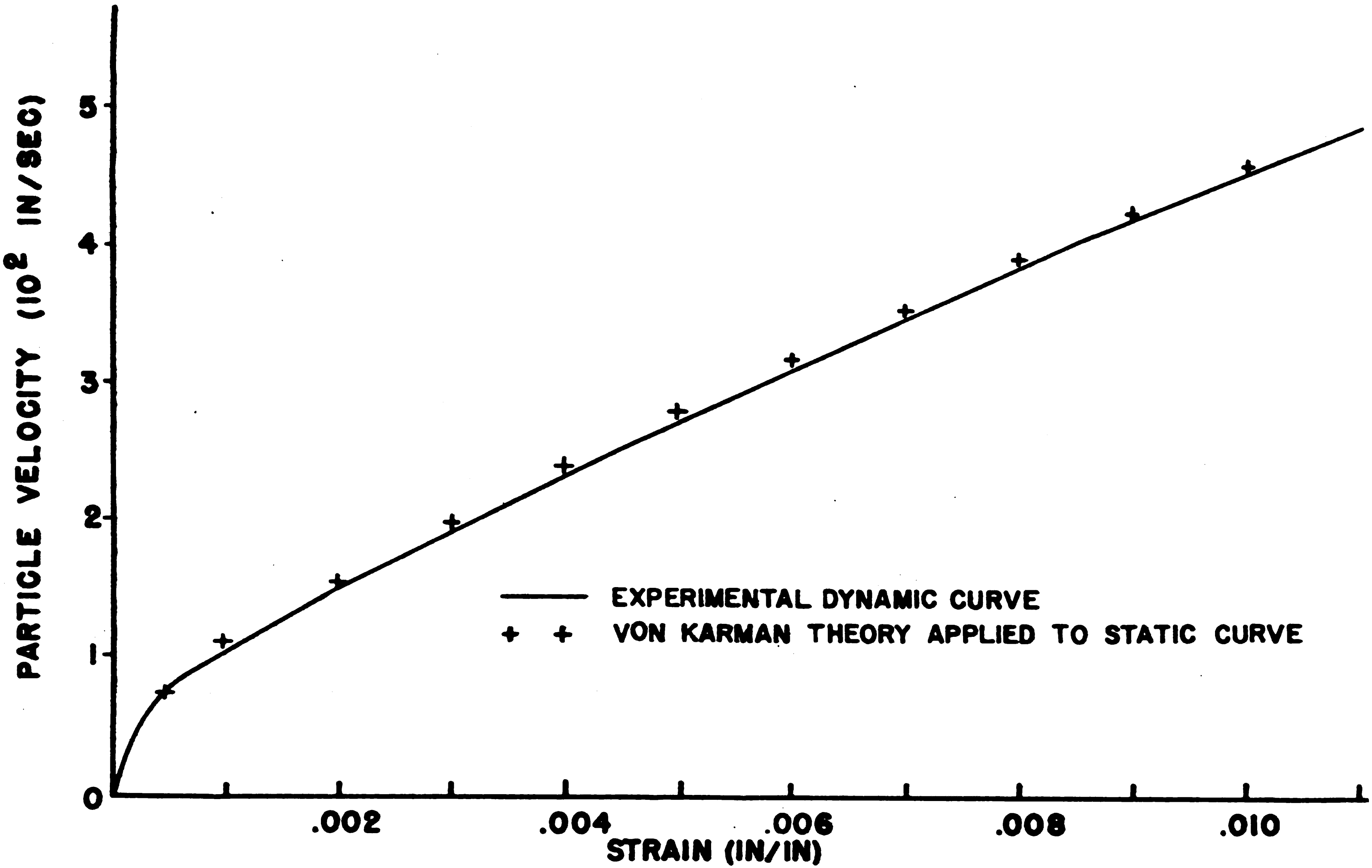

FIG (4.7) PARTICLE VELOCITY VS. STRAIN

relation to the strain rate levels, as was shown in the tabulated comparisons at the beginning of this section.

4.3 Surface Strain Results

Records from the four strain gage tests are shown in Fig. (4.8). We note the initial elastic wave followed by the more slowly rising plastic portion of the pulse. The final negative step in two of the trace records indicates the arrival of the unloading wave front. The records end before the reflection from the far end has yet reached station 4. At no gage station in any test did the strain appear to reach equilibrium. This condition is readily noticeable at station 4.

The residual strains in specimens 9 and 10, for which static measurements were made with the N-unit immediately prior to and after the dynamic tests, are tabulated on page 81 and compared with the final level of the transient record photo.

Post-test micrometer measurements of bar diameter indicated a plateau of residual strain extending from $x = 0$ to beyond the fourth gage station in all tests. The slight slope of the plateau indicated by the strain gage readings from specimens nos.9 and 10 was too small to be detected by this means. The bar then tapered until a point was reached which had no detectable residual strain. The lengths of the total region of residual strain and of the plateau were related to the magnitude of the impact loading.

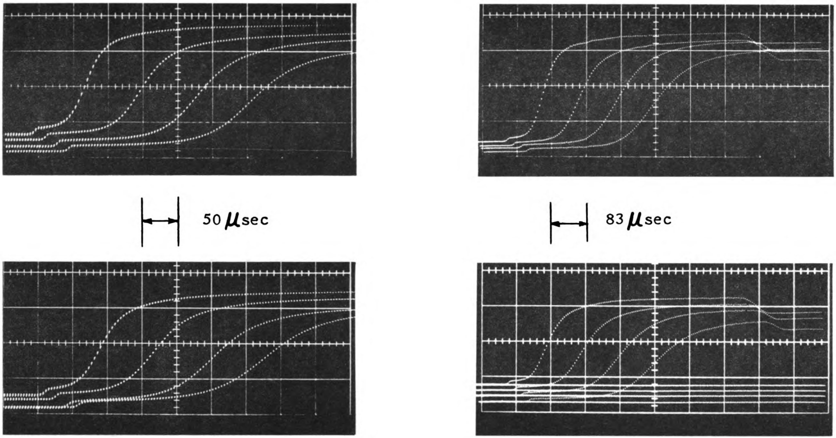

FIG. (4.8) TRACE RECORDS - ETCHED FOIL RESISTANCE STRAIN GAGES
(SWITCHING RATE - 960 KC)

Specimen		RESIDUAL MICROSTRAIN AT STATION 1	2	3	4
9	N-Unit	7110	6995	6830	6520
	Photo	7170	7080	6940	6760
10	N-Unit	8965	8725	8560	8245
	Photo	8950	8780	8710	8490

4.4 Discussion of Test Results

One feature of the test records on which some attention should be focused is the "knee" in the curve marking the transition from elastic to plastic wave propagation. All strain levels in the elastic range propagate at a single speed. Such a "knee" is not indicated in any of the results reported by Bell[26,27] using his diffraction grating technique on annealed aluminum bars. A comparison of my static stress-strain curve with that of Bell[27,43] for "dead-annealed" aluminum shows that his was relatively softer, and had a much lower yield point.

Wave propagation speeds for various levels of strain as found from the velocity and surface strain tests are compared to those predicted by the rate-independent theory from the static stress-strain relation in Fig. (4.9). The curve for the velocity tests is obtained from Fig. (4.5) and the relation $c = \sqrt{\frac{d\sigma}{d\epsilon}/\rho}$. This is equivalent to using the single dynamic curve of Fig. (4.6), and shows that the single dynamic curve predicts that strains below about $\epsilon = 0.0055$ have higher propagation speeds than predicted with the static curve, while strains above $\epsilon = 0.0055$ have lower propagation speeds.

It is readily seen that the foil gages indicated markedly lower propagation speeds than the velocity transducer at all levels of plastic strain. It should, however, be noted that the rise time of the strain pulse was fairly constant for all tests, and hence, the maximum strain and the strain rate at any gage section varied proportionately. The average e strain rates for the four foil gage tests are approximately in the ratio 3.5:4:6:9. The apparent lag in the strain record at any propagation speed for a constant rise time pulse appears to be inversely related to the strain rate. This does not appear to agree with Bell's observations[31] (see Art. 1.2) that the lag in resistance strain gage records is proportional to strain rate. Again noting that rise times of the strain pulse in all tests are fairly constant and that records of residual strain from the trace records and static N-Unit

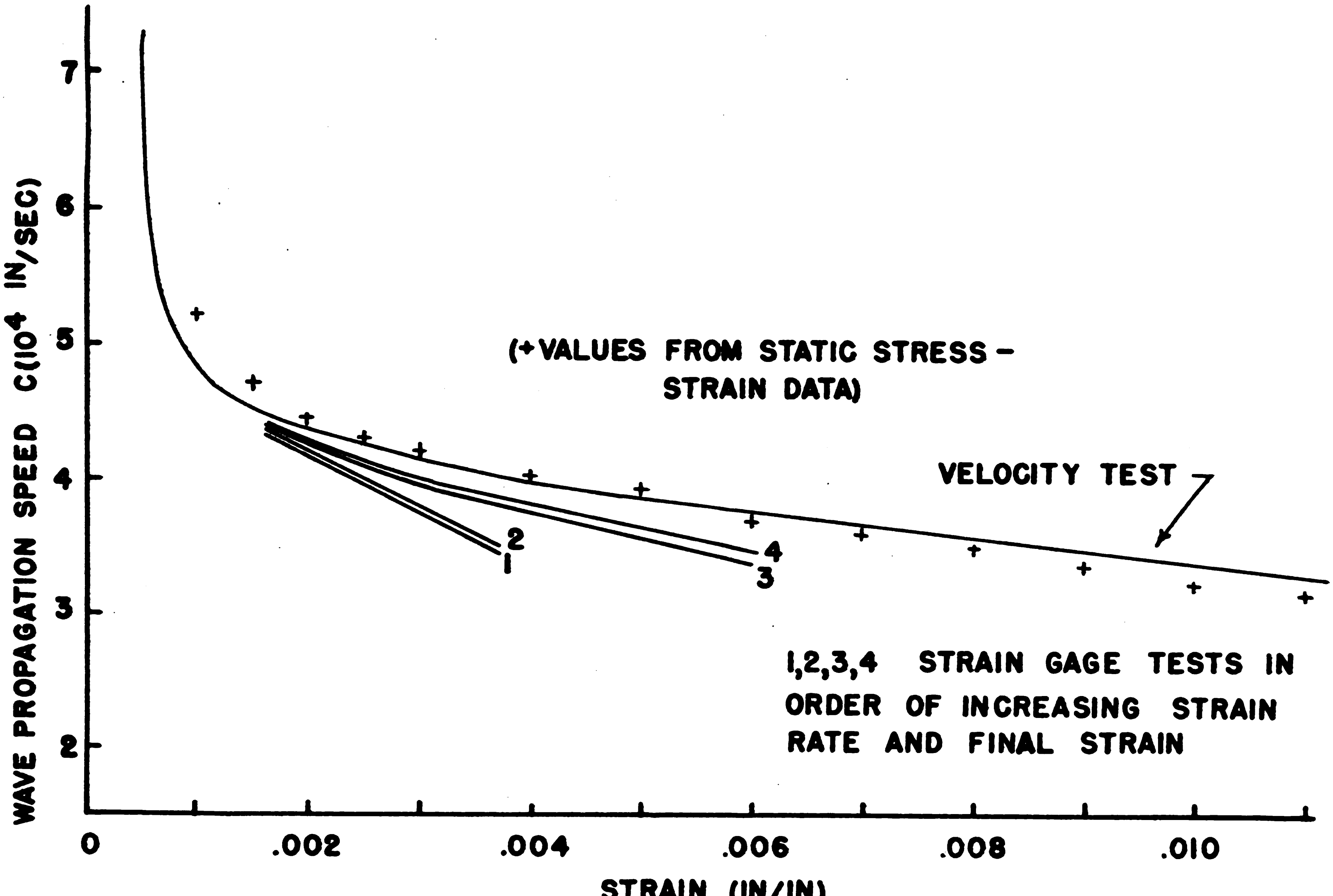

FIG (4.9) WAVE PROPAGATION SPEED VS. STRAIN LEVEL measurements show close agreement, we see that the gages seem to have a time constant which causes them to lag behind in response.

4.5 Numerical Results

(a) Linear Overstress Rate Dependence Theory

It has been noted in Section 1.2 that the numerical solution obtained by Malvern[10] for a hardened aluminum alloy subjected to constant velocity impact did not indicate the formation of a constant strain plateau in the neighborhood of $x = 0$. The material constants used were

$$\sigma_o = f(\epsilon) = 20{,}000 - \frac{10}{\epsilon}$$

$$E_o = 10^7 \text{ psi}$$

$$\sigma_y = 10^4 \text{ psi}$$

$$\rho = 2.5 \times 10^{-4} \text{ lb sec}^2/\text{in}^4$$

The constitutive equation then becomes

$$E_o \dot{\epsilon} = \dot{\sigma} + k\left(\sigma - 20{,}000 + \frac{10}{\epsilon}\right)$$

The assumed value of the constant k was

$$k = 10^6 \text{ sec}^{-1}$$

which gives an increase in stress over the static value of approximately ten per cent for a strain rate of 200 in/in/sec.

The boundary condition imposed at $x = 0$ was

$$v(0,t) = v_o = -600 \text{ ips}$$

The strain distribution in the bar at $t = 102.4\ \mu$ sec is shown in Fig. (4.10). Attempts to carry out the solution further into the x,t-plane using the CDC-3600 computer resulted in an oscillatory behavior of the solution in the neighborhood of $x = 0$. This may have been due to an accumulation of errors in the finite difference method used.

As an alternative to this solution, the constant stress boundary condition was investigated with the aid of the CDC-3600 computer. The boundary condition $\sigma(0,t) = 18{,}650$ psi (which is the asympotically approached value of stress at $x = 0$ according to von Karman theory for $v(0,t) = -600$ in/sec) gave results similar to Malvern in that no plateau seemed to appear even after $300\ \mu$ sec. However, lowering the impact stress to $\sigma(0,t) = 17{,}500$ psi and then to $\sigma(0,t) = 15{,}000$ psi did produce the sought-for plateau. The results are illustrated in Figs. (4.11) and (4.12). The curves for the rate-independent solution are for von Karman theory based on the static curve.

It is seen that the velocity at $x = 0$ very quickly asymptotically approaches a constant. The value is that which would be predicted by von Karman rate-independent theory. The significant feature of the solution is the appearance of the constant strain plateau. Hence, contrary to what has long been thought, the Malvern formulation for a rate-of-strain dependence does predict the formation of a region of constant strain near the impact end of the bar for a nearly

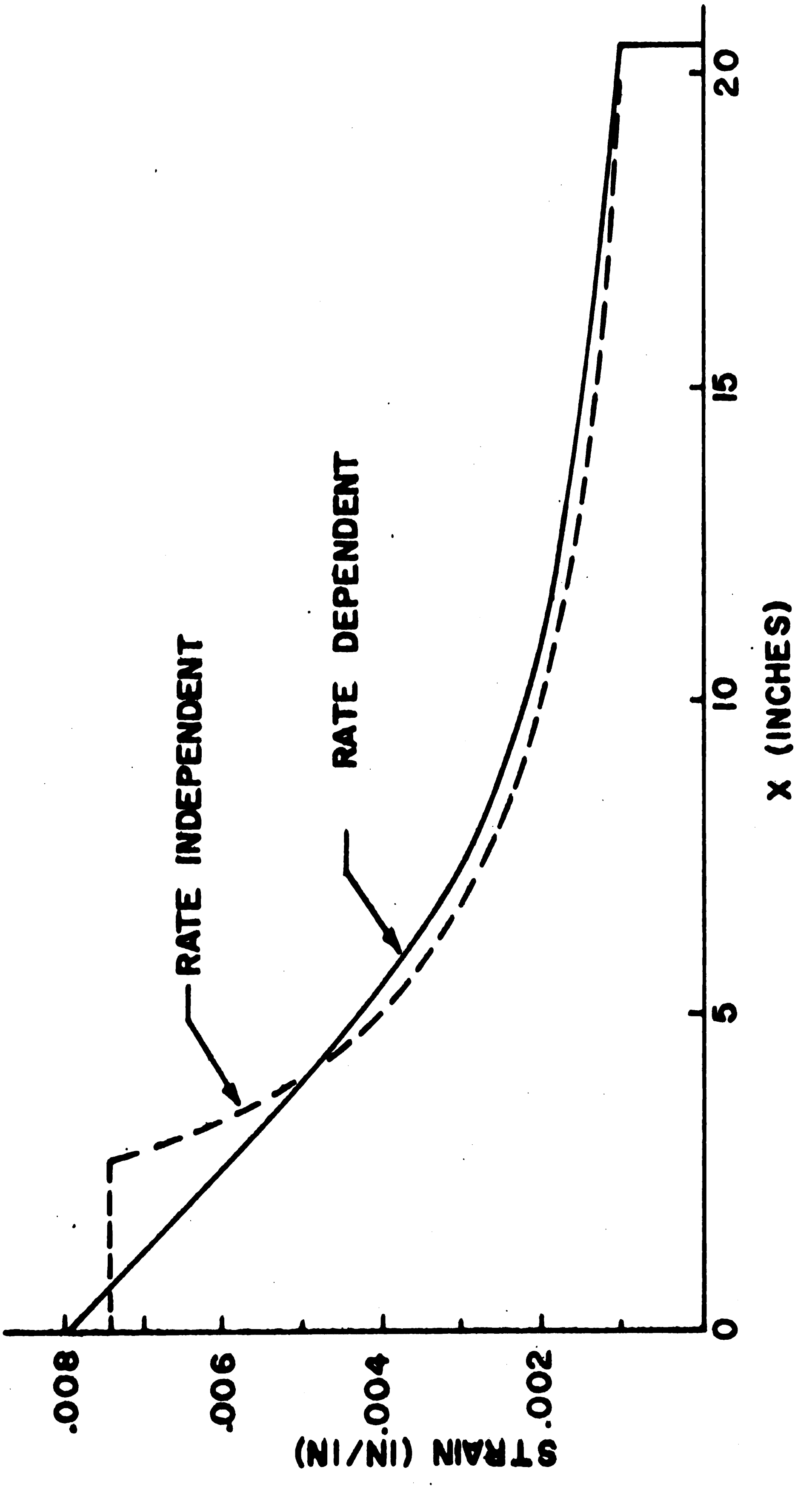

FIG (4.10) STRAIN DISTRIBUTION (AFTER MALVERN)

(T=102.4 μ SEC)

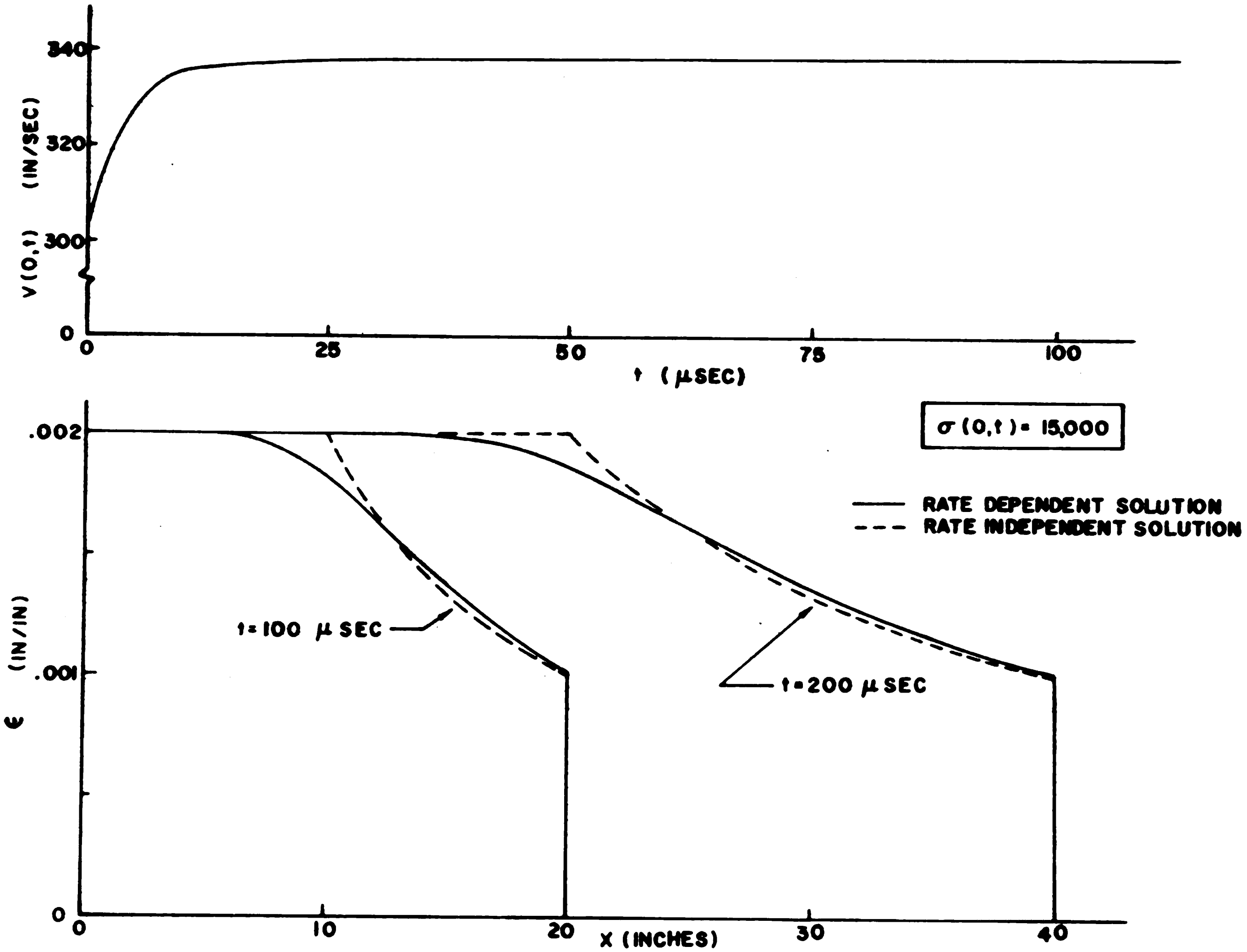

FIG (4.11) SOLUTION—CONSTANT STRESS BOUNDARY CONDITION AND LINEAR OVERSTRESS RATE DEPENDENCE

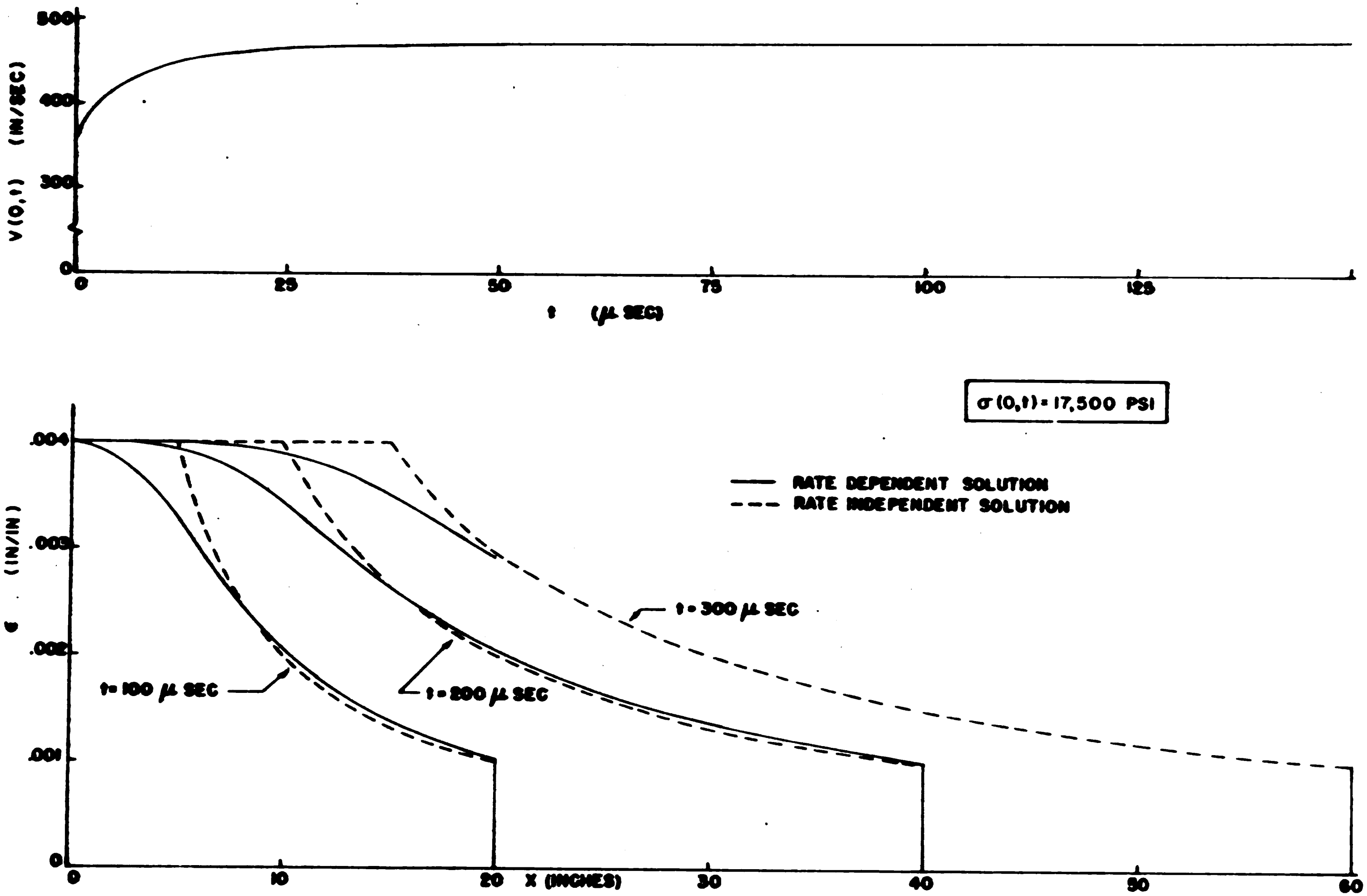

FIG (4.12) SOLUTION—CONSTANT STRESS BOUNDARY CONDITION AND LINEAR OVERSTRESS RATE DEPENDENCE constant velocity imposed at x = 0, if the pulse is long enough for the material near the impact face to reach equilibrium, as has been previously pointed out by Mercado.[44] By applying the method of characteristics to a non-linear visco-elastic model (with a linear plastic strain rate dependence) representative of Fort Peck sand, Mercado has demonstrated that a plateau of residual strain occurs close to x = 0 for a constant stress boundary condition with appropriate values of the dynamic constants.

It is noted from Figs. (4.11) and (4.12) that as the stress (and hence velocity) boundary condition increases in magnitude, the time required for a plateau to form increases so that the time required for the boundary condition σ = 18,500 psi would certainly be considerably greater than 100 microseconds.

As seen in Fig. (4.10), Malvern found a strain at x = 0 greater than that indicated from rate independent theory, but this may have been due to the error accumulation.

(b) Power Law Rate Theory with Input Data from Velocity Transducer

(i) Convergence Difficulties

The velocity record from station 1, specimen No.7 [see Fig. (4.3)] obtained from the velocity transducer was considered as a velocity boundary condition for a bar. A strain-rate dependence of the form

$$\sigma = \sigma_1 \dot{\epsilon}^{\,n}$$

was assumed, and the constant value of $n = 0.017$ used was that obtained by Chiddister[45] for strains on the order of five per cent in the same material at room temperature.

Due to a problem of convergence of the numerical iterative scheme, the static stress-strain curve was assumed to be valid for $\dot{\epsilon} = 10^{-2}$ in/in/sec and thus

$$\sigma_1 = \sigma_o(100)^n$$

where σ_o is the static stress-strain relation $\sigma_o = f(\epsilon) = 39{,}400\,\epsilon^{0.366}$. Thus, we finally arrive at

$$\sigma = 39{,}400\,\epsilon^{0.366}\,(100\,\dot{\epsilon})^{0.017}$$

for use in the numerical solution.

For the computer solution, yield was chosen at $v = 1.3$ m/sec $= 51.18$ in/sec because this point on the velocity records had been observed to propagate at the elastic wave speed. This choice was made, since what was being studied was the post yield behavior, and there was no obvious point on the fitted static curve to choose for the yield value. Conditions along the leading wave front are those previously discussed in Art. (2.2) for a gradual transition from an elastic to a plastic wave, except that the fitted static curve implies a non-linear elastic behavior before yield.

From Equations (2.38) for a general interior point and Equations (2.40) for an impact end point with a velocity boundary condition, we have

$$E_p = C_1 + \tfrac{1}{2}\Delta T\, G_p$$

$$S_p = C_2 - \tfrac{1}{2}\Delta T\, G_p$$

and hence, from Equation (2.51)

$$\phi_1 = x_1 = E = C_1 + \tfrac{1}{2}\Delta T\, G(E,S)$$

$$\phi_2 = x_2 = S = C_2 - \tfrac{1}{2}\Delta T\, G(E,S)$$

with

$$\frac{\partial \phi_1}{\partial E} = \frac{\Delta T}{2}\frac{\partial G}{\partial E} \qquad \frac{\partial \phi_1}{\partial S} = \frac{\Delta T}{2}\frac{\partial G}{\partial S}$$

$$\frac{\partial \phi_2}{\partial E} = -\frac{\Delta T}{2}\frac{\partial G}{\partial E} \qquad \frac{\partial \phi_2}{\partial S} = -\frac{\Delta T}{2}\frac{\partial G}{\partial S}$$

and the inequalities of Equations (2.53) and (2.54) become

$$\left|\frac{\partial \phi_1}{\partial E}\right| + \left|\frac{\partial \phi_1}{\partial S}\right| = \frac{\Delta T}{2}\left(\left|\frac{\partial G}{\partial E}\right| + \left|\frac{\partial G}{\partial S}\right|\right) = \beta_1 < 1$$

$$\left|\frac{\partial \phi_2}{\partial E}\right| + \left|\frac{\partial \phi_2}{\partial S}\right| = \frac{\Delta T}{2}\left(\left|-\frac{\partial G}{\partial E}\right| + \left|-\frac{\partial G}{\partial S}\right|\right) = \beta_2 < 1$$

$$\left|\frac{\partial \phi_1}{\partial E}\right| + \left|\frac{\partial \phi_2}{\partial E}\right| = \frac{\Delta T}{2}\left(\left|\frac{\partial G}{\partial E}\right| + \left|-\frac{\partial G}{\partial E}\right|\right) = \Delta T\left|\frac{\partial G}{\partial E}\right| = \beta_3 < 1$$

$$\left|\frac{\partial \phi_1}{\partial S}\right| + \left|\frac{\partial \phi_2}{\partial S}\right| = \frac{\Delta T}{2}\left(\left|\frac{\partial G}{\partial S}\right| + \left|-\frac{\partial G}{\partial S}\right|\right) = \Delta T\left|\frac{\partial G}{\partial S}\right| = \beta_4 < 1$$

From $\sigma = \sigma_1 \dot{\epsilon}^n$ we obtain $G = 10^{-8} \left[C \frac{S}{E^B} \right]^Q$ where $C = \frac{E_o}{A}$ and $Q = n^{-1}$. For G(E,S) in this form we obtain

$$\frac{\partial G}{\partial E} = - \frac{BQ}{E} G \quad , \quad \frac{\partial G}{\partial S} = \frac{Q}{S} G$$

In order to satisfy the sufficiency conditions for convergence of the iteration process, we desire

$$\beta_3 = Q \ \Delta T \ G \left| - \frac{B}{E} \right| < 1$$

$$\beta_4 = Q \ \Delta T \ G \left| \frac{1}{S} \right| < 1$$

or

$$\beta_1 = \beta_2 = \tfrac{1}{2}(\beta_3 + \beta_4) < 1$$

Thus, we note that as the strain rate, $\dot{\epsilon}$, increases and the degree of rate dependence, n, decreases (i.e. increasing Q) we may require a decrease in the mesh grid as determined by our choice of ΔT. For specimen No.7 the choice $\Delta T = 0.26$ ($\Delta t = 0.26 \ \mu$ sec) allowed a complete solution, but a value twice as large was found to be too large for convergence everywhere in the X,T-plane for the input data described.

A check on the propagation of errors in the solution due to round off in the computer was obtained by obtaining a solution with $\Delta T = 0.13$ ($\Delta t = 0.13 \ \mu$ sec). The results for stress, strain and velocity agreed with those of the previous solution with $\Delta T = 0.26$ to five or six digits at all points in the X,T-plane.

(ii) <u>Discussion of Calculation Results Based on Power Law Rate Theory with Input Data from Velocity Transducer</u>

Fig. (4.15) shows level lines of velocity in the x,t-plane. Since the level lines are straight (except for some slight curvature for v = 300 in/sec and v = 350 in/sec near x = 0) the propagation speed for any given level of particle velocity is predicted to be constant as the pulse travels down the bar and thus independent of the variations in strain rate encountered. The dashed lines in Fig. (4.15) are the level lines predicted by the von Karman rate-independent theory based on the fitted power-law static curve of Equation (4.2). Comparison with the solid curves shows that the rate-dependent solution predicts higher propagation speeds for velocity increments up to a little above 300 in/sec. The level lines of stress and strain are not shown separately in the figure since they so nearly coincide with velocity level lines as to be indistinguishable in plotting. What this means is that for the range of strain rates actually encountered in this solution and for the very slight rate dependence implied by the rate law with n = 0.017, the level lines are the same as would be predicted by using a single dynamic stress-strain curve instead of the static curve in the von Karman theory, except for very slight differences observable where the level lines plotted show a slight curvature. It was pointed out in Art. (4.4) that the average strain rates at the first and last gage stations were approximately in the ratio 3.5:9. It is not surprising, therefore, that the predictions of the rate-dependent theory can be correlated with a single dynamic curve, since there is so little variation in the strain rates in the solution, all of them being of the order of magnitude of 10,000 times the rate of $\dot{\epsilon} = 10^{-2}$ in/in/sec assumed for the "static" curve.

Additional information about the solution is contained in Figs. (4.16) and (4.14). Fig. (4.16) shows calculated stress versus time at $x = 0$ where the velocity input was taken from the first velocity gage station for specimen No.7. The solid curves in Fig. (4.14) show the input velocity at $x = 0$ and the calculated velocity versus time at $x = 3.07$ in, $x = 3.58$ in, $x = 6.14$ in, and $x = 9.21$ in. The dashed curve is the experimental record from the second gage station at $x = 3.25$ in on specimen No.7. Comparison of this with an interpolation between the two calculated curves for $x = 3.07$ in and $x = 3.58$ in indicates that the calculated propagation velocities are greater than the measured velocities. The greater part of the discrepancy is believed to be due to the use of the fitted power law for the static curve. As is seen in Fig. (4.13), the slopes of the fitted curve deviate considerably from those of the actual static curve. The curve in Fig. (4.14) indicated by the small

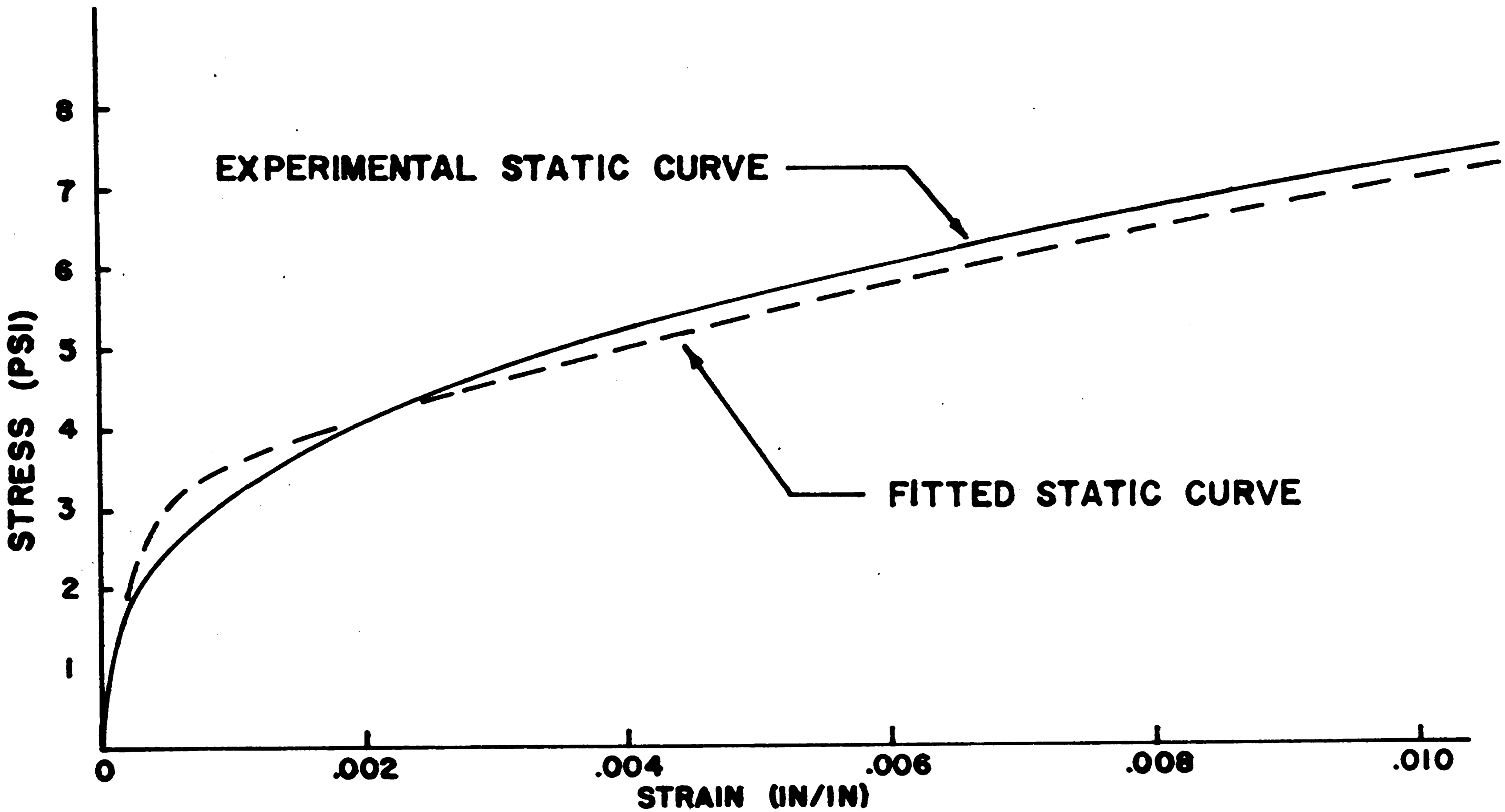

FIG (4.13) COMPARISON OF FITTED AND EXPERIMENTAL STATIC STRESS-STRAIN CURVES

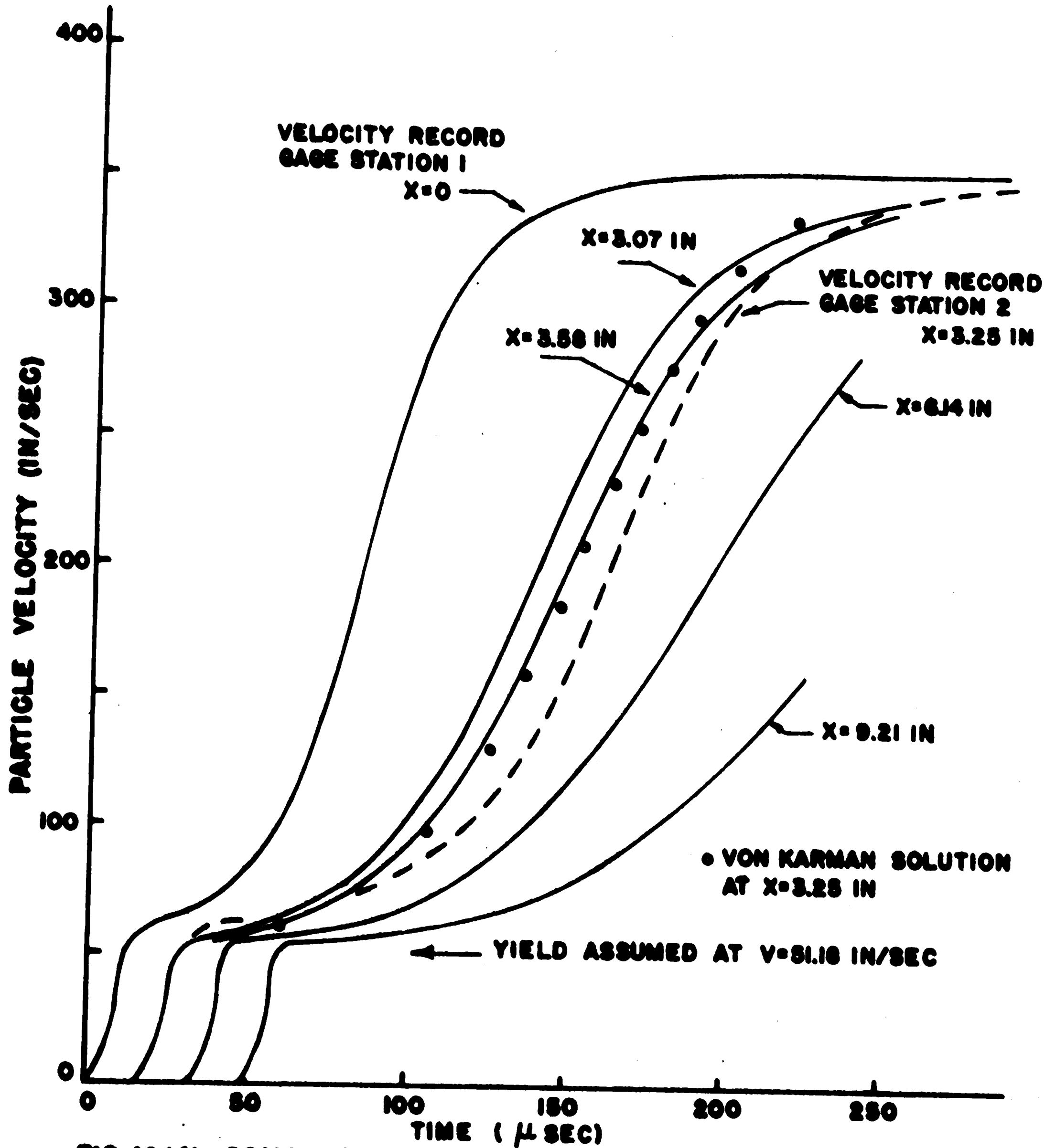

FIG (4.14) COMPUTER SOLUTION COMPARED WITH VON KARMAN SOLUTION AND EXPERIMENT

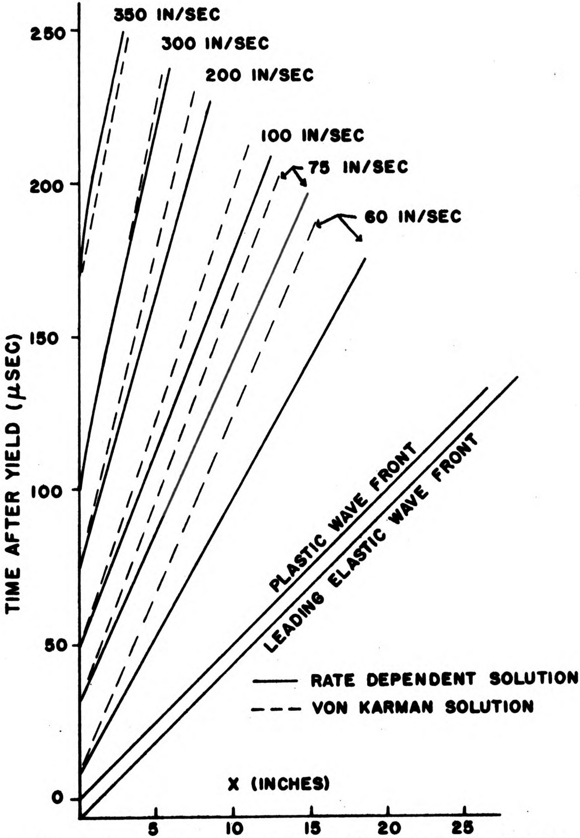

FIG (4.15) LEVEL LINES OF VELOCITY FOR SOLUTIONS WITH VELOCITY TEST DATA

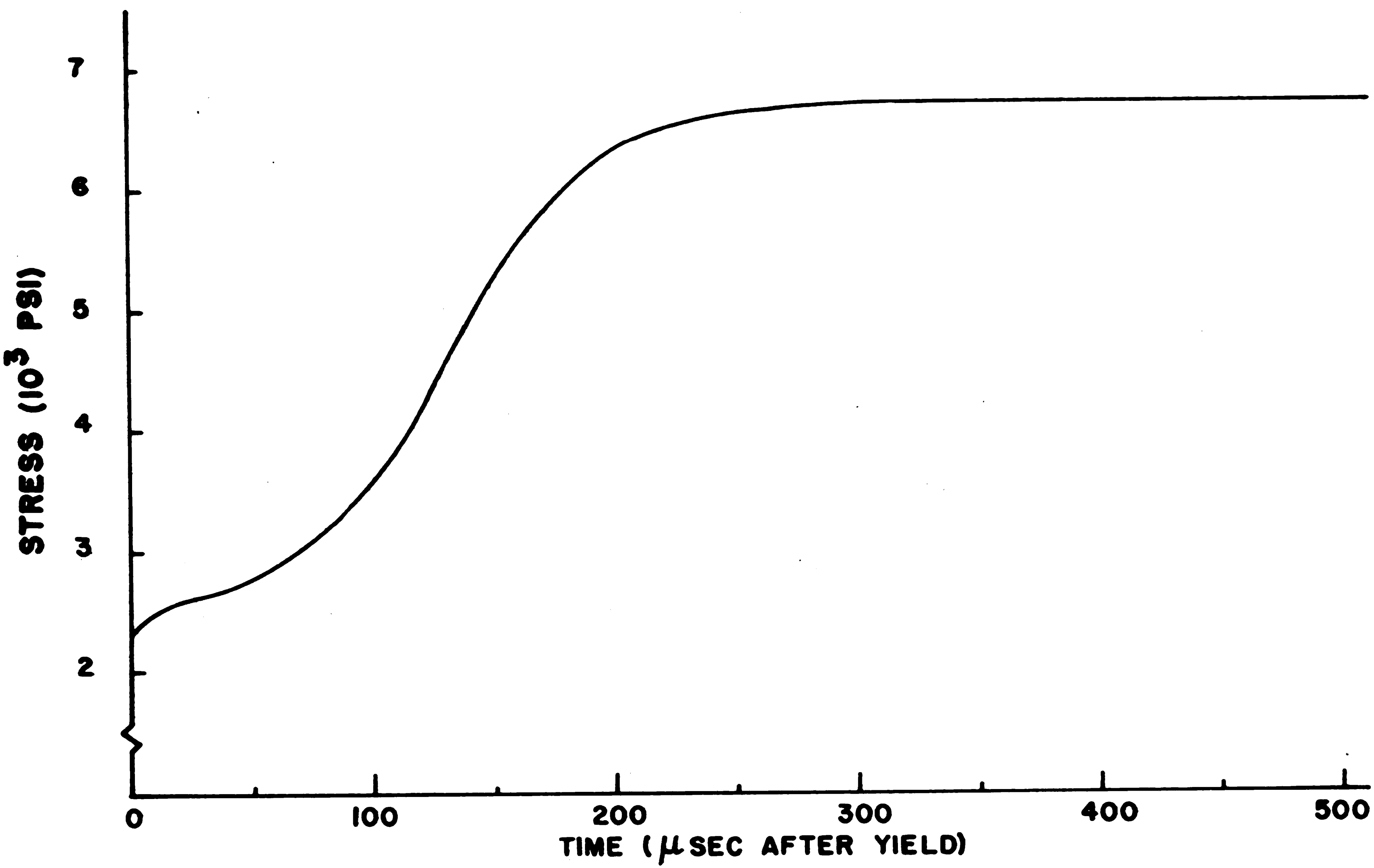

FIG(4.16) COMPUTED STRESS VS TIME AFTER YIELD AT X=0 circles is the predicted curve at the second gage station according to the von Karman rate-independent theory based on the fitted power-law static curve. The predictions are for levels of strain from $\epsilon = 0.0005$ to $\epsilon = 0.0065$ in increments of 0.0005 in/in. The rate-independent theory based on the fitted static curve thus also predicts a higher propagation velocity than was measured on specimen No.7. The small circles fall in between the dashed experimental curve and the interpolated solid curve (not shown) between $x = 3.07$ in and $x = 3.58$ in, but they fall closer to the interpolated curve than to the experimental curve, so that neither theoretical prediction agrees very well with the experimental curve. Part of this discrepancy may be due to variation of the experimental behavior of specimen No.7 from the averaged velocity behavior of all the specimens, which was seen in Art. (4.2) to correlate well with a single dynamic stress-strain curve prediction and fairly well with a static curve prediction. The greatest part of the discrepancy is, however, believed to be due to the use of the fitted power law instead of the actual static curve.

The computer solution may also be rather sensitive to the way the conditions representing yield were introduced into the solution. Picking a slightly higher value to represent yield seems likely to move the computed curves nearer to the experimental curve.

It was, however, considered not worthwhile to repeat the computer solution with a better fit on the static curve or to adjust the assumed yield value, since it was already clear from the results of Art. (4.2) that the averaged velocity data from the velocity experiments can be represented by a single dynamic curve.

CHAPTER V

SUMMARY AND CONCLUSIONS

Two independent series of dynamic plastic compression impact tests were performed on half-inch diameter bars of commercially pure aluminum. In the first series, an electro-magnetic transducer was used to obtain measurements of particle velocity at four stations along the bar, while in the second series, etched foil resistance strain gages yielded records of surface strain at the same gage locations. Strain rates on the order of 100 in/in/sec were reached.

Test results indicated that any given level of velocity or strain propagates along the bar with a constant velocity, not affected by the strain rate within the small range of strain rates encountered. However, the velocities of propagation observed differed noticeably from those predicted by von Karman rate-independent theory based on the static curve. Good agreement was found between the propagation speeds observed for different levels of velocity (averaged over all tests) and predictions of von Karman theory based on a single dynamic stress-strain curve differing from the static curve.

That the apparent applicability of a single dynamic curve and rate-independent theory to this kind of plastic wave propagation is consistent with rate-dependent theory for a material with a very slight rate dependence, was demonstrated by the results of computer solutions for rate-dependent theory in Art. (4.5). The nature of the process is such that the range of strain rates encountered for most of the observations is covered by a 3:1 ratio of strain rates, and almost all of the plastic deformation occurs at rates in the range from 3,000 to 10,000 times the "static curve" strain rate.

The wave propagation speed versus strain level plots from the transient strain records showed consistently lower propagation speeds than those based on the velocity records. It is believed that the strain gage response actually lags behind the strain in the material, as previously observed by Bell,[31] but our records are not consistent with a lag proportional to strain rate as reported by Bell, since, in fact, the higher strain rate tests came nearer to agreeing with the velocity measurements and the rate-independent theory than did the lower strain rate tests. Considerably more evidence is needed before final conclusions can be drawn about the lag in the strain measurements and the reasons for it.

Using the velocity records obtained from the first gage station (six diameters from the impact end of the bar) as an input boundary condition to predict values at stations farther along the bar, a numerical computer solution was obtained using the rate-dependent theory with a power law for rate dependence and the power $n = 0.017$ found in dynamic stress-strain tests on short specimens of the same material performed by Chiddister.[45] This computer solution did predict a constant wave propagation speed for any given level of velocity, but the constant values predicted did not agree well with the experimental values from the velocity records. This lack of agreement appears to be mainly the result of using a rather poor fit to the static curve in the computations, since von Karman rate-independent theory using the same fitted static curve also gave poor agreement with the experiments. Since the computer solutions with rate-dependent theory were consistent with a single dynamic curve, and since the velocity measurements correlate with a single dynamic curve, it appears that a little ingenuity in curve-fitting could produce agreement between the rate theory and the experiments. This did not seem to be worth the effort.

Such agreement between rate theory and the experiments would not of course prove that the rate theory was correct and von Karman theory based on a single dynamic curve was incorrect, since the two would predict virtually the same thing for a material with little rate sensitivity. The rate-independent theory is easier to apply and therefore preferable for a situation like this. Any real test of the rate-dependent theory must come in a situation with a greater range of strain rates in the test and for a material with more strain-rate sensitivity than annealed aluminum.

Further study in this area should include experimental and theoretical wave propagation studies and dynamic tests on materials not in the soft annealed condition, which may exhibit more strain rate dependence as suggested by Dorn et al.

Ferrous materials are also known to be rate sensitive, but in wave propagation tests of the kind described in this report, anomalies occur because of the yield delay time.[6] It might be possible to study tensile pulse propagation in bars pre-loaded statically into the work-hardening range and impacted while the static loading was continuing. Furthermore, the magnetic velocity transducer could not be used on ferrous specimens. Further study is also in order on transient strain recording in dynamic plasticity to develop a simple strain recording technique not subject to the lag exhibited by the strain gage records.

The velocity recording technique might be improved by using stronger and more uniform magnetic fields. These would yield an increase in output signal level as well as allow the use of wider gaps between pole pieces. The wider gap would enable construction of a wire support system capable of a greater translation during the passage of the wave.

The velocity recording technique for non-magnetic materials is believed to give good results, but if possible, it would be desirable to modify it to make it more nearly a routine type of test.

BIBLIOGRAPHY

1. Donnell, L. H., "Longitudinal Wave Transmission and Impact," Trans. ASME, Vol. 52, 1930, pp. 153-167.

2. von Karman, T., "On the Propagation of Plastic Deformation in Solids," NDRC Report No. A-29 (OSRD No. 365), 1942.

3. von Karman, T. and Duwez, P., "The Propagation of Plastic Deformations in Solids," J. Appl. Physics, Vol. 21, 1950, pp. 987-994.

4. Taylor, G. I., "The Plastic Wave in a Wire Extended by an Impact Load," The Scientific Papers of Sir Geoffrey Taylor, Cambridge Univ. Press, 1958, pp. 467-479.

5. Rakhmatulin, K. A., "Propagation of a Wave of Unloading," Prikl. Mat. i Mek., Vol. 9, 1945, pp. 91-100 (in Russian). Translation All - T2/15, Brown Univ., 1948.

6. Duwez, P. and Clark, D. S., "An Experimental Study of the Propagation of Plastic Deformation Under Conditions of Longitudinal Impact," Proc. Am. Soc. Test. Mat., Vol. 47, 1949, pp. 502-532.

7. Ludwik, P., "Über den Einfluss der Deformationgeschwindigkeit bei Bleibenden Deformationen mit Besonderer Berücksichtigung der Nachwirkungserscheinungen," Physikalische Zeitschrift, Vol. 10, 1909, pp. 411-417.

8. Deutler, H., "Experimentelle Untersuchen uber die Abhangigkeit der Zugspannungen von der Verformungsgeschwindigkeit," Physikalische Zeitschrift, Vol. 33, 1932, pp. 247-259.

9. Prandtl, L., "Ein Gedankenmodell Zur Kinetischen Theorie der Festen Körper," Zeitschrift fur Angewandtke Mathematik und Mechanik, Vol. 8, 1928, pp. 85-106.

10. Malvern, L. E., "The Propagation of Longitudinal Waves of Plastic Deformation in a Bar of Material Exhibiting a Strain-Rate Effect," J. Appl. Mech., Vol. 18, 1951, pp. 203-208.

11. Malvern, L. E., "Plastic Wave Propagation in a Bar of Material Exhibiting a Strain Rate Effect," Quart. Appl. Math., Vol. 8, 1950, pp. 405-411.

12. Sokolovsky, V. V., "The Propagation of Elastic-Viscous-Plastic Waves in Bars," Prikl. Mat. i Mek., Vol. 12, pp. 261-280, 1948 (Russian). Translation A11-T6, Brown University, 1949.

13. Bell, J. F., "Propagation of Plastic Waves in Pre-Stressed Bars," Dept. of Mechanical Engr., The Johns Hopkins University, Baltimore, Tech. Rep. No. 5, Navy Contract N6-ONR-243, 1951.

14. Sternglass, E. J., and Stuart, D. A., "An Experimental Study of Propagation of Transient Longitudinal Deformations in Elastoplastic Media," J. Appl. Mech., Vol. 20, 1953, pp. 427-434.

15. Alter, B. E. K. and Curtis, C. W., "Effects of Strain Rate on the Propagation of a Plastic Strain Pulse Along a Lead Bar," J. Appl. Phys., Vol. 27, 1956, pp. 1079-1085.

16. Davies, R. M., "A Critical Study of the Hopkinson Pressure Bar," Phil. Trans. Roy. Soc. Lond., Ser. A, Vol. 240, 1948, pp. 375-457.

17. Bell, J. F. and Stein, A., "The Incremental Loading Wave in the Pre-Stressed Plastic Field," J. de Mecanique, Vol. 1, No. 4, Dec. 1962.

18. Bodner, S. R. and Kolsky, H., "Stress Wave Propagation in Lead," in Proc. Third U. S. Nat. Congr. Appl. Mech., New York, 1958, ASME, pp. 495-501.

19. Simmons, J. A., Hauser, F., and Dorn, J. E., "Mathematical Theories of Plastic Deformation Under Impulsive Loading," Univ. of California MRL Publication, Series No. 133, Issue No. 1, December, 1959.

20. Campbell, J. D., Simmons, J. A. and Dorn, J. E., "On the Dynamic Behaviour of a Frank-Read Source," Univ. of California MRL publication, Series No. 133, Issue No. 2, May, 1959 (also J. Appl. Mech., Vol. 28, Sept. 1961, p. 447).

21. Hauser, F. E., Simmons, J. A., and Dorn, J. E., "Strain Rate Effects in Plastic Wave Propagation," Univ. of California MRL publication, Series No. 133, Issue No. 3, June, 1960.

22. Hauser, F. E. and Winter, C. A., "An Experimental Method for Determining Stress-Strain Relations at High Strain-Rates," Univ. of California MRL publication, Series No. 133, Issue No. 4, December, 1960.

23. Hauser, F. E., Simmons, J. A., and Dorn, J. E., "Strain Rate Effects in Plastic Wave Propagation," Response of Metals to High Velocity Deformation, Interscience, New York, 1961, pp. 93-114.

24. Rajnak, S. and Hauser, F., "Plastic Wave Propagation in Rods," Symposium on Dynamic Behavior of Materials, ASTM Special Technical Publication No. 336, 1963, pp. 167-179.

25. Bell, J. F., "Diffraction Grating Strain Gauge," Proc. SESA, Vol. 1, 1959, pp. 51-64.

26. Bell, J. F., "Propagation of Large Amplitude Waves in Annealed Aluminum," J. Appl. Phys., Vol. 31, No. 1, 1960, pp. 277-282.

27. Bell, J. F., "Study of Initial Conditions in Constant Velocity Impact," J. Appl. Phys., Vol. 31, No. 2, 1960, pp. 2188-2195.

28. Kolsky, H. and Douch, L. S., "Experimental Studies in Plastic Wave Propagation," J. Mech. Phys. Solids, Vol. 10, July/Sept. 1962, pp. 195-223.

29. Lindholm, U. S., "Some Experiments with the Split Hopkinson Pressure Bar," Technical Report No. 1, Contract No. DA-23-072-ORD-1674, SwRI Project No. 02-1102, Southwest Research Institute, San Antonio, Texas, March, 1964.

30. Ripperger, E. A. and Karnes, C. H., "Plastic Impact on Short Cylindrical Specimens," Symposium on Dynamic Behavior of Materials, ASTM Special Technical Publication No. 336, 1963, pp. 180-194.

31. Bell, J. F., Discussion, "Experimental Studies of Plastic Wave Propagation in Bars," Plasticity, Proceedings of the Second Symposium on Naval Structural Mechanics, Brown University, 1960, p. 485.

32. Hopkins, H. G., "Dynamic Anelastic Deformations of Metals," Appl. Mech. Rev., 1961, Vol. 14, No. 6, pp. 417-431.

33. Kolsky, H., "Stress Waves in Solids," J. Sound and Vibr., 1964, Vol. 1, pp. 88-110.

34. Lee, E. H., "The Theory of Wave Propagation in Anelastic Materials," in N. Davids, ed., Int. Symposium on Stress Wave Propagation in Solids, Interscience, 1960, pp. 199-228.

35. Craggs, J. W., "Plastic Waves," in Sneddon-Hill, eds., Progress in Solid Mechanics, Vol. II, Interscience, 1961, pp. 141-197.

36. Kolsky, H., Stress Waves in Solids, Oxford, 1953 (Dover, 1963), Ch. VII.

37. Courant, R. and Hilbert, D., Methods of Mathematical Physics, Vol. II, Interscience, New York, 1962.

38. Courant, R. and Friedrichs, K. O., Supersonic Flow and Shock Waves, Interscience, 1948, Ch. II.

39. Zaguskin, V. L., Handbook of Numerical Methods for the Solution of Algebraic and Transcendental Equations, Pergamon, New York, 1961.

40. Pugh, E. M. and Pugh, E. W., Principles of Electricity and Magnetism, Addison-Wesley, Reading, Mass., 1960, pp. 216-220.

41. Ripperger, E. A. and Yeakley, L. M., "Measurement of Particle Velocities Associated with Waves Propagating in Bars," Experimental Mechanics, Vol. 3, No. 2, February, 1963, pp. 47-56.

42. Ramberg, W. and Irwin, L. K., "A Pulse Method for Determining Dynamic Stress Strain Relations," Proc. Ninth International Congress of Applied Mechanics, Brussels, 1957, Vol. 8, pp. 480-489.

43. Bell, J. F., "An Experimental Study of the Interrelation between the Theory of Dislocations in Polycrystalline Media and Finite Amplitude Wave Propagation in Solids," Tech. Report No. 7, Air Force Contract AF49(638)-423, Johns Hopkins University, March, 1961.

44. Mercado, E. J., "Plane Wave Propagation in Nonlinear Viscoelastic Materials," Thesis, Rensselaer Polytechnic Institute, 1963.

45. Chiddister, Jerry L., "An Experimental Study of Aluminum at High Strain Rates and Elevated Temperatures," Thesis, Division of Engineering Research, Michigan State Univ., 1961.

APPENDIX

THE COMPUTER PROGRAM

In the following pages an asterisk (*) will denote multiplication and a slash(/) will denote division so that the equations in which they appear will be similar to the corresponding Fortran statements in the computer programs.

A.1 Leading Wave Front

For a transition from an elastic to plastic impact, the conditions along the leading wave front are given by

$$\sigma = \sigma_y$$

$$\epsilon = \epsilon_y$$

where the subscript y refers to the values at yield.

Assuming rate independent theory applicable until yield occurs, we have

$$v = v_y = \int_0^{\epsilon_y} \sqrt{\frac{1}{\rho}\frac{d\sigma}{d\epsilon}}\, d\epsilon$$

When the impact is initially plastic, we must consider a shock wave propagating along X = T ($x = c_o t$).

(a) Linear Overstress Rate Dependence (MALRATE)

From Equation (1.11)

$$E_o \dot{\epsilon} = \dot{\sigma} + k[\sigma - f(\epsilon)]$$

$$g(\sigma, \epsilon) = k[\sigma - f(\epsilon)]$$

$$k = 10^6 \text{ sec}^{-1}$$

(i.e. 10^{-6} sec = unit dimensionless time)

$$f(\epsilon) = 20{,}000 - \frac{10}{\epsilon}$$

$$G = \frac{g}{kE_o} = \frac{\sigma - 20{,}000 + \frac{10}{\epsilon}}{E_o}$$

$$= S - \frac{20{,}000}{E_o} + \frac{10}{E_oE}$$

$$= S - B + \frac{A}{E}$$

where

$$A = \frac{10}{E_o}, \quad B = \frac{2 \times 10^4}{E_o}$$

From Equation (2.48)

$$\frac{T}{2} = \int_{S(0,0)}^{S} \frac{ds}{s - B + \frac{A}{s}} = \int_{S_o}^{S} \frac{sds}{s^2 - Bs + A}$$

which yields

$$T = kt = 2\left[\frac{10{,}000}{\sigma - 10{,}000} - \frac{10{,}000}{\sigma(0,0) - 10{,}000}\right.$$

$$\left. + \ln\left(\frac{\sigma(0,0) - 10{,}000}{10{,}000} * \frac{10{,}000}{\sigma - 10{,}000}\right)\right]$$

$$= 2[P - Q + \ln(P/Q)]$$

where

$$P = \frac{10,000}{\sigma - 10,000}$$

$$Q = \frac{10,000}{\sigma(0,0) - 10,000}$$

At any mesh point along X = T we have T = (J-1) * T. Hence,

$$TAX = J - 1 = \frac{2}{\Delta T}\,[P - Q + \ln(P/Q)]$$

Thus, $\frac{T}{\Delta T} = f(P)$ is solved by the "Method of False Position" and $\sigma = \sigma(P) = \sigma(c_o t, t) = \sigma(T,T)$ is obtained along X = T.

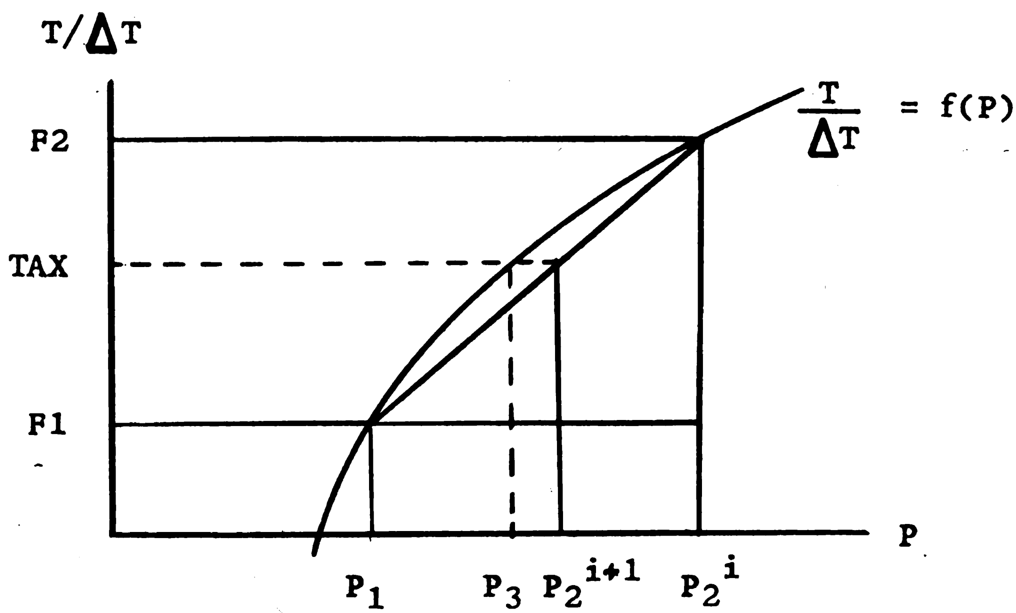

$$P_2^{i+1} = P_2^{i} - (P_2^{i} - P_1)\,\frac{F2 - TAX}{F2 - F1}$$

When $P_2^{i+1} - P_2^{i} < \delta$ we assume that P_2^{i+1} is sufficiently close to P_3 giving us the value of stress at any given time (TAX * ΔT) along the leading wave shock front.

(b) <u>Power Law Rate Dependence (POWRATE)</u>

$$\sigma(\epsilon,\dot{\epsilon}) = \sigma_1(\epsilon,1)\dot{\epsilon}^{\,n}$$

Assuming that the static-stress strain curve is applicable at $\dot{\epsilon} = 10^{-2}\ \mathrm{sec}^{-1}$ we have

$$\sigma_o = \sigma_1(0.01)^n$$

$$\sigma_1 = \sigma_o(0.01)^{-n}$$

and

$$\sigma(\epsilon,\dot{\epsilon}) = \sigma_o(100\,\dot{\epsilon}_p)^n \quad \text{for} \quad \dot{\epsilon} \geqq 0.01\ \mathrm{sec}^{-1}$$

$$\sigma(\epsilon,\dot{\epsilon}) = \sigma_o \qquad\qquad \dot{\epsilon} < 0.01\ \mathrm{sec}^{-1}$$

Hence

$$\dot{\epsilon}_p = 0.01\left(\frac{\sigma}{\sigma_o}\right)^{\frac{1}{n}} = 10^{-2}\left(\frac{\sigma}{\sigma_o}\right)^{Q}$$

And the constitutive equation becomes

$$E_o\,\dot{\epsilon} = \dot{\sigma} + 10^{-2}\,E_o\left(\frac{\sigma}{\sigma_o}\right)^{Q}$$

Therefore,

$$g(\sigma,\epsilon) = 10^{-2}\,E_o\left(\frac{\sigma}{\sigma_o}\right)^{Q}$$

Choosing $k = 10^6\ \sec^{-1}$ so that unit T is 10^{-6} second, we obtain

$$G = 10^{-8}\left(\frac{\sigma}{\sigma_o}\right)^Q$$

For a static stress-strain relation expressible in the form

$$\sigma_o = A\epsilon^B \qquad , \ B < 1$$

we have

$$G = 10^{-8}\ \frac{E_oS}{AE^B}^{\ Q}$$

$$= 10^{-8}\left(C\ \frac{S}{E^B}\right)^Q$$

where

$$C = \frac{E_o}{A}$$

For a plastic shock wave along X = T, we substitute into Equation (2.48) to obtain

$$T = -2 \times 10^8 \int_{S_o}^{S} \frac{ds}{(cs^{1-B})^Q}$$

$$= \frac{2 \times 10^8}{Q(1-B) - 1}\left\{\frac{S}{\left[C(S)^{1-B}\right]^Q} - \mathrm{DOT}\right\}$$

where

$$\mathrm{DOT} = \frac{S_o}{\left[C(S_o)^{1-B}\right]^Q} \qquad , \ S_o = S(0,0)$$

For $B<1$, $Q>1$, $C\gg 1$ and $0<S\ll 1$ we note that

$$\frac{dT}{dS} = -\frac{2}{G} < 0$$

Hence, the graph of $T/\Delta T$ versus s appears as shown below.

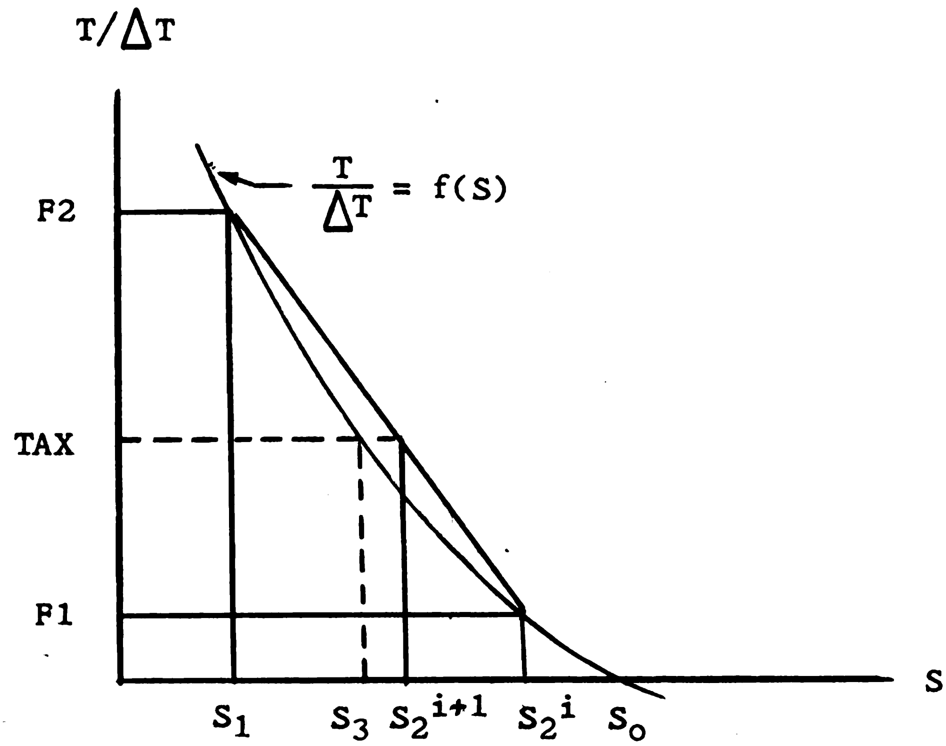

and

$$S_2^{i+1} = S_1 + (S_2^{i} - S_1)\,\frac{F2 - TAX}{F2 - F1}$$

The process is repeated as has been described previously for the case of linear rate dependence.

A.2 Computational Procedure

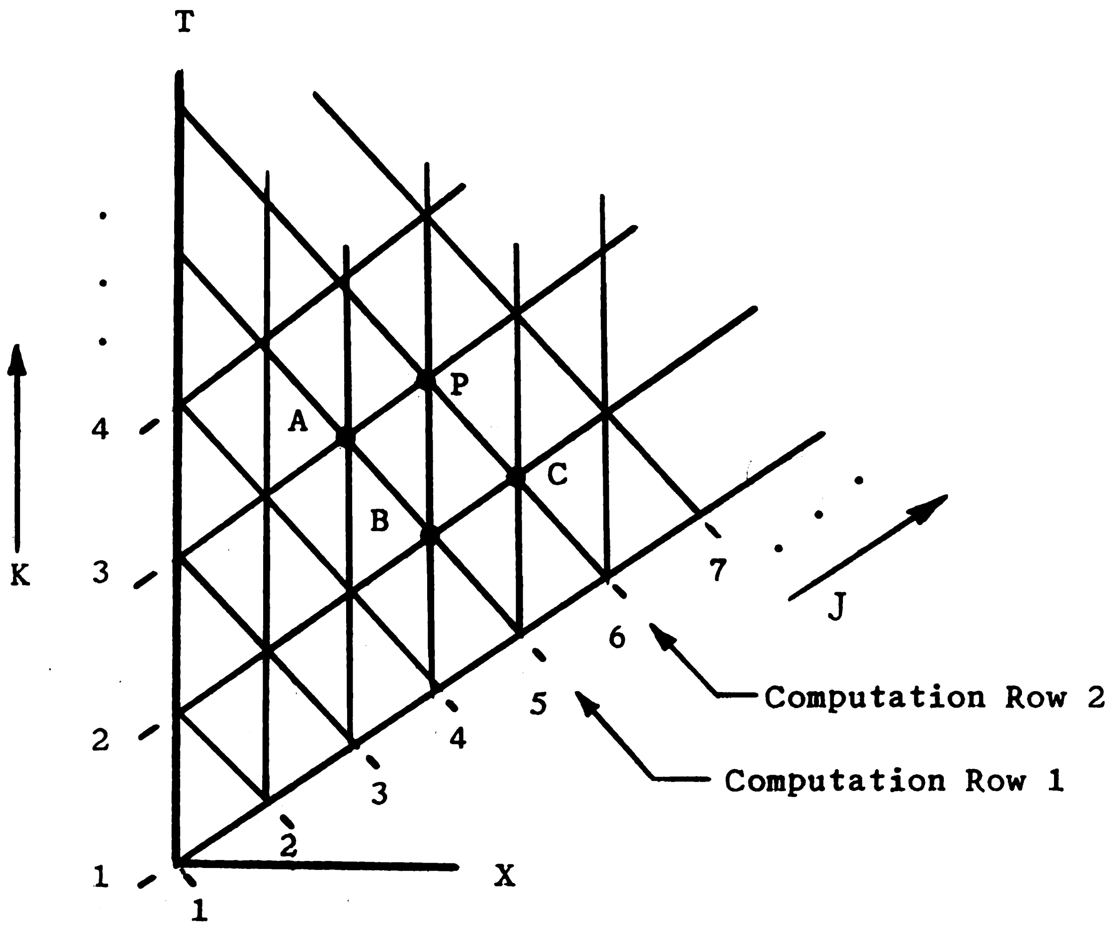

Point P is denoted by the array identification (2,N). Points A, B and C are identified by (1,N), (1,N-1) and (2,N-1) respectively. The variable N is given by the "column" number, K.

The solution works outwards from the origin and proceeds along a "row," J = constant. For K = N = 1, we make use of the equation for a gradual elastic-plastic wave transition interface (see last equation of Art. 2.2) or use the schemes of Sec. A.1 for shock waves. For K = N = J the boundary conditions will determine the appropriate relations [Equations (2.40), (2.42) or (2.44)] to be solved.

If we have not reached the last row, we will proceed to the next row and the values just obtained in the former "computation row 2" become the elements of the next "computation row 1."

In the vicinity of the origin, we chose the values of variables at B or C as initial estimates of the variables at P. Elsewhere, initial estimates in the field for $K<5$ make use of the first and second derivatives of the variable along the column K = constant. For $K>5$ we make use of the derivatives along J = constant.

The iterations appeared to converge as an oscillatory geometric progression. Hence, the following Aitkin - δ^2 process was used.[36]

Assume the solution is $\{a\}$ and iterated estimate $\{a_k\}$. For oscillatory convergence, $a - a_k$ is assumed to decrease approximately as the sequence of numbers

$$pr^k \cos(k\phi + \theta)$$

Such a sequence is the sum of two geometrical progressions with complex conjugate ratios

$$q_1 = r\,(\cos\phi + i\sin\phi)$$

$$q_2 = r\,(\cos\phi - i\sin\phi)$$

$a_{k+1} - a_k$ decreases approximately as the sequence

$$p^1 r^k \cos\,(k\phi + \theta^1)$$

where p^1 and θ^1 are in general different from p and θ, but r and ϕ are the same for the sequence $\{a - a_k\}$.

The improved value, $\tilde{a}_{k+1}$, is given by

$$\tilde{a}_{k+1} = a_k - \frac{\Delta a_{k-1}(\Delta a_k - r^2\,\Delta a_{k-1})}{\Delta^2 a_{k-1} - r^2\,\Delta^2\,a_{k-2}}$$

Here

$$r^2 = \frac{\begin{vmatrix} \Delta a_{k-2} & \Delta a_{k-1} \\ \Delta a_{k-1} & \Delta a_k \end{vmatrix}}{\begin{vmatrix} \Delta a_{k-3} & \Delta a_{k-2} \\ \Delta a_{k-2} & \Delta a_{k-1} \end{vmatrix}} = \frac{\Delta a_{k-2}\,\Delta a_k - (\Delta a_{k-1})^2}{\Delta a_{k-3}\,\Delta a_{k-1} - (\Delta a_{k-2})^2}$$

where

$$\Delta a_i = a_{i+1} - a_i$$

$$\Delta^2 a_i = \Delta a_{i+1} - \Delta a_i$$

Thus,

$$\tilde{a}_5 = a_4 - \frac{(a_4 - a_3)\left[(a_5 - a_4) - r^2(a_4 - a_3)\right]}{\left[(a_5 - a_4) - (a_4 - a_3)\right] - r^2\left[(a_4 - a_3) - (a_3 - a_2)\right]}$$

where

$$r^2 = \frac{(a_3 - a_2)(a_5 - a_4) - (a_4 - a_3)^2}{(a_2 - a_1)(a_4 - a_3) - (a_3 - a_2)^2}$$

If necessary, this process is repeated after four more Seidel iterations. Each time the Aitkin - δ^2 process is used, the magnitude of the correction term denominator in the equations for a_5 is checked to make sure that it is greater than zero. If the denominator vanishes, we omit the Aitkin - δ^2 process and perform another Seidel iteration.

A.3 Interpretation of Code Words

Words Common to Both Programs

J		Grid Row Number
K		Grid Column Number
LOOK	= 1	V(0,T) = VOL = constant
	= 2	V(0,T) is a known variable
	= 3	S(0,T) is a known variable
	= 4	E(0,T) is a known variable
JAZZ	= 1	S(0,T) is tabulated V(0,T) is tabulated
	= 2	S(0,T) is σ_o - then zero V(0,T) has exponential rise
MAX		Maximum permissible iterations
M1		First Row to be printed after initial impact point (1,1)
M2		First Column in first row to be printed out
M3		Increment along column for print out
M4		Increment along row for print out
LL		Last row after which stress = 0 for LOOK = 3, JAZZ = 2 or strain = constant for LOOK = 4
IMPACT	= 1	Plastic Impact - Calculations Required Along X = T
	= 2	Elastic-Plastic transition - Conditions Constant along X = T
MARK	1,2	Value changes from 1 to 2 when $\sigma = f(\epsilon)$ at an interior or impact boundary point

T	$\Delta T = 10^6 \Delta t$
EO	Young's Modulus (psi)
RHO	Mass Density ($lb/sec^2/in^4$)
YIELD	Yield Stress (psi)
VMAX	V_{max}(in/sec)
TFIX	t_{fix}(μsec)
CENT	.01a

(For case of exponential velocity rise at X = 0, $v|_{x=o}$ = a% of v_{max} when $t = t_{fix}$)

VOL	v(0,t) = constant (in/sec)
STRS	$\sigma(0,t)$ = constant (psi)
ALPHA BETA	Constants in $v(0,t) = v_{max}[1 - e^{-(\beta+\alpha T)}]$ (calculated in computer)

Program Malrate

A, B	$G = S - B + \frac{A}{E}$
C	Along X = T, $P = \frac{S - C}{C}$, $C = \frac{10^4}{E_o}$
D	ΔP, Increment in P along X = T
F, Q, P	$T = 2[P - Q + Ln(F*P)]$, $F = Q^{-1}$

Program Powrate

A, B	$\sigma_o = A\epsilon^B$
C	$C = \frac{E_o}{A}$
D	ΔP, Increment in P along X = T

P		P = S along X = T
Q		$\sigma = \sigma_1 \dot{\epsilon}^n$, $Q = \frac{1}{n}$
F		NOT USED
MAD	= 1	Normal Run
	= 2	Program will restart after last row with new mesh
	= 3	Program is a restart ($J \neq 1$)
TIM		Factor by which ΔT is multiplied in going from MAD = 2 to MAD = 3

A.4 Computation Flow Chart

The computation flow chart on the following page gives a schematic representation of the process by which the actual computer program carries out the solution in the characteristic X,T-plane. Using the flow chart and the "comment" cards within the actual program, it is hoped that the reader will be able to follow the Fortran coding.

The routine for changing the mesh size (i.e. increasing ΔT) during computation is presently only found in PROGRAM POWRATE but could easily be incorporated in PROGRAM MALRATE.

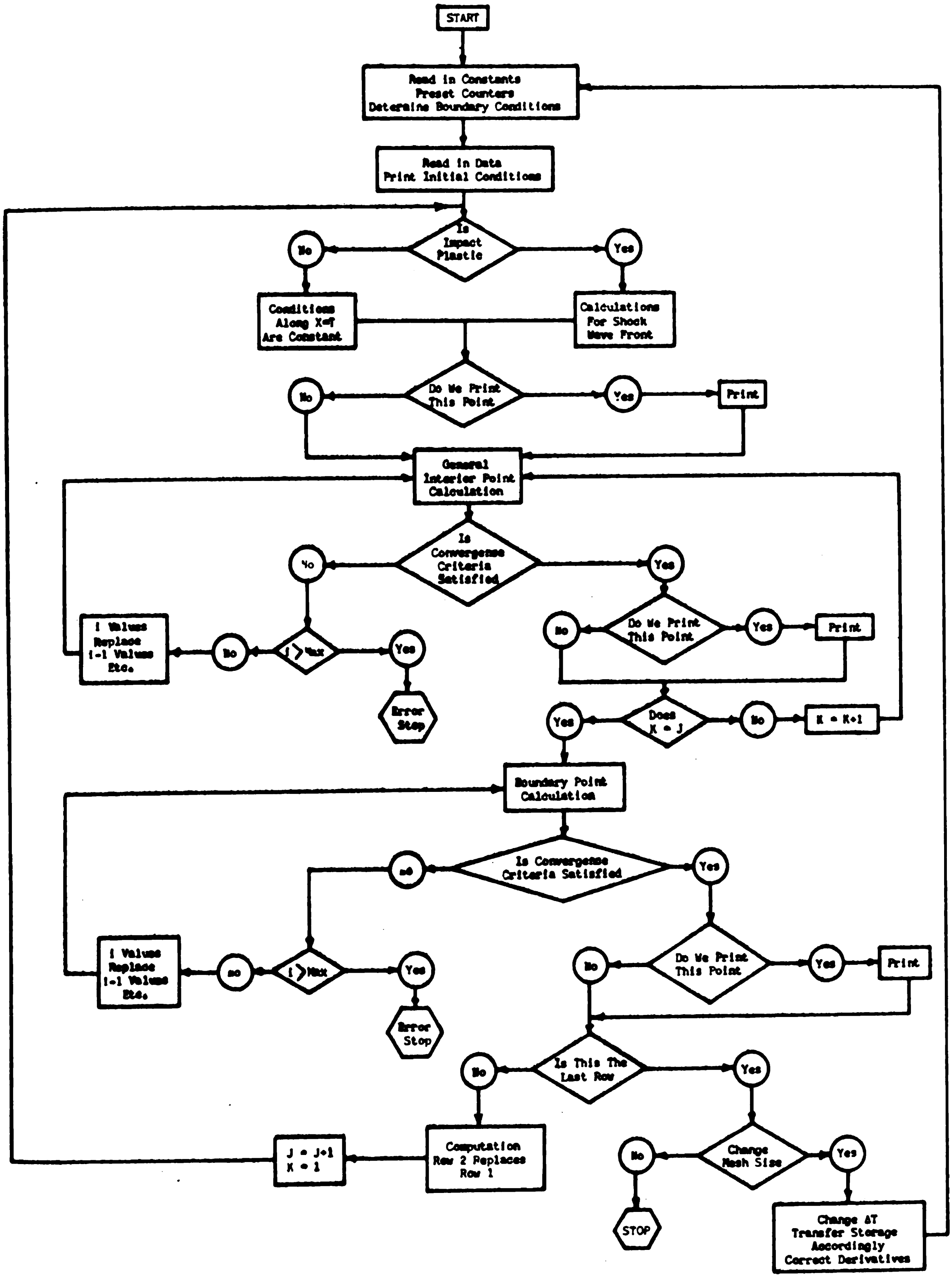

COMPUTATION FLOW CHART

A.5 Fortran Programs

The following Fortran programs (with illustrative data cards) have been programmed for the CDC-3600 and use an iteration convergence criteria of agreement to ten significant figures for two successive iterations. The following items should be taken into account before attempting to use either program.

1. The programs are presented with the warning that all of the possible boundary conditions have not been used to date, and hence, errors may exist.

2. Computer must provide a minimum of ten digit storage capability plus sufficient storage for program and variables.

3. Beware of time requirements.

PROGRAM	L	Impact B.C.	Approximate Machine Time on CDC-3600
MALRATE	401	$\sigma(0,t)$ = constant	4½ minutes
POWRATE	501	velocity data from Gage Station One Spec. No.7	20 minutes

4. Proper choice of ΔT is not necessarily known a' priori. Given an initial set of input data for which the choice of ΔT gives convergence only into a small (or not

at all) region of the characteristic X,T-plane, interpolation of already punched data may be used with another choice of ΔT. The illustrative examples given below were the schemes actually used with the velocity input data from the velocity transducer.

<u>TO HALVE ΔT</u>

```
201     READ 4, (V(2,N), N=J,L,2)
        DO 202 N=J,L,2
202     V(2,N) =  V(2,N)/CO
        LLL = L-1
        DO 203 N=2,LLL,2
203     V(2,N) = 0.5*(V(2,N-1) + V(2,N+1))
        CONTINUE
```

<u>TO QUARTER ΔT</u>

```
201     READ 4,(V(2,N), N=J,L,4)
        DO 202 N=J,L,4
202     V(2,N) = -V(2,N)/CO
        LLL = L-3
        DO 203 N=2,LLL,4
        TEMP = V(2,N+3) - V(2,N-1)
        V(2,N) = V(2,N-1) + 0.25*TEMP
        V(2,N+1) = V(2,N-1) + 0.50*TEMP
203     V(2,N+2) = V(2,N-1) + 0.75*TEMP
        CONTINUE
```

```
      PROGRAM MALRATE
    1 FORMAT (1X,3HROW,3X,6HCOLUMN,9X,6HSTRESS,13X,6HSTRAIN,
     111X,8HVELOCITY,9X,10HG FUNCTION,8X,10HITERATIONS/)
    2 FORMAT (1X,I3,5X,I3,4X,4(E16.10,3X),3X,I3)
    3 FORMAT (14(I4,1X))
    4 FORMAT (5(E16.10))
   41 FORMAT(1X,2HJ=,I3,3X,2HK=,I3,3X,7HNUMBER=,I3)
    5 FORMAT (1X,2HJ=,I3,4X,5HLOOK=,I2,4X,3HM1=,I3,4X,3HM3=,
     1I3,4X,4HMAX=,I3/1X,2HK=,I3,4X,5HJAZZ=,I2,4X,3M72=,I3,
     24X,3HM4=,I3,4X,2HL=,I3,3X,3HLL=,I3,3X,7HIMPACT=,I3,3X,
     34HMAD=,I3/)
    6 FORMAT (1X,3HEO=,E16.10,4X,4HRHO=,E16.10,4X,3HCO=,
     1E16.10,4X,2HT=,E16.10/)
    7 FORMAT (1X,2HA=,E16.10,4X,2HB=,E16.10,4X,2HC=,E16.10,
     14X,2HD=,E16.10,4X,2HP=,E16.10/,/1X,6HYIELD=,E16.10,4X,
     25HVMAX=,E16.10,4X,5HTFIX=,E16.10,4X,5HCENT=,E16.10/,
     3/1X,2HQ=,E16.10,4X,2HF=,E16.10,4X,4HTIM=,E16.10/,/)
    8 FORMAT (1X,6HALPHA=,E16.10,4X,5HBETA=,E16.10,4X,
     116HYIELD REACHED AT,1X,E16.10,2X,
     225HMICROSECONDS AFTER IMPACT/,/)
    9 FORMAT (/1X,25HG FUNCTION = .1E-07 AT J=,I4,3X,2HK=,
     1I4/)
      DIMENSION S(2,401),E(2,401),V(2,401),G(2,401),SP(5),
     1SPP(5),EP(5),EPP(5)
      READ 3,J,K,L,LOOK,JAZZ,MAX,M1,M2,M3,M4,LL,IMPACT
      READ 4,T,EO,RHO,A,B,C,D,P,YIELD,VMAX,TFIX,CENT,Q,F
      CO=SQRTF(EO/RHO)
      PRINT 5,J,LOOK,M1,M3,MAX,K,JAZZ,M2,M4,L,LL,IMPACT
      PRINT 6,EO,RHO,CO,T
      PRINT 7,A,B,C,D,P,YIELD,VMAX,TFIX,CENT,Q,F
      NUMBER=0
      MARK=1
      E1=0.0
      E2=0.0
      E3=0.0
      E4=0.0
      S1=0.0
      S2=0.0
      S3=0.0
      S4=0.0
      DO 98 N=1,401
      S(1,N)=0.0
      S(2,N)=0.0
      E(1,N)=0.0
      E(2,N)=0.0
      V(1,N)=0.0
      V(2,N)=0.0
      G(1,N)=0.0
   98 G(2,N)=0.0
      DO 99 N=1,5
```

```
      EP(N)=0.0
      EPP(N)=0.0
      SP(N)=0.0
   99 SPP(N)=0.0
C     VELOCITY , STRESS OR STRAIN BOUNDARY CONDITIONS AT X=0
      GO TO (100,200,300,400),LOOK
C     IMPACT VELOCITY IS CONSTANT
  100 READ 4,VOL
      V(1,1)=VOL/CO
      E(1,1)=-V(1,1)
      S(1,1)=-V(1,1)
      DO 101 N=1,L
  101 V(2,N)=V(1,1)
      GO TO 500
C     IMPACT VELOCITY IS A KNOWN VARIABLE
  200 GO TO (201,210),JAZZ
C     IMPACT VELOCITY IS A TABULATED VARIABLE    IN/SEC
  201 READ 4,(V(2,N),N=1,L)
      DO 202 N=1,L
  202 V(2,N)=V(2,N)/CO
      GO TO 225
C     IMPACT VELOCITY IS GIVEN AS AN EXPONENTIAL FUNCTION
  210 TEMP=1.0/(1.0-CENT)
      ALPHA=LOGF(TEMP)/TFIX
      TEMP=EO*VMAX
      BETA=LOGF(TEMP/(TEMP+CO*YIELD))
      TEMP=BETA/ALPHA
      PRINT 8,ALPHA,BETA,TEMP
      DO 220 N=1,L
      WER=2*(N-1)
      TEMP=EXPF(ALPHA*T*WER+BETA)
  220 V(2,N)=VMAX*(1.0-1.0/TEMP)/CO
  225 V(1,1)=V(2,1)
      S(1,1)=-V(1,1)
      E(1,1)=-V(1,1)
      S(2,1)=S(1,1)
      E(2,1)=E(1,1)
      G(2,1)=S(2,1)-B+A/E(2,1)
      GO TO 500
C     IMPACT STRESS IS A KNOWN VARIABLE
  300 GO TO (301,310),JAZZ
C     IMPACT STRESS IS TABULATED   PSI
  301 READ 4,(S(2,N),N=1,L)
      DO 302 N=1,L
  302 S(2,N)=S(2,N)/EO
      GO TO 325
C     IMPACT STRESS IS A CONSTANT -- THEN ZERO
  310 READ 4,STRS
      DO 311 N=1,LL
  311 S(2,N)=STRS/EO
```

```
      LL=LL+1
      IF(LL-L) 312,312,325
  312 DO 313 N=LL,L
  313 S(2,N)=0.0
  325 S(1,1)=S(2,1)
      E(1,1)=S(1,1)
      V(1,1)=-S(1,1)
C     WILL BE RECOMPUTED BELOW IF INITIAL IMPACT IS PLASTIC
      E(2,1)=E(1,1)
      V(2,1)=V(1,1)
      G(2,1)=S(2,1)-B+A/E(2,1)
      GO TO 500
C     STRAIN HISTORY IS GIVEN
  400 READ 4,(E(2,N),N=1,LL)
      IF(LL-L) 412,425,425
C     STRAIN IS NOW CONSTANT
  412 LLL=LL+1
      DO 413 N=LLL,L
  413 E(2,N)=E(2,LL)
  425 S(1,1)=E(2,1)
      E(1,1)=E(2,1)
      V(1,1)=-E(2,1)
C     WILL BE RECOMPUTED BELOW IF INITIAL IMPACT IS PLASTIC
      S(2,1)=E(2,1)
      V(2,1)=-E(2,1)
      G(2,1)=S(2,1)-B+A/E(2,1)
      GO TO 500
C     PRINT OUT OF IMPACT CONDITIONS
  500 PRINT 1
      STRESS=S(1,1)*EO
      VELOC=V(1,1)*CO
      G(1,1)=S(1,1)-B+A/E(1,1)
      PRINT 2,J,K,STRESS,E(1,1),VELOC,G(1,1)
C     GO TO FIRST POINT AFTER IMPACT
      J=J+1
      GO TO (1000,1045),IMPACT
C     CALC. ALONG X=CO*T FOR PLASTIC INITIAL IMPACT
 1000 TT=2.0/T
      F1=TT*(P-Q+LOGF(F*P))
 1001 TAX=J-1
 1002 P1=P
      P=P+D
      F2=TT*(P-Q+LOGF(F*P))
      DI=F2-TAX
      IF(DI) 1010,1010,1020
 1010 F1=F2
      GO TO 1002
 1020 IF(DI-.1E-09) 1040,1040,1030
C     FALSE POSITION ITERATION
 1030 R=F2-F1
```

```
      P=P-(P-P1)*DI/R
      F2=TT*(P-Q+LOGF(F*P))
      DI=F2-TAX
      NUMBER=NUMBER+1
      GO TO 1020
 1040 S(2,1)=C+C/P
      E(2,1)=S(2,1)
      V(2,1)=-S(2,1)
      G(2,1)=S(2,1)-B+A/S(2,1)
      F1=F2
      D=1.01*D
C     DO WE PRINT THIS ROW
 1045 IF(J-M1) 1060,1050,1060
C     DO WE PRINT THIS COLUMN
 1050 IF(K-M2) 1060,1055,1060
C     PRINT THIS POINT
 1055 M2=M2+M3
      STRESS=E0*S(2,K)
      VELOC=C0*V(2,K)
      PRINT 2,J,K,STRESS,E(2,K),VELOC,G(2,K),NUMBER
C     MOVE TO THE NEXT POINT IN COLUMN
 1060 K=K+1
      NO=0
      NUMBER=0
      GO TO 1100
C     ARE WE IN THE FIRST FIVE ROWS
 1100 IF(K-5) 1110,1110,1120
C     ARE WE IN THE LAST TWO ROWS IN THIS COLUMN
 1110 IF(J-K-2) 1114,1112,1112
C     INITIAL ESTIMATES FOR THE FIRST FIVE ROWS
 1112 DELS=SP(K)+SPP(K)
      DELE=EP(K)+EPP(K)
      DELG=DELS-A*DELE/(E(1,K)*E(1,K))
      Z=G(1,K)+DELG
      GO TO 1130
C     INITIAL ESTIMATES FOR THE LAST TWO ROWS IN THIS COLUMN
 1114 Z=G(2,K-1)
      GO TO 1130
C     ESTIMATE FOR GENERAL INTERIOR POINT
 1120 DELS=2.0*S(2,K-1)-3.0*S(2,K-2)+S(2,K-3)
      DELE=2.0*E(2,K-1)-3.0*E(2,K-2)+E(2,K-3)
      DELG=DELS-A*DELE/(E(2,K-1)*E(2,K-1))
      Z=G(2,K-1)+DELG
      GO TO 1130
C     CONSTANTS WHICH ARE FUNCTIONS OF ADJACENT STATE POINTS
 1130 DC=S(2,K-1)+V(2,K-1)-.5*T*G(2,K-1)
      DB=-S(1,K-1)+E(1,K-1)+T*G(1,K-1)
      DA=S(1,K)-V(1,K)-.5*T*G(1,K)
C     INTERIOR OR END POINT
      IF(J-K) 2047,1150,1140
```

```
C      INTERIOR POINT CALCULATION
 1140 C2=.5*(DA+DC)
      C1=C2+DB
      TEMP=.5*T*Z
      E4=C1+TEMP
      S4=C2-TEMP
      Z=S4-B+A/E4
      GO TO 1240
C      END POINT -- CHECK BOUNDARY CONDITION
 1150 GO TO (1160,1160,1180,1190),LOOK
C      VELOCITY BOUNDARY CONDITION
 1160 C4=DC-V(2,K)
      C3=C4+DB
      TEMP=.5*T*Z
      E4=C3+TEMP
      S4=C4-TEMP
      Z=S4-B+A/E4
      GO TO 1260
C      STRESS BOUNDARY CONDITION
 1180 X=S(2,K)
      C5=DB+X
      E4=C5+T*Z
      C6=X-B
      Z=C6+A/E4
      GO TO 1280
C      STRAIN BOUNDARY CONDITION
 1190 X=E(2,K)
      C7=X-DB
      C8=-C7+DC
      S4=C7-T*Z
      C9=-B+A/X
      Z=S4+C9
      GO TO 1220
C      END POINT -- STRAIN B. C. --  SEIDEL OR AITKEN CORRECTION
 1220 IF(NO-4) 1224,1224,1221
C      AITKEN CORRECTION METHOD
 1221 DELS1=S2-S1
      DELS2=S3-S2
      DELS3=S4-S3
      DELS4=S5-S4
      RSSQ=(DELS2*DELS4-DELS3*DELS3)/(DELS1*DELS3-DELS2*DELS2)
      DELSS2=DELS3-DELS2
      DELSS3=DELS4-DELS3
      DENOMS=DELSS3-RSSQ*DELSS2
C      DENOMINATOR CHECK
      IF(ABSF(DENOMS)) 1224,1224,1223
C      DENOMINATOR DOES NOT VANISH
 1223 S5=S4-DELS3*(DELS4-RSSQ*DELS3)/DENOMS
      Z=S5+C9
      NO=1
```

```
      NUMBER=NUMBER+1
      GO TO 1220
C     SEIDEL ITERATION
 1224 S1=S2
      S2=S3
      S3=S4
      S4=S5
 1225 S5=C7-T*Z
      Z=S5+C9
      NUMBER=NUMBER+1
      DIFF=ABSF(S5-S4)
C     CONVERSION CHECK TO TEN DIGITS
      IF(S5-0.01) 1226,1228,1228
 1226 IF(S5-0.001) 1227,1229,1229
 1227 IF(S5-0.0001) 1231,1230,1230
 1228 IF(DIFF-.1E-10)  1235,1235,1237
 1229 IF(DIFF-.1E-11) 1235,1235,1237
 1230 IF(DIFF-.1E-12) 1235,1235,1237
 1231 IF(DIFF-.1E-13) 1235,1235,1237
 1235 V(2,K)=C8+.5*T*Z
      S(2,K)=S5
      G(2,K)=Z
C     SEARCH FOR FIRST POINT WHERE G-FUNCTION VANISHES
      GO TO (2030,2032),MARK
 2030 IF(Z) 2031,2031,2032
 2031 PRINT 9,J,K
      MARK=2
 2032 CONTINUE
C     ARE WE IN THE FIRST FIVE ROWS
      IF(K-5) 1236,1236,1300
C     NEW PARTIAL DERIVATIVES ALONG THE ROW
 1236 TEMP=S(2,K)-S(1,K)
      SPP(K)=TEMP-SP(K)
      TEMP=E(2,K)-E(1,K)
      EPP(K)=TEMP-EP(K)
      EP(K)=TEMP
      GO TO 1300
C     COUNTER FOR AITKEN CORRECTION
 1237 NO=NO+1
C     ARE THE ITERATIONS BOUNDED
      IF(NUMBER-MAX) 1220,1220,2047
C     INTERIOR POINT -- SEIDEL OR AITKEN DELTA SQUARE ITERATION
 1240 IF(NO-4) 1244,1244,1241
C     AITKEN CORRECTION METHOD
 1241 DELE1=E2-E1
      DELE2=E3-E2
      DELE3=E4-E3
      DELE4=E5-E4
      DELS1=S2-S1
      DELS2=S3-S2
```

```
      DELS3=S4-S3
      DELS4=S5-S4
      RESQ=(DELE2*DELE4-DELE3*DELE3)/(DELE1*DELE3-DELE2*DELE2)
      RSSQ=(DELS2*DELS4-DELS3*DELS3)/(DELS1*DELS3-DELS2*DELS2)
      DELEE2=DELE3-DELE2
      DELEE3=DELE4-DELE3
      DELSS2=DELS3-DELS2
      DELSS3=DELS4-DELS3
      DENOME=DELEE3-RESQ*DELEE2
      DENOMS=DELSS3-RSSQ*DELSS2
C     DENOMINATOR CHECK IN AITKEN METHOD
      IF(ABSF(DENOMS)) 1244,1244,1242
 1242 IF(ABSF(DENOME)) 1244,1244,1243
C     DENOMINATORS DO NOT VANISH
 1243 E5=E4-DELE3*(DELE4-RESQ*DELE3)/DENOME
      S5=S4-DELS3*(DELS4-RSSQ*DELS3)/DENOMS
      Z=S5-B+A/E5
      NO=1
      NUMBER=NUMBER+1
      GO TO 1240
C     SEIDEL ITERATION
 1244 E1=E2
      E2=E3
      E3=E4
      E4=E5
      S1=S2
      S2=S3
      S3=S4
      S4=S5
 1245 TERM=.5*T*Z
      E5=C1+TERM
      TEMP1=-B+A/E5
      Z=S4+TEMP1
      TERM=.5*T*Z
      S5=C2-TERM
      Z=S5+TEMP1
      NUMBER=NUMBER+1
      DIFF=ABSF(E5-E4)
C     CONVERGENCE CHECK TO TEN DIGITS
      IF(E5-0.01) 1246,1248,1248
 1246 IF(E5-0.001) 1247,1249,1249
 1247 IF(E5-0.0001) 1251,1250,1250
 1248 IF(DIFF-.1E-10) 1255,1255,1257
 1249 IF(DIFF-.1E-11) 1255,1255,1257
 1250 IF(DIFF-.1E-12) 1255,1255,1257
 1251 IF(DIFF-.1E-13) 1255,1255,1257
 1255 S(2,K)=S5
      E(2,K)=E5
      V(2,K)=.5*(-DA+DC)
      G(2,K)=Z
```

```
C      SEARCH FOR FIRST POINT ATTAINING STATIC S-E VALUE
       GO TO (2000,2002),MARK
 2000  IF(Z) 2001,2001,2002
 2001  PRINT 9,J,K
       MARK=2
 2002  CONTINUE
C      ARE WE IN THE FIRST FIVE ROWS
       IF(K-5) 1256,1256,1045
C      NEW PARTIAL DERIVATIVES ALONG THE ROW
 1256  TEMP=S(2,K)-S(1,K)
       SPP(K)=TEMP-SP(K)
       SP(K)=TEMP
       TEMP=E(2,K)-E(1,K)
       EPP(K)=TEMP-EP(K)
       EP(K)=TEMP
       GO TO 1045
C      COUNTER FOR AITKEN CORRECTION
 1257  NO=NO+1
C      ARE THE ITERATIONS BOUNDED
       IF(NUMBER-MAX) 1240,1240,2047
C      END POINT -- VELOCITY B. C. -- SEIDEL OR AITKEN CORRECTION
 1260  IF(NO-4) 1264,1264,1261
C      AITKEN CORRECTION METHOD
 1261  DELE1=E2-E1
       DELE2=E3-E2
       DELE3=E4-E3
       DELE4=E5-E4
       DELS1=S2-S1
       DELS2=S3-S2
       DELS3=S4-S3
       DELS4=S5-S4
       RESQ=(DELE2*DELE4-DELE3*DELE3)/(DELE1*DELE3-DELE2*DELE2)
       RSSQ=(DELS2*DELS4-DELS3*DELS3)/(DELS1*DELS3-DELS2*DELS2)
       DELEE2=DELE3-DELE2
       DELEE3=DELE4-DELE3
       DELSS2=DELS3-DELS2
       DELSS3=DELS4-DELS3
       DENOME=DELEE3-RESQ*DELEE2
       DENOMS=DELSS3-RSSQ*DELSS2
C      DENOMINATOR CHECK
       IF(ABSF(DENOMS)) 1264,1264,1262
 1262  IF(ABSF(DENOME)) 1264,1264,1263
C      DENOMINATORS DO NOT VANISH
 1263  E5=E4-DELE3*(DELE4-RESQ*DELE3)/DENOME
       S5=S4-DELS3*(DELS4-RSSQ*DELS3)/DENOMS
       Z=S5-B+A/E5
       NO=1
       NUMBER=NUMBER+1
       GO TO 1260
C      SEIDEL ITERATION
```

```
 1264 E1=E2
      E2=E3
      E3=E4
      E4=E5
      S1=S2
      S2=S3
      S3=S4
      S4=S5
 1265 TERM=.5*T*Z
      E5=C3+TERM
      TEMP1=-B+A/E5
      Z=S4+TEMP1
      TERM=.5*T*Z
      S5=C4-TERM
      Z=S5+TEMP1
      NUMBER=NUMBER+1
      DIFF=ABSF(E5-E4)
C     CONVERSION CHECK TO TEN DIGITS
      IF(E5-0.01) 1266,1268,1268
 1266 IF(E5-0.001) 1267,1269,1269
 1267 IF(E5-0.0001) 1271,1270,1270
 1268 IF(DIFF-.1E-10) 1275,1275,1277
 1269 IF(DIFF-.1E-11) 1275,1275,1277
 1270 IF(DIFF-.1E-12) 1275,1275,1277
 1271 IF(DIFF-.1E-13) 1275,1275,1277
 1275 S(2,K)=S5
      E(2,K)=E5
      G(2,K)=Z
C     SEARCH FOR FIRST POINT ATTAINING STATIC S-E VALUE
      GO TO (2010,2012),MARK
 2010 IF(Z) 2011,2011,2012
 2011 PRINT 9,J,K
      MARK=2
 2012 CONTINUE
C     ARE WE IN THE FIRST FIVE ROWS
      IF(K-5) 1276,1276,1300
C     NEW PARTIAL DERIVATIVES ALONG THE ROW
 1276 TEMP=S(2,K)-S(1,K)
      SPP(K)=TEMP-SP(K)
      SP(K)=TEMP
      TEMP=E(2,K)-E(1,K)
      EPP(K)=TEMP-EP(K)
      EP(K)=TEMP
      GO TO 1300
C     COUNTER FOR AITKEN CORRECTION
 1277 NO=NO+1
C     ARE THE ITERATIONS BOUNDED
      IF(NUMBER-MAX) 1260,1260,2047
C     END POINT -- VELOCITY B. C. -- SEIDEL OR AITKEN CORRECTION
 1280 IF(NO-4) 1284,1284,1281
```

```
C       AITKEN CORRECTION METHOD
 1281 DELE1=E2-E1
      DELE2=E3-E2
      DELE3=E4-E3
      DELE4=E5-E4
      RESQ=(DELE2*DELE4-DELE3*DELE3)/(DELE1*DELE3-DELE2*DELE2)
      DELEE2=DELE3-DELE2
      DELEE3=DELE4-DELE3
      DENOME=DELEE3-RESQ*DELEE2
C       DENOMINATOR CHECK
      IF(ABSF(DENOME)) 1284,1284,1283
C       DENOMINATOR DOES NOT VANISH
 1283 E5=E4-DELE3*(DELE4-RESQ*DELE3)/DENOME
      Z=X-B+A/E5
      NO=1
      NUMBER=NUMBER+1
      GO TO 1280
C       SEIDEL ITERATION
 1284 E1=E2
      E2=E3
      E3=E4
      E4=E5
 1285 E5=C5+T*Z
      Z=C6+A/E5
      NUMBER=NUMBER+1
      DIFF=ABSF(E5-E4)
C       CONVERSION CHECK TO TEN DIGITS
      IF(E5-0.01) 1286,1288,1288
 1286 IF(E5-0.001) 1287,1289,1289
 1287 IF(E5-0.0001) 1291,1290,1290
 1288 IF(DIFF-.1E-10) 1295,1295,1297
 1289 IF(DIFF-.1E-11) 1295,1295,1297
 1290 IF(DIFF-.1E-12) 1295,1295,1297
 1291 IF(DIFF-.1E-13) 1295,1295,1297
 1295 V(2,K)=DC-X-.5*T*Z
      E(2,K)=E5
      G(2,K)=Z
C       SEARCH FOR FIRST POINT ATTAINING STATIC S-E VALUE
      GO TO (2020,2022),MARK
 2020 IF(Z) 2021,2021,2022
 2021 PRINT 9,J,K
      MARK=2
 2022 CONTINUE
C       ARE WE IN THE FIRST FIVE ROWS
      IF(K-5) 1296,1296,1300
C       NEW PARTIAL DERIVATIVES ALONG THE ROW
 1296 TEMP=S(2,K)-S(1,K)
      SPP(K)=TEMP-SP(K)
      SP(K)=TEMP
      TEMP=E(2,K)-E(1,K)
```

```
      EPP(K)=TEMP-EP(K)
      EP(K)=TEMP
      GO TO 1300
C     COUNTER FOR AITKEN CORRECTION
 1297 NO=NO+1
C     ARE THE ITERATIONS BOUNDED
      IF(NUMBER-MAX) 1280,1280,2047
C     ARE WE PRINTING THIS ROW
 1300 IF(J-M1) 1330,1310,1330
C     DO WE PRINT THIS COLUMN
 1310 IF(K-M2) 1330,1320,1330
C     PRINT THIS POINT
 1320 STRESS=EO*S(2,K)
      VELOC=CO*V(2,K)
      PRINT2,J,K,STRESS,E(2,K),VELOC,G(2,K),NUMBER
C     NEXT ROW AND COLUMN TO BE PRINTED
      M1=M1+M4
      M2=1
C     HAVE WE CALCULATED THE LAST ROW
 1330 IF(J-L) 1340,2047,2047
C     STORAGE TRANSFER BEFORE MOVING ON TO NEXT COLUMN
 1340 DO 1350 N=1,J
      S(1,N)=S(2,N)
      E(1,N)=E(2,N)
      V(1,N)=V(2,N)
 1350 G(1,N)=G(2,N)
C     GO TO FIRST POINT IN NEXT COLUMN
      J=J+1
      K=1
      NUMBER=0
C     CHECK B. C. -- IS LEADING WAVE FRONT CALC. NEEDED
      GO TO (1001,1045),IMPACT
C     HAVE WE REACHED LAST ROW
 2047 IF (J-L) 2046,2045,2046
C     ERROR STOP -- OUTPUTS STORAGE
 2046 PRINT 41,J,K,NUMBER
C     PROGRAM OVER
 2045 STOP
      END
      END
```

SAMPLE DATA -- PROGRAM MALRATE -- CONSTANT STRESS BOUNDARY CONDITION

```
0001 0001 0401 0003 0002 0050 0011 0001 0010 0010 0401 0001
 .5000000000E 00 .1000000000E 08 .2500000000E-03 .1000000000E-05 .2000000000E
 .1000000000E-02 .1000000000E 00 .1450000000E 01 .1000000000E 05-.6000000000E
 .1000000000E 03 .9000000000E 00 .1333333333E+01 .7500000000E 00
 .1750000000E 05
```

```
      PROGRAM POWRATE
    1 FORMAT (1X,3HROW,3X,6HCOLUMN,9X,6HSTRESS,13X,6HSTRAIN,
     111X,8HVELOCITY,9X,10HG FUNCTION,8X,10HITERATIONS/)
    2 FORMAT (1X,I3,5X,I3,4X,4(E16.10,3X),3X,I3)
    3 FORMAT (14(I4,1X))
   31 FORMAT (10(1X,I4))
   32 FORMAT (6(1X,E16.10))
   33 FORMAT (4(E16.10))
    4 FORMAT (5(E16.10))
   41 FORMAT (1X,2HJ=,I3,3X,2HK=,I3,3X,7HNUMBER=,I3)
    5 FORMAT (1X,2HJ=,I3,4X,5HLOOK=,I2,4X,3HM1=,I3,4X,3HM3=,
     1I3,4X,4HMAX=,I3/1X,2HK=,I3,4X,5HJAZZ=,I2,4X,3M72=,I3,
     24X,3HM4=,I3,4X,2HL=,I3,3X,3HLL=,I3,3X,7HIMPACT=,I3,3X,
     34HMAD=,I3/)
    6 FORMAT (1X,3HEO=,E16.10,4X,4HRHO=,E16.10,4X,3HCO=,
     1E16.10,4X,2HT=,E16.10/)
    7 FORMAT (1X,2HA=,E16.10,4X,2HB=,E16.10,4X,2HC=,E16.10,
     14X,2HD=,E16.10,4X,2HP=,E16.10/,/1X,6HYIELD=,E16.10,4X,
     25HVMAX=,E16.10,4X,5HTFIX=,E16.10,4X,5HCENT=,E16.10/,
     3/1X,2HQ=,E16.10,4X,2HF=,E16.10,4X,4HTIM=,E16.10/,/)
    8 FORMAT (1X,6HALPHA=,E16.10,4X,5HBETA=,E16.10,4X,
     116HYIELD REACHED AT,1X,E16.10,2X,
     225HMICROSECONDS AFTER IMPACT/,/)
    9 FORMAT (/1X,25HG FUNCTION = .1E-07 AT J=,I4,3X,2HK=,I4/)
   91 FORMAT (/,/)
      DIMENSION S(2,601),E(2,601),V(2,601),G(2,601),SP(601),
     1SPP(601),EP(601),EPP(601)
      MARK=1
      E1=0.0
      E2=0.0
      E3=0.0
      E4=0.0
      S1=0.0
      S2=0.0
      S3=0.0
      S4=0.0
      DO 98 N=1,401
      S(1,N)=0.0
      S(2,N)=0.0
      E(1,N)=0.0
      E(2,N)=0.0
      V(1,N)=0.0
      V(2,N)=0.0
      G(1,N)=0.0
   98 G(2,N)=0.0
      DO 99 N=1,401
      EP(N)=0.0
      EPP(N)=0.0
      SP(N)=0.0
   99 SPP(N)=0.0
```

```
  999 READ 3,J,K,L,LOOK,JAZZ,MAX,M1,M2,M3,M4,LL,IMPACT,MAD
      READ 4,T,EO,RHO,A,B,C,D,P,YIELD,VMAX,TFIX,CENT,Q,F,TIM
      C=EO/A
      CO=SQRTF(EO/RHO)
      PRINT 5,J,LOOK,M1,M3,MAX,K,JAZZ,M2,M4,L,LL,IMPACT,MAD
      PRINT 6,EO,RHO,CO,T
      PRINT 7,A,B,C,D,P,YIELD,VMAX,TFIX,CENT,Q,F,TIM
      NUMBER=0
C     VELOCITY , STRESS OR STRAIN BOUNDARY CONDITIONS AT X=0
      GO TO (100,200,300,400),LOOK
C     IMPACT VELOCITY IS A CONSTANT
  100 READ 4,VOL
      V(1,1)=-VOL/CO
      E(1,1)=-V(1,1)
      S(1,1)=-V(1,1)
      DO 101 N=1,L
  101 V(2,N)=V(1,1)
      GO TO 500
C     IMPACT VELOCITY IS A KNOWN VARIABLE
  200 GO TO (201,210),JAZZ
C     IMPACT VELOCITY IS A TABULATED VARIABLE    IN/SEC
  201 READ 4,(V(2,N),N=J,L,1)
      DO 202 N=J,L,1
  202 V(2,N)=V(2,N)/CO
      GO TO 225
C     IMPACT VELOCITY IS GIVEN AS AN EXPONENTIAL FUNCTION
  210 TEMP=1.0/(1.0-CENT)
      ALPHA=LOGF(TEMP)/TFIX
      TEMP=EO*VMAX
      BETA=LOGF(TEMP/(TEMP+CO*YIELD))
      PRINT 8,ALPHA,BETA,TEMP
      DO 220 N=J,L
      WER=2*(N-1)
      TEMP=EXPF(ALPHA*T*WER+BETA)
  220 V(2,N)=VMAX*(1.0-1.0/TEMP)/CO
  225 V(1,1)=V(2,1)
      E(1,1)=(-SQRTF(RHO/(A*B))*B+1.0)*V(1,1)*0.5*CO)**
     1(2.0/(B+1.0))
      S(1,1)=(A*(E(1,1)**B))/EO
      S(2,1)=S(1,1)
      E(2,1)=E(1,1)
      G(2,1)=.1E-07*(C*S(2,1)/(E(2,1)**B))**Q
      GO TO 500
C     IMPACT STRESS IS A KNOWN VARIABLE
  300 GO TO (301,310),JAZZ
C     IMPACT STRESS IS TABULATED    PSI
  301 READ 4,(S(2,N),N=J,L)
      DO 302 N=J,L
  302 S(2,N)=S(2,N)/EO
      GO TO 325
```

```
  310 READ 4,STRS
      DO 311 N=J,LL
  311 S(2,N)=STRS/EO
      LL=LL+1
      IF(LL-L) 312,312,325
  312 DO 313 N=LL,L
  313 S(2,N)=0.0
  325 S(1,1)=S(2,1)
      E(1,1)=S(1,1)
      V(1,1)=-S(1,1)
C     WILL BE RECOMPUTED BELOW IF INITIAL IMPACT IS PLASTIC
      E(2,1)=E(1,1)
      V(2,1)=V(1,1)
      G(2,1)=.1E-07*(C*S(2,1)/(E(2,1)**B))**Q
      GO TO 500
C     STRAIN HISTORY IS GIVEN
  400 READ 4,(E(2,N),N=J,LL)
      IF(LL-L) 412,425,425
C     STRAIN IS NOW CONSTANT
  412 LLL=LL+1
      DO 413 N=LLL,L
  413 E(2,N)=E(2,LL)
  425 S(1,1)=E(2,1)
      E(1,1)=E(2,1)
      V(1,1)=-E(2,1)
C     WILL BE RECOMPUTED BELOW IF IMPACT IS INITIALLY PLASTIC
      S(2,1)=E(1,1)
      V(2,1)=V(1,1)
      G(2,1)=.1E-07*(C*S(2,1)/(E(2,1)**B))**Q
      GO TO 500
C     PRINT OUT OF IMPACT CONDITIONS
  500 PRINT 1
  503 G(1,1)=.1E-07*(C*S(1,1)/(E(1,1)**B))**Q
  504 STRESS=S(1,1)*EO
      VELOC=V(1,1)*CO
      PRINT 2,J,K,STRESS,E(1,1),VELOC,G(1,1)
C     GO TO FIRST POINT AFTER IMPACT
      J=J+1
      GO TO (1000,1045),IMPACT
C     CALC. ALONG X=CO*T FOR PLASTIC INITIAL IMPACT
 1000 TT=(2.0/T)*.1E+09/(Q*(1.0-B)-1.0)
      DOT=S(1,1)/(C*S(1,1)**(1.0-B))**Q
      TEMP=P/(C*P**(1.0-B))**Q
      F1=TT*(TEMP-DOT)
 1001 TAX=J-1
 1002 P2=P
      P=P+D
      TEMP=P/(C*P**(1.0-B))**Q
      F2=TT*(TEMP-DOT)
      DI=F2-TAX
```

```
     IF(DI) 1010,1010,1020
1010 F1=F2
     GO TO 1002
1020 IF(DI-.1E-09) 1041,1041,1030
1030 P2=P1
     P1=P
1031 R=F2-F1
     P2=P1+(P2-P1)*DI/R
     TEMP=P2/(C*P2**(1.0-B))**Q
     F1=TT*(TEMP-DOT)
     DI=TAX-F1
     NUMBER=NUMBER+1
     IF(DI-.1E-09) 1040,1040,1031
1040 P=P2
1041 S(2,1)=P
     E(2,1)=P
     V(2,1)=-P
     G(2,1)=.1E-07*(C*P/(P**B))**Q
     F1=F2
     D=.99*D
C    DO WE PRINT THIS ROW
1045 IF (J-M1) 1060,1050,1060
C    DO WE PRINT THIS COLUMN
1050 IF(K-M2) 1060,1055,1060
C    PRINT THIS POINT
1055 M2=M2+M3
     STRESS=E0*S(2,K)
     VELOC=C0*V(2,K)
     PRINT 2,J,K,STRESS,E(2,K),VELOC,G(2,K),NUMBER
C    MOVE TO THE NEXT POINT IN COLUMN
1060 K=K+1
     NO=0
     NUMBER=0
     GO TO 1100
1100 IF(J-K-3) 1110,1120,1125
1110 IF(J-K-1) 1111,1113,1113
1111 E4=E(1,K-1)-EP(K-1)
     S4=S(1,K-1)-SP(K-1)
     GO TO 1129
1113 E4=E(1,K)+EP(K-1)-EPP(K-1)
     S4=S(1,K)+SP(K-1)-SPP(K-1)
     GO TO 1129
1120 E4=E(1,K)+EP(K)
     S4=S(1,K)+SP(K)
     GO TO 1129
1125 E4=E(1,K)+EP(K)+EPP(K)
     S4=S(1,K)+SP(K)+SPP(K)
     GO TO 1129
C    IMPACT STRESS IS A CONSTANT -- THEN ZERO
1129 Z=.1E-07*(C*S4/(E4**B))**Q
```

```
C       CONSTANTS WHICH ARE FUNCTIONS OF ADJACENT STATE POINTS
 1130 DC=S(2,K-1)+V(2,K-1)-.5*T*G(2,K-1)
      DB=-S(1,K-1)+E(1,K-1)+T*G(1,K-1)
      DA=S(1,K)-V(1,K)-.5*T*G(1,K)
C       INTERIOR OR END POINT
      IF(J-K) 2047,1150,1140
C       INTERIOR POINT CALCULATION
 1140 C2=.5*(DA+DC)
      C1=C2+DB
      TEMP=.5*T*Z
      E4=C1+TEMP
      S4=C2-TEMP
      Z=.1E-07*(C*S4/(E4**B))**Q
      GO TO 1245
C       END POINT -- CHECK BOUNDARY CONDITION
 1150 GO TO (1160,1160,1180,1190),LOOK
C       VELOCITY BOUNDARY CONDITION
 1160 C4=DC-V(2,K)
      C3=C4+DB
      TEMP=.5*T*Z
      E4=C3+TEMP
      S4=C4-TEMP
      Z=.1E-07*(C*S4/(E4**B))**Q
      GO TO 1265
C       STRESS BOUNDARY CONDITION
 1180 X=S(2,K)
      C5=DB+X
      E4=C5+T*Z
      Z=.1E-07*(C*X/(E4**B))**Q
      GO TO 1285
C       STRAIN BOUNDARY CONDITION
 1190 X=E(2,K)
      C7=X-DB
      C8=-C7+DC
      SUN=C/(X**B)
      IF(J-L) 1192,1191,1192
 1191 S5=((.50E+08*ABSF(E(2,K)-E(1,K-1))/T)**(1.0/Q))/SUN
      GO TO 1193
 1192 S5=((.25E+08*ABSF(E(2,K+1)-E(1,K-1))/T)**(1.0/Q))/SUN
 1193 Z=.1E-07*(S5*SUN)**Q
 1235 V(2,K)=C8+.5*T*Z
      S(2,K)=S5
      G(2,K)=Z
C       SEARCH FOR FIRST POINT ATTAINING STATIC S-E VALUE
      GO TO (2030,2032),MARK
 2030 IF(Z-.1E-07) 2031,2031,2032
 2031 PRINT 9,J,K
      MARK=2
 2032 CONTINUE
C       ARE WE IN THE FIRST FIVE ROWS
```

```
      IF(K-5) 1236,1236,1300
C     NEW PARTIAL DERIVATIVES ALONG THE ROW
 1236 TEMP=S(2,K)-S(1,K)
      SPP(K)=TEMP-SP(K)
      TEMP=E(2,K)-E(1,K)
      EPP(K)=TEMP-EP(K)
      EP(K)=TEMP
      GO TO 1300
C     INTERIOR POINT -- SEIDEL OR AITKEN DELTA SQUARE ITERATION
 1240 IF(NO-4) 1244,1244,1241
C     AITKEN CORRECTION METHOD
 1241 DELE1=E2-E1
      DELE2=E3-E2
      DELE3=E4-E3
      DELE4=E5-E4
      DELS1=S2-S1
      DELS2=S3-S2
      DELS3=S4-S3
      DELS4=S5-S4
      RESQ=(DELE2*DELE4-DELE3*DELE3)/(DELE1*DELE3-DELE2*DELE2)
      RSSQ=(DELS2*DELS4-DELS3*DELS3)/(DELS1*DELS3-DELS2*DELS2)
      DELEE2=DELE3-DELE2
      DELEE3=DELE4-DELE3
      DELSS2=DELS3-DELS2
      DELSS3=DELS4-DELS3
      DENOME=DELEE3-RESQ*DELEE2
      DENOMS=DELSS3-RSSQ*DELSS2
C     DENOMINATOR CHECK IN AITKEN METHOD
      IF(ABSF(DENOMS)) 1244,1244,1242
 1242 IF(ABSF(DENOME)) 1244,1244,1243
C     DENOMINATORS DO NOT VANISH
 1243 E5=E4-DELE3*(DELE4-RESQ*DELE3)/DENOME
      S5=S4-DELS3*(DELS4-RSSQ*DELS3)/DENOMS
      Z=.1E-07*(C*S5/(E5**B))**Q
      NO=1
      NUMBER=NUMBER+1
      GO TO 1240
C     SEIDEL ITERATION
 1244 E1=E2
      E2=E3
      E3=E4
      E4=E5
      S1=S2
      S2=S3
      S3=S4
      S4=S5
 1245 TERM=.5*T*Z
      E5=C1+TERM
      TEMP1=C/(E5**B)
      Z=.1E-07*(S4*TEMP1)**Q
```

```
      TERM=.5*T*Z
      S5=C2-TERM
      Z=.1E-07*(S5*TEMP1)**Q
      NUMBER=NUMBER+1
      DIFF=ABSF(E5-E4)
C     CONVERGENCE CHECK TO TEN DIGITS
      IF(E5-0.01) 1246,1248,1248
 1246 IF(E5-0.001) 1247,1249,1249
 1247 IF(E5-0.0001) 1251,1250,1250
 1248 IF(DIFF-.1E-10) 1255,1255,1257
 1249 IF(DIFF-.1E-11) 1255,1255,1257
 1250 IF(DIFF-.1E-12) 1255,1255,1257
 1251 IF(DIFF-.1E-13) 1255,1255,1257
 1255 S(2,K)=S5
      E(2,K)=E5
      V(2,K)=.5*(-DA+DC)
      G(2,K)=Z
C     SEARCH FOR FIRST POINT ATTAINING STATIC S-E VALUE
      GO TO (2000,2002),MARK
 2000 IF(Z-.1E-07) 2001,2001,2002
 2001 PRINT 9,J,K
      MARK=2
 2002 CONTINUE
C     ARE WE IN THE FIRST FIVE ROWS
      IF(K-5) 1256,1256,1045
C     NEW PARTIAL DERIVATIVES ALONG THE ROW
 1256 TEMP=S(2,K)-S(1,K)
      SPP(K)=TEMP-SP(K)
      SP(K)=TEMP
      TEMP=E(2,K)-E(1,K)
      EPP(K)=TEMP-EP(K)
      EP(K)=TEMP
      GO TO 1045
C     COUNTER FOR AITKEN CORRECTION
 1257 NO=NO+1
C     ARE THE ITERATIONS BOUNDED
      IF(NUMBER-MAX) 1240,1240,2047
C     END POINT -- VELOCITY B. C. -- SEIDEL OR AITKEN CORRECTION
 1260 IF(NO-4) 1264,1264,1261
C     AITKEN CORRECTION METHOD
 1261 DELE1=E2-E1
      DELE2=E3-E2
      DELE3=E4-E3
      DELE4=E5-E4
      DELS1=S2-S1
      DELS2=S3-S2
      DELS3=S4-S3
      DELS4=S5-S4
      RESQ=(DELE2*DELE4-DELE3*DELE3)/(DELE1*DELE3-DELE2*DELE2)
      RSSQ=(DELS2*DELS4-DELS3*DELS3)/(DELS1*DELS3-DELS2*DELS2)
```

```
      DELEE2=DELE3-DELE2
      DELEE3=DELE4-DELE3
      DELSS2=DELS3-DELS2
      DELSS3=DELS4-DELS3
      DENOME=DELEE3-RESQ*DELEE2
      DENOMS=DELSS3-RSSQ*DELSS2
C     DENOMINATOR CHECK
      IF(ABSF(DENOMS)) 1264,1264,1262
 1262 IF(ABSF(DENOME)) 1264,1264,1263
C -   DENOMINATORS DO NOT VANISH
 1263 E5=E4-DELE3*(DELE4-RESQ*DELE3)/DENOME
      S5=S4-DELS3*(DELS4-RSSQ*DELS3)/DENOMS
      Z=.1E-07*(C*S5/(E5**B))**Q
      NO=1
      NUMBER=NUMBER+1
      GO TO 1260
C     SEIDEL ITERATION
 1264 E1=E2
      E2=E3
      E3=E4
      E4=E5
      S1=S2
      S2=S3
      S3=S4
      S4=S5
 1265 TERM=.5*T*Z
      E5=C3+TERM
      TEMP1=C/(E5**B)
      Z=.1E-07*(S4*TEMP1)**Q
      S5=C4-TERM
      Z=.1E-07*(S5*TEMP1)**Q
      NUMBER=NUMBER+1
      DIFF=ABSF(E5-E4)
C     CONVERSION CHECK TO TEN DIGITS
      IF(E5-0.01) 1266,1268,1268
 1266 IF(E5-0.001) 1267,1269,1269
 1267 IF(E5-0.0001) 1271,1270,1270
 1268 IF(DIFF-.1E-10) 1275,1275,1277
 1269 IF(DIFF-.1E-11) 1275,1275,1277
 1270 IF(DIFF-.1E-12) 1275,1275,1277
 1271 IF(DIFF-.1E-13) 1275,1275,1277
 1275 S(2,K)=S5
      E(2,K)=E5
      G(2,K)=Z
C     SEARCH FOR FIRST POINT ATTAINING STATIC S-E VALUE
      GO TO (2010,2012),MARK
 2010 IF(Z-.1E-07) 2011,2011,2012
 2011 PRINT 9,J,K
      MARK=2
 2012 CONTINUE
```

```
C       ARE WE IN THE FIRST FIVE ROWS
        IF(K-5) 1276,1276,1300
C       NEW PARTIAL DERIVATIVES ALONG THE ROW
 1276 TEMP=S(2,K)-S(1,K)
        SPP(K)=TEMP-SP(K)
        SP(K)=TEMP
        TEMP=E(2,K)-E(1,K)
        EPP(K)=TEMP-EP(K)
        EP(K)=TEMP
        GO TO 1300
C       COUNTER FOR AITKEN CORRECTION
 1277 NO=NO+1
C       ARE THE ITERATIONS BOUNDED
        IF(NUMBER-MAX) 1260,1260,2047
C       END POINT -- STRESS B. C. -- SEIDEL OR AITKEN CORRECTION
 1280 IF(NO-4) 1284,1284,1281
C       AITKEN CORRECTION METHOD
 1281 DELE1=E2-E1
        DELE2=E3-E2
        DELE3=E4-E3
        DELE4=E5-E4
        RESQ=(DELE2*DELE4-DELE3*DELE3)/(DELE1*DELE3-DELE2*DELE2)
        DELEE2=DELE3-DELE2
        DELEE3=DELE4-DELE3
        DENOME=DELEE3-RESQ*DELEE2
C       DENOMINATOR CHECK
        IF(ABSF(DENOME)) 1284,1284,1283
C       DENOMINATOR DOES NOT VANISH
 1283 E5=E4-DELE3*(DELE4-RESQ*DELE3)/DENOME
        Z=.1E-07*(C*X/(E5**B))**Q
        NO=1
        NUMBER=NUMBER+1
        GO TO 1280
C       SEIDEL ITERATION
 1284 E1=E2
        E2=E3
        E3=E4
        E4=E5
 1285 E5=C5+T*Z
        Z=.1E-07*(C*X/(E5**B))**Q
        NUMBER=NUMBER+1
        DIFF=ABSF(E5-E4)
C       CONVERSION CHECK TO TEN DIGITS
        IF(E5-0.01) 1286,1288,1288
 1286 IF(E5-0.001) 1287,1289,1289
 1287 IF(E5-0.0001) 1291,1290,1290
 1288 IF(DIFF-.1E-10) 1295,1295,1297
 1289 IF(DIFF-.1E-11) 1295,1295,1297
 1290 IF(DIFF-.1E-12) 1295,1295,1297
 1291 IF(DIFF-.1E-13) 1295,1295,1297
```

```
 1295 V(2,K)=DG-X-.5*T*Z
      E(2,K)=ES
      G(2,K)=Z
C     SEARCH FOR FIRST POINT ATTAINING STATIC S-E VALUE
      GO TO (2020,2022),MARK
 2020 IF(Z-.1E-07) 2021,2021,2022
 2021 PRINT 9,J,K
      MARK=2
 2022 CONTINUE
C     ARE WE IN THE FIRST FIVE ROWS
      IF(K-5) 1296,1296,1300
C     NEW PARTIAL DERIVATIVES ALONG THE ROW
 1296 TEMP=S(2,K)-S(1,K)
      SPP(K)=TEMP-SP(K)
      SP(K)=TEMP
      TEMP=E(2,K)-E(1,K)
      EPP(K)=TEMP-EP(K)
      EP(K)=TEMP
      GO TO 1300
C     COUNTER FOR AITKEN CORRECTION
 1297 NO=NO+1
C     ARE THE ITERATIONS BOUNDED
      IF(NUMBER-MAX) 1280,1280,2047
C     ARE WE PRINTING THIS ROW
 1300 IF(J-M1) 1330,1310,1330
C     DO WE PRINT THIS COLUMN
 1310 IF(K-M2) 1330,1320,1330
C     PRINT THIS POINT
 1320 STRESS=EO*S(2,K)
      VELOC=CO*V(2,K)
      PRINT2,J,K,STRESS,E(2,K),VELOC,G(2,K),NUMBER
      M1=M1+M4
      M2=1
C     HAVE WE CALCULATED THE LAST ROW
 1330 IF(J-L) 1340,2047,2047
C     STORAGE TRANSFER BEFORE MOVING ON TO NEXT COLUMN
 1340 DO 1350 N=1,J
      S(1,N)=S(2,N)
      E(1,N)=E(2,N)
      V(1,N)=V(2,N)
 1350 G(1,N)=G(2,N)
C     GO TO FIRST POINT IN NEXT COLUMN
      J=J+1
      K=1
      NUMBER=0
C     CHECK B. C. -- IS LEADING WAVE FRONT CALC. NEEDED
      GO TO (1001,1045),IMPACT
C     HAVE WE REACHED THE LAST ROW
 2047 IF(J-L) 2046,2045,2046
C     ERROR STOP -- OUTPUTS STORAGE
```

```
 2046 PRINT 41,J,K,NUMBER
C     PROGRAM OVER
 2045 IF(MAD-2) 2042,2044,2042
 2044 MIT=TIM
      DO 2043 N=1,L,MIT
      NN=1+(N-1)/MIT
      SP(NN)=TIM*SP(N)
      SPP(NN)=TIM*SPP(N)
      EP(NN)=EP(N)*TIM
      EPP(NN)=EPP(N)*TIM
      S(1,NN)=S(2,N)
      E(1,NN)=E(2,N)
      V(1,NN)=V(2,N)
      G(1,NN)=G(2,N)
      S(2,NN)=S(2,N)
      E(2,NN)=E(2,N)
      V(2,NN)=V(2,N)
 2043 G(2,NN)=G(2,N)
      PRINT 91
      GO TO 999
 2042 CONTINUE
      STOP
      END
      END
```

SAMPLE DATA -- PROGRAM POWRATE -- TABULATED VELOCITY INPUT DATA

```
0001 0001 0051 0002 0001 0050 0011 0001 0010 0010 0051 0002 0001
 .5200000000E-00 .9800000000E+07 .2530000000E-03 .3940362000E+05 .3657000000E+00
 .0000000000E 00 .0000000000E 00 .0000000000E 00 .0000000000E 00 .0000000000E 00
 .0000000000E 00 .0000000000E 00 .5880000000E 02 .0000000000E 00 .0000000000E 00
-.5118100000E+02-.5354300000E+02-.5511800000E+02-.5669300000E+02-.5787400000E+02
-.5826800000E+02-.5885800000E+02-.5925200000E+02-.6023600000E+02-.6102400000E+02
-.6141700000E+02-.6220500000E+02-.6259800000E+02-.6279500000E+02-.6318900000E+02
-.6377900000E+02-.6456700000E+02-.6535400000E+02-.6614200000E+02-.6692900000E+02
-.6732300000E+02-.6811000000E+02-.6889800000E+02-.6968500000E+02-.7047200000E+02
-.7086600000E+02-.7165300000E+02-.7244100000E+02-.7322800000E+02-.7401600000E+02
-.7480300000E+02-.7598400000E+02-.7716500000E+02-.7834600000E+02-.7952700000E+02
-.8070900000E+02-.8228300000E+02-.8385800000E+02-.8543300000E+02-.8700800000E+02
-.8937000000E+02-.9094500000E+02-.9291300000E+02-.9488200000E+02-.9724400000E+02
-.9921200000E+02-.1011810000E+03-.1035430000E+03-.1055120000E+03-.1082680000E+03
-.1114170000E+03
```